

Phase Space Formulation of S-matrix

Joon-Hwi Kim^a

^a *Walter Burke Institute for Theoretical Physics,
California Institute of Technology, Pasadena, CA 91125*

E-mail: joonhwi@caltech.edu

ABSTRACT: We establish an exact relation between the S-symplectomorphism and the S-matrix by means of the phase space formulation of quantum mechanics. The adjoint action of the S-matrix defines a fuzzy diffeomorphism on phase space whose classical limit is the S-symplectomorphism. The relation between classical and quantum eikonals is immediate via \hbar -deformation of each Poisson bracket in the Magnus formula. Diagrammatic computation of quantum eikonal is illustrated for quantizations in both symmetric and normal orderings.

Contents

1	Introduction	2
2	Phase Space Formulation	5
2.1	Classical Mechanics	5
2.2	Quantum Mechanics	7
3	Scattering Theory	18
3.1	Classical Interaction Picture	19
3.2	S-symplectomorphism	19
3.3	Quantum Interaction Picture	21
3.4	Fuzzy S-diffeomorphism	21
3.5	S-matrix	23
4	Classical Limits	24
4.1	Eikonal Matrix \rightarrow Classical Eikonal	24
4.2	Adjoint Action of S-matrix \rightarrow S-symplectomorphism	24
4.3	S-matrix \rightarrow No Good Limit	25
4.4	Impulse Formulae	25
5	Quantum Eikonal from Magnus Expansion	27
5.1	Classical Eikonal	28
5.2	Quantum Eikonal (Symmetric Ordering)	33
5.3	Quantum Eikonal (Normal Ordering)	38
6	Summary and Outlook	46
A	Appendices	49
A.1	More on Interaction Pictures	49
A.2	In Background Perturbation Theory	50
A.3	More on Wightman Tensor	52
A.4	Field Theory	53

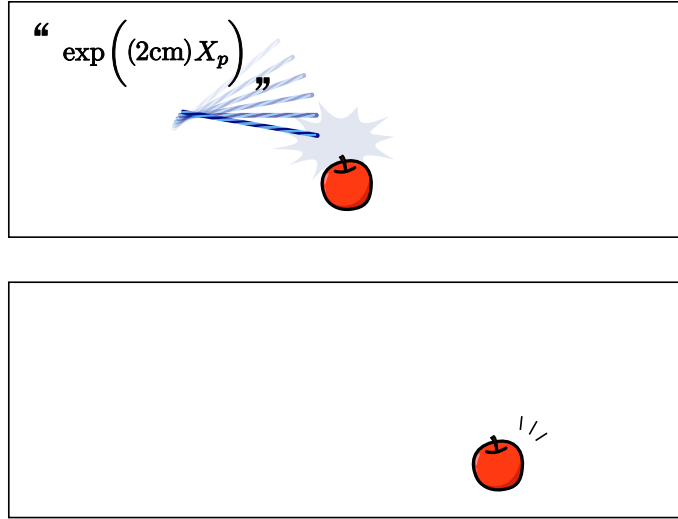


Figure 1. Translation is a symplectomorphism, whose generator is the momentum p .

1 Introduction

A variety of formulations exist for classical mechanics. Among them, Hamiltonian mechanics could stand out in terms of its geometrical approach based on phase space. In a view, the appeal of Hamiltonian mechanics is that it naturally encourages an “operator-like”—or “object-oriented”—way of approaching classical mechanics. Classical time evolution is an *operator* that acts on the phase space as an *object*. In Fig. 1, spatial translation is implemented by exponentiating a Hamiltonian vector field $X_p = \{p, \}$ as an *operator*.

Indeed, this mode of thinking provides glimpses into the more fundamental framework, i.e., quantum mechanics. Quantum time evolution is a unitary *operator* that acts on the Hilbert space as an *object*. Spatial translation is generated by an exponential *operator* that arises from the momentum.

In the fancy terms of category theory [1–9], we say that Hamiltonian mechanics is based on the category **Symp**. *Objects* are phase spaces as symplectic manifolds. *Morphisms* are maps between phase spaces that preserve the symplectic structure, which are referred to as symplectomorphisms. Classical time evolution is a symplectomorphism on phase spaces. Transformations such as spatial translations are also symplectomorphisms on phase spaces.

Similarly, quantum mechanics is based on the category **Hilb**. *Objects* are Hilbert spaces. *Morphisms* are operators. Quantum time evolution is a unitary operator. Spatial translation is also a unitary operator.

When applied to scattering theory, the above analogy between classical and quantum mechanics elicits the idea of “S-symplectomorphism.” The S-matrix is the unitary operator mapping the initial Hilbert space of scattering states to the final Hilbert space of scattering states. Thus, its classical counterpart shall be the symplectomorphism mapping the initial phase space of scattering states to the final phase space of scattering states, which we dub

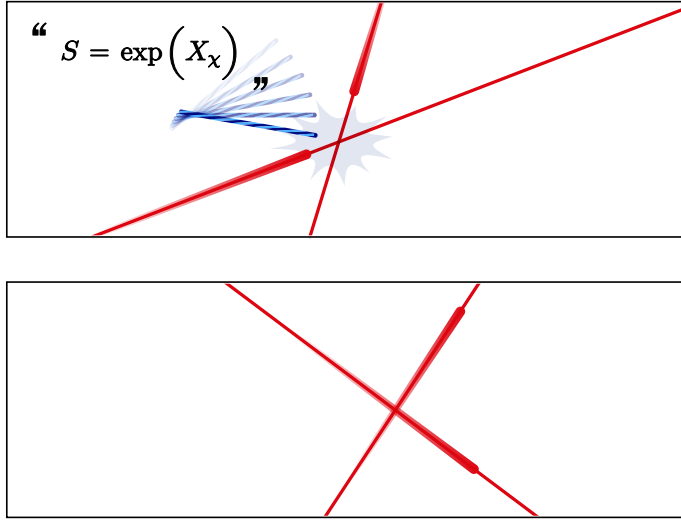


Figure 2. Scattering is a symplectomorphism, whose generator is the eikonal χ .

S-symplectomorphism.

A cartoon is provided in Fig. 2, depicting the action of an S-symplectomorphism for a two-particle system. Just like the translation operator in Fig. 1, the S-symplectomorphism S can be represented as the exponentiation of a Hamiltonian vector field $X_\chi = \{\chi, \cdot\}$. This generator χ is referred to as the classical eikonal, as it serves as the analog of the eikonal matrix $\hat{\chi}$ in quantum mechanics: $\hat{S} = \exp(\hat{\chi}/i\hbar)$.

Historically, the concept of S-symplectomorphism was proposed by Hunziker [10] in 1968 and had been investigated in works [11–16] in the '70s and '80s (called “S-map,” “S-transformation,” or “canonical S-transformation”). An impressive application of the idea is given by Ref. [14], as is reviewed in Ref. [16]. It is shown that the classical analog of Levinson’s theorem [17] follows from the volume-preserving property of S-symplectomorphism, relating the phase-space volume occupied by bound orbits in an attractive potential to an integral over time delay for scattering orbits.

The idea of S-symplectomorphism has been also independently accessed by the present author during the work [18], which could be concretized through later works [19, 20]. The purely classical formulation of S-symplectomorphism has been established in Ref. [21].

The identification of the classical eikonal χ as the generator of S-symplectomorphism traces back to the work [15] by Narnhofer and Thirring, where it is found—yet for simple examples—that “The quasiclassical phase shift is identified as the generator of the classical canonical S transformation.” This observation has been established to full extent of generality by Refs. [19, 20], where a nested bracket structure is essential.

The analogies between the S-symplectomorphism S and the S-matrix \hat{S} , and also the classical eikonal χ and the eikonal matrix $\hat{\chi}$, have been argued from the correspondence principle or related ideas [11–16, 18–20]. However, to our best understanding, it has been not shown that the S-symplectomorphism arises as the faithful $\hbar \rightarrow 0$ limit of a quantum-

mechanical construct. The claims have remained at the levels of analogies or arguments, which do not describe exact mathematical equalities.

The physical relevance of this problem would be evaluated from the angle of modern applications of scattering theory. As the work [22] by Kosower, Maybee, and O’Connell has nicely reviewed and systematized, the punchline has been “Extract classical observables from the quantum S-matrix.” A formalism based on the eikonal matrix has also emerged, proposed in Ref. [19] while tracing back to Refs. [23, 24] as well. The latter formalism has shown that the S-symplectomorphism provides a purely classical framework for the classical eikonal, the point of which is explicitly emphasized in Ref. [21]. Hence the punchline shifts to “Extract classical observables from the S-symplectomorphism.” To understand the precise relation between these two paradigms, however, an exact relationship needs to be clarified between the S-symplectomorphism $S = \exp(X_\chi)$ and the S-matrix $\hat{S} = \exp(\hat{\chi}/i\hbar)$.

An immediate issue is a mismatch in “data types.” The S-matrix \hat{S} is a linear transformation on a Hilbert space. The literal $\hbar \rightarrow 0$ limit cannot equate it to the diffeomorphism S on a phase space, suddenly turning the Hilbert space into a symplectic manifold. In the same way, the eikonal matrix $\hat{\chi}$ cannot be directly equated with a scalar-valued function χ . So to speak, they are “apples and oranges” living in two separate worlds, so any comparison is grammatically nonsense unless a “translator” is provided. Furthermore, the classical limit of $\hat{S} = \exp(\hat{\chi}/i\hbar)$ is still divergent even if the classical limit of $\hat{\chi}$ could describe χ .

In this paper, we derive the precise relation between the S-matrix and the S-symplectomorphism in terms of exact mathematical equalities. Crucially, this is facilitated by the phase space formulation of quantum mechanics, which provides the “translator” that re-casts operators on Hilbert spaces as scalar functions on phase spaces.

The phase space formulation of quantum mechanics was put forward by Moyal and Groenewold [25, 26] in the ’40s, based on earlier constructions by Weyl and Wigner [27, 28]. It is equivalent to the density matrix formulation of quantum mechanics, where one focuses on operators instead of wavefunctions. See Refs. [29–31] for comprehensive expositions on the subject. It is also roughly synonymous to deformation quantization [32–38], in which case the geometrical picture describes a fuzzy (noncommutative) phase space.

In Sec. 2, we review the phase space formulation of quantum mechanics in a friendly and concrete fashion, since the formulation may not be standard or well-known depending on the community. In Sec. 3, we develop scattering theory in the phase space formulation of quantum mechanics, which is new to our best knowledge. In Sec. 4, we establish the main statements about the classical limit. The adjoint action of the S-matrix is equivalent to the deformation of the S-symplectomorphism. The eikonal matrix is equivalent to the deformation of the classical eikonal.

Our formalism facilitates a systematic diagrammatic evaluation of quantum eikonal to all loop orders, as shown in Sec. 5. Explicitly, we compute the all-loop quantum eikonal at three vertices in both symmetric and normal orderings. Our approach and results are new, despite the recent work [39] appeared during the preparation of this paper. Mathematically, the implication is that Magnus expansion [40] in deformation quantization defines two new graph functions on directed acyclic kinds of graphs, generalizing the one due to Murua [70].

2 Phase Space Formulation

2.1 Classical Mechanics

To initiate our journey in a friendly fashion, let us suppose a simple concrete example: a particle on a one-dimensional line \mathbb{R} . The classical state of this particle is represented as the pair (x, p) of position x and momentum p . The **phase space** is the space $\mathcal{P} = \mathbb{R}^2$ of this pair (x, p) , where each point represents a classical state. Classical observables are smooth functions on the phase space, the space of which is denoted as $C^\infty(\mathcal{P})$.

The mathematical model of phase space is **symplectic geometry**, which we presume within this paper. The symplectic form is a nondegenerate closed two-form:

$$\Omega = dp \wedge dx. \quad (2.1)$$

The symplectic form Ω induces the following geometric structures on the phase space.

First, the phase space is equipped with the **Poisson bracket**. The Poisson bracket is a linear bi-differential operator that takes two classical observables $f, g \in C^\infty(\mathcal{P})$ as input and returns another classical observable $\{f, g\} \in C^\infty(\mathcal{P})$ as output. For our one-dimensional particle, the Poisson bracket is defined by the canonical relations

$$\{x, x\} = 0, \quad \{x, p\} = 1, \quad \{p, p\} = 0. \quad (2.2)$$

The Poisson bracket in Eq. (2.2) is in an “inverse” relationship with the symplectic form in Eq. (2.1), so knowing the former implies knowing the latter and vice versa.

Second, the phase space is equipped with the **Liouville measure**, a top-degree differential form that provides an invariant integration measure over the phase space. It is constructed from the symplectic form as

$$\mu = \frac{dp \wedge dx}{\varepsilon}. \quad (2.3)$$

Here, ε is an ad-hoc constant whose sole purpose is to make μ dimensionless.

The time evolution of the particle’s classical state is described by the **Hamiltonian equations of motion**. For a generic time-dependent Hamiltonian $H(t) \in C^\infty(\mathcal{P})$, the Hamiltonian equations of motion read

$$\dot{x} = \{x, H(t)\}, \quad \dot{p} = \{p, H(t)\}. \quad (2.4)$$

For example, $H(t) = p^2/2m - F(t)x$ will implement a particle of mass m driven by a time-dependent external force $F(t)$. Evidently, Eq. (2.4) is a first-order differential equation that describes how a point on \mathcal{P} moves within time.

More generally, one can describe an ensemble of the same particle in terms of the **Liouville equation**:

$$\dot{\rho}(t) = \{H(t), \rho(t)\}. \quad (2.5)$$

Here, $\rho(t) \in C^\infty(\mathcal{P})$ is a time-dependent probability distribution on \mathcal{P} . It is unit-normalized with respect to the Liouville measure, encoding the unity of total probability:

$$\int \frac{dp \wedge dx}{\varepsilon} \rho(t) = 1. \quad (2.6)$$

The classical time evolution can be studied by either of Eqs. (2.4) or (2.5). Physically, the former is a special case of the latter: a single particle is an extreme case of an ensemble of particles. Geometrically, the former describes a map that sends a point in \mathcal{P} to another, whereas the latter describes the evolution of test functions on \mathcal{P} . These are two equivalent ways for representing a diffeomorphism on \mathcal{P} [41].

Intuitively speaking, one can picture classical time evolution as a fluid that fills in and streams through the phase space \mathcal{P} . To grasp the flow of this fluid, one could put a neutrally buoyant bubble at each point in \mathcal{P} and track its trajectory. Alternatively, one could also study how splashes of inks on the fluid would change their shapes under time.

With this remark made, let us stick to the latter description in light of its practical and conceptual advantages as well as its relevance that will become evident shortly. In this approach, the classical time evolution can be explicitly *computed* as the following.

First of all, for each function $f \in C^\infty(\mathcal{P})$ on phase space, define X_f as the first-order differential operator such that

$$X_f[g] = \{f, g\}, \quad \forall g \in C^\infty(\mathcal{P}). \quad (2.7)$$

X_f is known as the **Hamiltonian vector field** of f . This terminology appeals to the well-known mathematical equivalence between vector fields and first-order differential operators. Importantly, Hamiltonian vector fields are differential operators that preserve the algebraic structure of classical observables due to pointwise addition, pointwise multiplication, and Poisson bracket:

$$X_f[g + h] = X_f[g] + X_f[h], \quad (2.8a)$$

$$X_f[gh] = (X_f[g])h + g(X_f[h]), \quad (2.8b)$$

$$X_f[\{g, h\}] = \{X_f[g], h\} + \{g, X_f[h]\}. \quad (2.8c)$$

This implies that Hamiltonian vector fields preserve the symplectic structure.

Second of all, provided the definition in Eq. (2.7), the Liouville equation in Eq. (2.5) can be rewritten and solved as

$$\dot{\rho}(t) = X_{H(t)}[\rho(t)] \implies \rho(T) = U^*[\rho(0)], \quad (2.9)$$

where we have arbitrarily set the initial and final times as $t = 0$ and $t = T$. In Eq. (2.9), U^* is a differential operator that transforms the initial classical (ensemble) state $\rho(0)$ to the final classical state $\rho(T)$. Well-established results due to Dyson [42] and Magnus [40] facilitate the explicit formulae

$$U^* = \text{Texp} \left(\int_0^T dt X_{H(t)} \right) = \exp(X_G), \quad (2.10)$$

respectively. In Eq. (2.10), $G \in C^\infty(\mathcal{P})$ is given by

$$\begin{aligned} G = & \int dt_1 H(t_1) + \frac{1}{2} \int_{t_1 > t_2} d^2t \{H(t_1), H(t_2)\} \\ & + \frac{1}{6} \int_{t_1 > t_2 > t_3} d^3t \left(\{H(t_1), \{H(t_2), H(t_3)\}\} + \{H(t_3), \{H(t_2), H(t_1)\}\} \right) + \dots, \end{aligned} \quad (2.11)$$

where the default integral bounds are $[0, T]$.

An important feature of Eq. (2.11) is that each integrand is composed by nesting Poisson brackets. This property crucially counts on the Jacobi identity

$$[X_f, X_g] = X_{\{f,g\}}, \quad (2.12)$$

which encodes that Hamiltonian vector fields as first-order differential operators are closed under the commutator. Note that Eq. (2.12) demands the closure of the symplectic form.

The formula $U^* = \exp(X_G)$ in Eq. (2.10) establishes that U^* is the exponentiation of a Hamiltonian vector field. This fact has the following implications. Firstly, there exists a diffeomorphism $U : \mathcal{P} \rightarrow \mathcal{P}$ such that U^* implements its pullback: $U^* = f \mapsto f \circ U^{-1}$. This is because U^* is the exponentiation of a first-order differential operator, which can be checked by verifying the following conditions for a pullback:

$$U^*[f + g] = U^*[f] + U^*[g], \quad (2.13a)$$

$$U^*[fg] = U^*[f]U^*[g]. \quad (2.13b)$$

Secondly, the diffeomorphism U preserves the symplectic structure. This is because X_G is not just an any first-order differential operator but a Hamiltonian vector field, which preserves the symplectic structure as per Eq. (2.8c). Explicitly, for any classical observables $f, g \in C^\infty(\mathcal{P})$ it holds that

$$U^*[\{f, g\}] = \{U^*[f], U^*[g]\}, \quad (2.13c)$$

which is the exponentiated version of Eq. (2.8c).

Diffeomorphisms that preserve the symplectic structure is called *symplectomorphisms*. The groups of diffeomorphisms and symplectomorphisms on the phase space are denoted as $\text{Diff}(\mathcal{P})$ and $\text{Diff}(\mathcal{P}, \Omega)$, respectively. The latter is a Lie subgroup of the former.

From this analysis, we conclude that the solution to the Liouville equation, Eq. (2.9), has computed a symplectomorphism on the phase space,

$$U \in \text{Diff}(\mathcal{P}, \Omega), \quad (2.14)$$

by representing it as the differential operator U^* implementing the pullback. To reiterate, $U^* : \rho(0) \mapsto \rho(T)$ transforms the initial classical state to the final classical state. Therefore, the symplectomorphism U in Eq. (2.14) is the map from the initial phase space to the final phase space due to the classical time evolution. Hence, U in Eq. (2.14) is referred to as the *time-evolution symplectomorphism*.

Of course, the fact that classical time evolution is a symplectomorphism on phase space is a well-known postulate of Hamiltonian mechanics. The purpose of the above calculation and discussion is to remind ourselves how this postulate is concretely approached by solving the Liouville equation in Eq. (2.5) (or the Hamiltonian equations of motion in Eq. (2.4)).

2.2 Quantum Mechanics

Now let us concern the quantum mechanics of the particle. In the standard formulation, the starting point is the declaration of the *Hilbert space* as the space of square-integrable functions on the real line: $\mathcal{H} = L^2(\mathbb{R})$. As is well-known, this is the space where well-behaved wavefunctions dwell in.

An operator is a linear map $\mathcal{H} \rightarrow \mathcal{H}$ that sends a wavefunction to another. Especially, the position and momentum operators are defined as

$$\begin{aligned}\hat{x} &: \left(x \mapsto \psi(x) \right) \mapsto \left(x \mapsto x\psi(x) \right), \\ \hat{p} &: \left(x \mapsto \psi(x) \right) \mapsto \left(x \mapsto -i\hbar \frac{\partial}{\partial x} \psi(x) \right).\end{aligned}\tag{2.15}$$

The canonical commutation relations hold as

$$[\hat{x}, \hat{x}] = 0, \quad [\hat{x}, \hat{p}] = i\hbar \hat{1}, \quad [\hat{p}, \hat{p}] = 0.\tag{2.16}$$

2.2.1 The Quantization Map

Let $\text{Ops}(\mathcal{H})$ be the space of operators, subject to one's favorite mathematical assumptions. To construct the quantum theory fully, one identifies the quantum-mechanical counterpart $\hat{f} \in \text{Ops}(\mathcal{H})$ of each function $f \in C^\infty(\mathcal{P})$ on the phase space $\mathcal{P} = \mathbb{R}^2$. Mathematically, this means to define a linear map

$$\mathcal{Q} : C^\infty(\mathcal{P}) \rightarrow \text{Ops}(\mathcal{H}),\tag{2.17}$$

such that $\mathcal{Q}(x) = \hat{x}$ and $\mathcal{Q}(p) = \hat{p}$ [43]. This is known as the *quantization map*.

To this end, however, it is well-known that one must pick an *ordering prescription*. For example, consider the function $f(x, p) = xp^2$. There are at least three different possibilities for its quantization: $\hat{x}\hat{p}^2$, $\hat{p}\hat{x}\hat{p}$, and $\hat{p}^2\hat{x}$, each differing from each other by terms of $\mathcal{O}(\hbar^1)$.

A popular convention is the symmetric ordering, which performs an equal-weight average: $\hat{f} = (\hat{x}\hat{p}^2 + \hat{p}\hat{x}\hat{p} + \hat{p}^2\hat{x})/3$. A unique feature of this prescription is that all coordinates on the phase space, namely position and momentum, are put on an equal footing.

For simplicity, suppose we stick to the symmetric ordering for the moment. To re-capitulate its definition, the quantization map \mathcal{Q} in the symmetric ordering prescription sends $x^n p^m$ to the average of all possible orderings of n factors of \hat{x} and m factors of \hat{p} . Equivalently, a useful formula due to McCoy [44] reads

$$\mathcal{Q}(x^n p^m) = \frac{1}{2^n} \sum_{k=0}^n \binom{n}{k} \hat{x}^k \hat{p}^m \hat{x}^{n-k} = \frac{1}{2^m} \sum_{k=0}^m \binom{m}{k} \hat{p}^k \hat{x}^n \hat{p}^{m-k}.\tag{2.18}$$

Using Eq. (2.18), it is not difficult to prove that [27]

$$\mathcal{Q}(f) = \int \frac{dp \wedge dx}{2\pi\hbar} f(x, p) \hat{\Delta}(x, p),\tag{2.19}$$

where we have denoted

$$\hat{\Delta}(x, p) = \int dy |x + y/2\rangle e^{ipy/\hbar} \langle x - y/2|.\tag{2.20}$$

The above operator $\hat{\Delta}(x, p)$, labeled with phase space coordinates, is known as the *Stratonovich kernel* [45, 46] for symmetric ordering. The Stratonovich kernel completely defines the quantization map \mathcal{Q} , from which a unique operator \hat{f} is paired to each phase-space function f and vice versa. The Stratonovich kernel satisfies several axioms such as Hermiticity, normalization, and orthocompleteness, which one can directly verify or derive from its explicit definition in Eq. (2.20).

2.2.2 The Inverse of Quantization Map

Notably, the axioms of the Stratonovich kernel together ensures a reinterpretation of quantum mechanics reminiscent of statistical mechanics in phase space [45, 46], as is explicitly advertized in the title of Ref. [25]: “Quantum Mechanics as a Statistical Theory.”

The key idea is to pay attention to the inverse of the quantization map [28]:

$$\mathcal{Q}^{-1}(\hat{f})(x, p) = \text{tr}(\hat{\Delta}(x, p)\hat{f}). \quad (2.21)$$

It is left as an exercise to check that Eq. (2.21) is the inverse of Eq. (2.19) by using Eq. (2.20). Notably, the inverse of the quantization map, \mathcal{Q}^{-1} , designates a unique phase-space function $f \in C^\infty(\mathcal{P})$ to each operator $\hat{f} \in \text{Ops}(\mathcal{P})$:

$$\mathcal{Q}^{-1} : \text{Ops}(\mathcal{H}) \rightarrow C^\infty(\mathcal{P}). \quad (2.22)$$

First of all, consider two operators \hat{f}, \hat{g} and their images f, g under \mathcal{Q}^{-1} . Eqs. (2.19) and (2.21) imply that the operator product $\hat{f}\hat{g}$ corresponds to the phase space function

$$\mathcal{Q}^{-1}(\hat{f}\hat{g}) = f \star g, \quad (2.23)$$

where $(f \star g)(x, p)$ is defined by the integral

$$\int \frac{dp_1 dx_1}{2\pi\hbar} \frac{dp_2 dx_2}{2\pi\hbar} \text{tr}(\hat{\Delta}(x, p)\hat{\Delta}(x_1, p_1)\hat{\Delta}(x_2, p_2)) f(x_1, p_1) g(x_2, p_2). \quad (2.24)$$

By explicit evaluation of this integral, it can be found that

$$f \star g = f \exp\left(\frac{i\hbar}{2}\left(\frac{\overleftarrow{\partial}}{\partial x}\frac{\overrightarrow{\partial}}{\partial p} - \frac{\overleftarrow{\partial}}{\partial p}\frac{\overrightarrow{\partial}}{\partial x}\right)\right) g, \quad (2.25)$$

where the arrows indicate the directions on which derivatives act. Mathematically, Eq. (2.25) defines a noncommutative product between functions f and g , known as the *star product* due to Moyal [25]. Therefore, the conclusion reads that the quantum-mechanical operator product is equivalent to a noncommutative product on phase-space functions.

The noncommutativity of a star product is measured by

$$\{f, g\}^* = \frac{1}{i\hbar}(f \star g - g \star f), \quad (2.26)$$

which will be referred to as the *deformed Poisson bracket*. It should be clear that Eq. (2.26) is the phase space counterpart of the operator commutator, divided by $i\hbar$: $\{f, g\}^* = \mathcal{Q}^{-1}([\hat{f}, \hat{g}])/i\hbar$. The correspondence principle arises from the fact that Eq. (2.26) approaches to the Poisson bracket $\{f, g\}$ in the $\hbar \rightarrow 0$ limit.

Next, consider the image $\rho \in C^\infty(\mathcal{P})$ of a density matrix $\hat{\rho} \in \text{Ops}(\mathcal{H})$ under \mathcal{Q}^{-1} [28]. The axioms of the Stratonovich kernel imply that

$$\text{tr}(\hat{\rho}) = 1 \iff \int \frac{dp \wedge dx}{2\pi\hbar} \rho = 1. \quad (2.27)$$

Notably, Eq. (2.27) resembles Eq. (2.6), the equation satisfied by the probability distribution in classical statistical mechanics. Specifically, the ad-hoc constant ε will be replaced and identified with $2\pi\hbar$, encoding the fundamental quantum of phase space volume. Hence, it is suggested that the phase-space function ρ might describe a probability distribution.

However, explicit examples reveal that the local value of the phase-space function ρ can be negative in general; see Refs. [29, 30, 47–49] for demonstrations. In fact, it is known that only Gaussian wavepackets can achieve strict positiveness [50]; the minimal-uncertainty wavepacket, for instance. Therefore, the precise statement reads that ρ defines a *quasiprobability distribution* over the phase space. Here, the prefix “quasi-” means that some of the Kolmogorov probability axioms are relaxed.

To establish the probabilistic interpretation of ρ , one can consider the identities

$$\langle x|\hat{\rho}|x\rangle = \int \frac{dp}{2\pi\hbar} \rho(x, p), \quad \langle p|\hat{\rho}|p\rangle = \int dx \rho(x, p), \quad (2.28)$$

and their application to a pure state $\hat{\rho} = |\psi\rangle\langle\psi|$. One can also examine the expectation value $\text{tr}(\hat{\rho}\hat{f})$ or the absolute-value-squared of a wavefunction overlap $\langle\psi_1|\psi_2\rangle$.

Finally, suppose a time-dependent density matrix $\hat{\rho}(t)$, whose evolution is governed by a time-dependent Hamiltonian $\hat{H}(t)$. As is well-known, the equation $\hat{\rho}(t)$ satisfies reads

$$\dot{\hat{\rho}}(t) = \frac{1}{i\hbar} [\hat{H}(t), \hat{\rho}(t)], \quad (2.29)$$

which is known as the *quantum Liouville equation*. From the results established above, we find that Eq. (2.29) is equivalent to a partial differential equation on the domain $\mathcal{P} \times \mathbb{R}$:

$$\dot{\rho}(t) = \{H(t), \rho(t)\}^*. \quad (2.30)$$

Here, $\rho(t)$ and $H(t)$ are the images of $\hat{\rho}(t)$ and $\hat{H}(t)$ under \mathcal{Q}^{-1} , respectively. The product manifold $\mathcal{P} \times \mathbb{R}$, the three-dimensional space of x , p , and t , is sometimes called the extended phase space [51]. Notably, the partial differential equation in Eq. (2.30) is first-order in the time derivative but is infinite-order in the x, p derivatives.

To sum up, the above analysis shows that every operator equation can be equivalently restated as an equation about phase-space functions via the map \mathcal{Q}^{-1} . This establishes the so-called *phase space formulation of quantum mechanics* [25–28], summarized below.

1. The point of departure is the density matrix formulation of quantum mechanics, built upon operator equations. (That is, do not talk about wavefunctions or kets/bras.)
2. The quantization map is uniquely determined given a choice of ordering prescription.
3. Provided the inverse of the quantization map,
 - (a) *operators* translate to *phase-space functions*,
 - (b) *density matrices* translate to *quasiprobability distributions* over phase space,
 - (c) the *operator product* translates to a noncommutative product on phase space functions dubbed *star product*.
4. The quantum-mechanical time evolution is defined by the quantum Liouville equation as a partial differential equation on the extended phase space.

It shall be highlighted that the phase space formulation is equivalent to the density matrix formulation: every calculation viable in the former should be possible in the latter and vice versa. This correspondence is exact and two-way, provided a well-behaved, invertible quantization map \mathcal{Q} for a fixed ordering prescription. For instance, no approximation or truncation has been made so far for any parameter. Note that the density matrix formulation is capable of describing not only pure states but also mixed states (ensembles).

2.2.3 Time Evolution as Fuzzy Diffeomorphism

It remains to solve the quantum Liouville equation explicitly, just like the treatment of the classical Liouville equation in Sec. 2.1.

First of all, for each function $f \in C^\infty(\mathcal{P})$ on phase space, define X_f^* as the first-order differential operator such that

$$X_f^*[g] = \{f, g\}^*, \quad \forall g \in C^\infty(\mathcal{P}). \quad (2.31)$$

X_f^* will be referred to as the *deformed Hamiltonian vector field* of f , as its classical limit is exactly the Hamiltonian vector field in Eq. (2.7). Importantly, deformed Hamiltonian vector fields are differential operators that preserve the algebraic structure of phase-space functions due to pointwise addition and star product:

$$X_f^*[g + h] = X_f^*[g] + X_f^*[h], \quad (2.32a)$$

$$X_f^*[g \star h] = (X_f^*[g]) \star h + g \star (X_f^*[h]). \quad (2.32b)$$

In other words, deformed Hamiltonian vector fields preserve the quantum operator algebra boiled down into the phase space formulation.

Second of all, provided the definition in Eq. (2.31), the quantum Liouville equation in Eq. (2.30) can be rewritten and solved as

$$\dot{\rho}(t) = X_{H(t)}^*[\rho(t)] \implies \rho(T) = U^*[\rho(0)], \quad (2.33)$$

where we have arbitrarily set the initial and final times as $t = 0$ and $t = T$. In Eq. (2.33), U^* is a differential operator that transforms the initial quantum (ensemble) state $\rho(0)$ to the final quantum state $\rho(T)$ as quasiprobability distributions. Again, well-established results due to Dyson [42] and Magnus [40] facilitate the explicit formulae

$$U^* = \text{Texp}\left(\int_0^T dt X_{H(t)}^*\right) = \exp\left(X_{G^*}^*\right), \quad (2.34)$$

respectively. In Eq. (2.34), $G^* \in C^\infty(\mathcal{P})$ is given by

$$\begin{aligned} G^* = & \int dt_1 H(t_1) + \frac{1}{2} \int_{t_1 > t_2} d^2t \{H(t_1), H(t_2)\}^* \\ & + \frac{1}{6} \int_{t_1 > t_2 > t_3} d^3t \left(\{H(t_1), \{H(t_2), H(t_3)\}^*\}^* + \{H(t_3), \{H(t_2), H(t_1)\}^*\}^* \right) + \dots, \end{aligned} \quad (2.35)$$

where the default integral bounds are $[0, T]$.

An important feature of Eq. (2.35) is that each integrand is composed by nesting deformed Poisson brackets. This property crucially counts on the Jacobi identity

$$[X_f^*, X_g^*] = X_{\{f,g\}^*}^*, \quad (2.36)$$

which encodes that deformed Hamiltonian vector fields as differential operators are closed under the commutator. Note that Eqs. (2.32b) and (2.36) demand associativity of the star product.

The formula $U^* = \exp(X_G^*)$ in Eq. (2.34) establishes that U^* is the exponentiation of a deformed Hamiltonian vector field. Unlike as in the classical case, this fact does not imply that a diffeomorphism exists such that U^* implements a pullback, as X_G^* is not a first-order differential operator; hence we have not put a superscript $*$. Still, however, it holds that

$$U^*[f + g] = U^*[f] + U^*[g], \quad (2.37a)$$

$$U^*[f \star g] = (U^*[f]) \star (U^*[g]), \quad (2.37b)$$

for any phase-space functions $f, g \in C^\infty(\mathcal{P})$. This is the exponentiated version of Eq. (2.32).

To elicit the geometrical interpretation of U^* , we might want to temporarily switch gears: a brief mathematical digression based on ideas in noncommutative geometry.

Roughly speaking, there is a sense in which examining the algebra of functions on a space studies the geometry of that space itself [52–57]. This idea provides an algebraic perspective on geometry. Especially, it facilitates the very definition of noncommutative geometry as a space endowed with a noncommutative algebra of functions.

In an ordinary (classical) geometry, smooth functions form a commutative ring $\mathcal{A} = (C^\infty(\mathcal{P}), +, \cdot)$ under the pointwise addition and multiplication. In the algebraic approach to geometry, diffeomorphisms are viewed as automorphisms of this ring \mathcal{A} . Namely, they are transformations that preserve the pointwise addition and multiplication. In fact, we have already explored this idea in Eqs. (2.13a) and (2.13b).

In a noncommutative geometry, smooth functions form a noncommutative ring $\mathcal{A}_\star = (C^\infty, +, \star)$ due to the pointwise addition and a star product \star . As the direct generalization of the identification made in the previous paragraph, diffeomorphisms of the noncommutative geometry can be defined as automorphisms of this ring \mathcal{A}_\star . Namely, they are transformations that preserve the pointwise addition and the star product. Evidently, this statement is the exact content of Eqs. (2.37a) and (2.37b).

In this precise mathematical sense, our map $U^* = \exp(X_G^*)$ describes and defines a diffeomorphism in a noncommutative geometry, or a **fuzzy diffeomorphism** in short. Here, “fuzzy” is a technical term referring to “noncommutative” in noncommutative geometry. The space of fuzzy diffeomorphisms may be denoted as $\text{Diff}(\mathcal{P}, \star)$, so $U^* \in \text{Diff}(\mathcal{P}, \star)$.

It is also instructive to approach this fact in terms of vector fields. In an ordinary geometry, vector fields are derivations on the commutative algebra $\mathcal{A} = (C^\infty(\mathcal{P}), +, \cdot)$. Namely, they are differential operators that preserve the pointwise addition and multiplication. In fact, we have already explored this idea in Eqs. (2.8a) and (2.8b). Similarly, Hamiltonian vector fields are derivations on the Poisson algebra $\mathcal{A}_{\{, \}} = (C^\infty(\mathcal{P}), +, \cdot, \{, \})$, as they additionally preserve the Poisson bracket. We have already adopted this view in Eq. (2.8c).

In a noncommutative geometry, vector fields are derivations on the noncommutative algebra $\mathcal{A}_\star = (C^\infty(\mathcal{P}), +, \star)$. Namely, they are differential operators that preserve the pointwise addition and the star product. Evidently, this statement is the exact content of Eqs. (2.32a) and (2.32b). Therefore, vector fields in a noncommutative geometry, or **fuzzy vector fields** in short, are exactly the differential operators such as the deformed Hamiltonian vector fields defined in Eq. (2.31).

Exponentiating, it follows that the map $U^\star = \exp(X_{G^\star}^\star)$ preserves the algebra \mathcal{A}_\star : U^\star is a \star -preserving map since $X_{G^\star}^\star$ is \star -preserving. Specifically, one shows that $U^\star = \exp(X_{G^\star}^\star)$ satisfies Eq. (2.37) if $X_{G^\star}^\star$ satisfies Eq. (2.32).

Note how Eq. (2.8) has described the (semi)classical vestige of Eq. (2.32). Similarly, it should be clear that $U^\star = \exp(X_{G^\star}^\star)$ in Eq. (2.34) reproduces $U = \exp(X_G)$ in Eq. (2.10) in the classical limit. A \star -preserving diffeomorphism $U^\star \in \text{Diff}(\mathcal{P}, \star)$ becomes an Ω -preserving diffeomorphism $U \in \text{Diff}(\mathcal{P}, \Omega)$ in the small fuzziness limit. A \star -preserving vector field X_G^\star becomes an Ω -preserving vector field X_G in the small fuzziness limit. Ω is the vestige of \star . Classical geometry of phase space emerges from the quantum geometry of phase space.

Eventually, let us return to the physics side and conclude. In the phase space formulation of quantum mechanics, the phase space \mathcal{P} is endowed with a noncommutative product \star on its functions, encoding the quantum-mechanical operator algebra. The pair (\mathcal{P}, \star) will be called the **fuzzy phase space**, which defines an instance of noncommutative geometry.

Intuitively, the fuzzy phase space is a geometry where each point becomes dissolved or spread out a bit due to the uncertainty principle, the extent of which is characterized by the quantum of phase space volume $\varepsilon = 2\pi\hbar$. In fact, the Poisson structure of the classical phase space shall be viewed as vestiges of this fuzziness, emerging in the limit $\hbar \rightarrow 0$.

Provided this geometrical interpretation, it follows that the solution to the quantum Liouville equation, Eq. (2.33), has computed a fuzzy diffeomorphism,

$$U^\star \in \text{Diff}(\mathcal{P}, \star), \quad (2.38)$$

incarnated as a \star -preserving differential operator. As $U^\star : \rho(0) \mapsto \rho(T)$ transforms the initial quantum state to the final quantum state as quasiprobability distributions, its interpretation is the quantum-mechanical time evolution reformulated as a fuzzy diffeomorphism. Hence, U^\star in Eq. (2.38) would be referred to as the **fuzzy time-evolution diffeomorphism**.

Of course, from the perspective of the standard operator formalism, this might be a merely pedantic way of assessing the fact that the quantum-mechanical time evolution is a map that preserves the operator product. Still, its geometrical reinterpretation in terms of noncommutative geometry could be interesting in light of its exotic semantics.

A few remarks are in order. Firstly, the consistency between the normalization $\text{tr}(\hat{\rho}(t)) = 1$ and the quantum Liouville equation in Eq. (2.29) is ensured by the property $\text{tr}(\hat{f}\hat{g}) = \text{tr}(\hat{g}\hat{f})$. In the phase space formulation, this consistency is ensured through the identity

$$\int \frac{dp \wedge dx}{2\pi\hbar} f \star g = \int \frac{dp \wedge dx}{2\pi\hbar} g \star f \iff \int \frac{dp \wedge dx}{2\pi\hbar} X_f^\star[g] = 0, \quad (2.39)$$

which arises by the axioms of the Stratonovich kernel. Formally, Eq. (2.39) is analogous to the vanishing total integral of a total derivative.

The above clarification establishes that the action of a deformed Hamiltonian vector field on quasiprobability distributions preserves the unity of quantum-mechanical probability, which reinterprets unitarity of quantum time evolution. Compare this with the fact that the action of a Hamiltonian vector field on probability distributions preserves the unity of classical probability, which is due to the invariance of the Liouville measure. This encodes symplecticity of classical time evolution.

Next, it is sometimes stated that the Liouville theorem breaks down at the quantum level. At face value, this is correct since $X_{H(t)}^*$ or $X_{G^*}^*$ are not Hamiltonian vector fields but deformed ones. In fact, they are not even first-order differential operators and thus cannot be interpreted as a vector field or an infinitesimal diffeomorphism. (What is the Lie derivative “ $\mathcal{L}_{X_{H(t)}^*} \Omega$ ”?) Namely, while their action on test functions is well-defined, their action on points in the phase space is not defined; see Ref. [58], for instance. Intuitively speaking, this means that they dissolve a point into a scattered cloud, instead of mapping it to another solid point. This precisely demonstrates their fuzzy nature.

In this regard, a better comparison may be evaluating the proper noncommutative geometry generalization of the Liouville theorem: the preservation of the *star product* by $X_{H(t)}^*$ or $X_{G^*}^*$. This generalized Liouville theorem is exactly satisfied and encodes the very unitarity as discussed above. So probability is still conserved, albeit quantum-mechanically.

2.2.4 Adjoint Actions and Intertwining Identities

Before moving on, it is helpful to establish a few mathematical identities regarding adjoint actions to clarify the origin of fuzzy diffeomorphisms.

As is well-known, the *adjoint actions* are defined as

$$\text{ad}_{\hat{f}}[\hat{g}] = [\hat{f}, \hat{g}], \quad \text{Ad}_{\hat{U}}[\hat{f}] = \hat{U} \hat{f} \hat{U}^{-1}, \quad (2.40)$$

for any operators $\hat{f}, \hat{g}, \hat{U} \in \text{Ops}(\mathcal{H})$ with the assumption that \hat{U} is invertible. In particular, it is well-known that exponentiation intertwines between ad and Ad [59]:

$$\text{Ad}_{\exp(\hat{f})} = \exp\left(\text{ad}_{\hat{f}}\right). \quad (2.41)$$

To put it intuitively, adjoint actions are “operators on operators.” Importantly, adjoint actions are maps that preserve the operator algebra. This fact follows from the identities

$$\text{ad}_{\hat{f}}[\hat{g} + \hat{h}] = \text{ad}_{\hat{f}}[\hat{g}] + \text{ad}_{\hat{f}}[\hat{h}], \quad (2.42a)$$

$$\text{ad}_{\hat{f}}[\hat{g}\hat{h}] = (\text{ad}_{\hat{f}}[\hat{g}])\hat{h} + \hat{g}(\text{ad}_{\hat{f}}[\hat{h}]), \quad (2.42b)$$

as well as

$$\text{Ad}_{\hat{U}}[\hat{f} + \hat{g}] = \text{Ad}_{\hat{U}}[\hat{f}] + \text{Ad}_{\hat{U}}[\hat{g}], \quad (2.43a)$$

$$\text{Ad}_{\hat{U}}[\hat{f}\hat{g}] = (\text{Ad}_{\hat{U}}[\hat{f}])(\text{Ad}_{\hat{U}}[\hat{g}]). \quad (2.43b)$$

In the mathematical language, $\text{ad}_{\hat{f}}$ describes a derivation on the operator algebra, while $\text{Ad}_{\hat{U}}$ describes an automorphism of the operator algebra. The astute reader will notice the parallel with X_f^* and U^* in Eqs. (2.32) and (2.37).

To render this parallel structure into precise mathematical statements, we establish a couple of identities that would be called *intertwining identities*, which assume a well-behaved quantization map \mathcal{Q} . The first intertwining identity reads the following:

$$\text{ad}_{\mathcal{Q}(f)/i\hbar} \circ \mathcal{Q} = \mathcal{Q} \circ X_f^*. \quad (2.44)$$

The proof is straightforward from the definitions in Eqs. (2.23) and (2.26). The second intertwining identity, on the other hand, is the exponentiated version of Eq. (2.44):

$$\text{Ad}_{\exp(\mathcal{Q}(f)/i\hbar)} \circ \mathcal{Q} = \mathcal{Q} \circ \exp(X_f^*). \quad (2.45)$$

It can be seen that Eq. (2.45) is implied by Eqs. (2.41) and (2.44).

To evaluate physical implications, one solves the quantum Liouville equation in Eq. (2.29) in the operator language:

$$\dot{\hat{\rho}}(t) = \text{ad}_{\hat{H}(t)/i\hbar}[\hat{\rho}(t)] \implies \hat{\rho}(T) = \text{Ad}_{\hat{U}}[\hat{\rho}(0)]. \quad (2.46)$$

In Eq. (2.46), the *time-evolution unitary operator* \hat{U} is given by

$$\hat{U} = \text{Texp}\left(\frac{1}{i\hbar} \int_0^T dt \hat{H}(t)\right) = \exp(\hat{G}/i\hbar), \quad (2.47)$$

where the operator \hat{G} is given by

$$\begin{aligned} \hat{G} = & \int dt_1 \hat{H}(t_1) + \frac{1}{2(i\hbar)^1} \int_{t_1 > t_2} d^2t [\hat{H}(t_1), \hat{H}(t_2)] \\ & + \frac{1}{6(i\hbar)^2} \int_{t_1 > t_2 > t_3} d^3t \left([\hat{H}(t_1), [\hat{H}(t_2), \hat{H}(t_3)]] + [\hat{H}(t_3), [\hat{H}(t_2), \hat{H}(t_1)]] \right) + \dots \end{aligned} \quad (2.48)$$

An important feature of Eq. (2.48) is that each integrand is composed by nesting commutators. This property crucially counts on the Jacobi identity,

$$[\text{ad}_{\hat{f}}, \text{ad}_{\hat{g}}] = \text{ad}_{[\hat{f}, \hat{g}]} . \quad (2.49)$$

Clearly, Eqs. (2.42b) and (2.49) demand associativity of the operator algebra.

Evidently, Eq. (2.48) is the image of Eq. (2.35) under \mathcal{Q} . This establishes that

$$\hat{G} = \mathcal{Q}(G^*). \quad (2.50)$$

Provided Eq. (2.50), the second intertwining identity in Eq. (2.45) establishes a precise relationship between the time-evolution unitary operator \hat{U} in Eq. (2.47) and the fuzzy time-evolution diffeomorphism U^* in Eq. (2.34):

$$\text{Ad}_{\hat{U}} \circ \mathcal{Q} = \mathcal{Q} \circ U^*. \quad (2.51)$$

Therefore, we conclude that the quantization map \mathcal{Q} intertwines between the adjoint action of the time-evolution unitary operator, $\text{Ad}_{\hat{U}}$, and the fuzzy time-evolution diffeomorphism, U^* . In other words, U^* is equivalent to the adjoint action $\text{Ad}_{\hat{U}}$ via the change in formulations (standard to phase space).

The above discussion should reveal the origin of the fuzzy time-evolution diffeomorphism in a transparent fashion. It might be also helpful to carry out explicit calculations at the level of the Stratonovich kernel such as $\hat{U}\hat{\Delta}(x, p)\hat{U}^{-1} = U^*[\hat{\Delta}(x, p)]$, which we leave as an exercise.

2.2.5 Normal Ordering

In Secs. 2.2.1 and 2.2.2, we have presumed the symmetric ordering prescription for concreteness of our exposition. However, another relevant prescription is the normal ordering for oscillator systems, exclusively adopted in field theories. For the reader's sake, below, we carry out the phase space formulation in the normal ordering prescription as well.

First, the starting point is the identification of the particle's phase space as a complex plane: $\mathcal{P} = \mathbb{R}^2 \cong \mathbb{C}^1$. Two coordinate systems, (x, p) and (a, \bar{a}) , are introduced on \mathcal{P} so that the symplectic structure in Eqs. (2.2) and (2.1) described also as

$$\Omega = i d\bar{a} \wedge da \iff \{a, a\} = 0, \quad \{a, \bar{a}\} = -i, \quad \{\bar{a}, \bar{a}\} = 0. \quad (2.52)$$

Explicitly, the coordinate transformations are given by

$$\begin{aligned} a &= \frac{m\omega x + ip}{\sqrt{2m\omega}}, & x &= \frac{1}{\sqrt{2m\omega}}(a + \bar{a}), \\ \bar{a} &= \frac{m\omega x - ip}{\sqrt{2m\omega}}, & p &= -i\sqrt{\frac{m\omega}{2}}(a - \bar{a}). \end{aligned} \quad (2.53)$$

The dimensionful constants m, ω are supplied by the free harmonic oscillator Hamiltonian,

$$H^\circ(a, \bar{a}) = \frac{p^2}{2m} + \frac{1}{2}m\omega^2x^2 = \omega\bar{a}a. \quad (2.54)$$

Second, the Hilbert space can be kept as the space $\mathcal{H} = L^2(\mathbb{R})$ of square-integrable functions on the position space, so the definition of the position and momentum operators remain the same as in Eq. (2.15). Then the lowering and raising operators are defined as

$$\begin{aligned} \hat{a} &: \left(x \mapsto \psi(x)\right) \mapsto \left(x \mapsto \frac{1}{\sqrt{2m\omega}} \left(m\omega x + \hbar \frac{\partial}{\partial x}\right) \psi(x)\right), \\ \hat{\bar{a}} &: \left(x \mapsto \psi(x)\right) \mapsto \left(x \mapsto \frac{1}{\sqrt{2m\omega}} \left(m\omega x - \hbar \frac{\partial}{\partial x}\right) \psi(x)\right), \end{aligned} \quad (2.55)$$

due to Eq. (2.53). As desired, Eq. (2.55) realizes the canonical commutation relations

$$[\hat{a}, \hat{a}] = 0, \quad [\hat{a}, \hat{\bar{a}}] = \hbar\hat{1}, \quad [\hat{\bar{a}}, \hat{\bar{a}}] = 0. \quad (2.56)$$

The coherent states are given as

$$\langle x|\lambda\rangle = \left(\frac{m\omega}{\pi\hbar}\right)^{1/4} \exp\left(-\frac{1}{\hbar}\left(\sqrt{\frac{m\omega}{2}}x - \lambda\right)^2 + \frac{\lambda^2}{2\hbar}\right) \implies \hat{a}|\lambda\rangle = \lambda|\lambda\rangle, \quad (2.57)$$

where $|\lambda\rangle : x \mapsto \langle x|\lambda\rangle$ is an element of \mathcal{H} . Our convention for their normalization is such that

$$\langle \bar{\lambda}_2|\lambda_1\rangle = e^{\bar{\lambda}_2\lambda_1/\hbar}, \quad \int \frac{i d\bar{\lambda} \wedge d\lambda}{2\pi\hbar} e^{-\bar{\lambda}\lambda/\hbar} |\lambda\rangle\langle\bar{\lambda}| = \hat{1}, \quad (2.58)$$

where the integration employs the Liouville measure over the phase space.

Third, the quantization map in the normal ordering prescription is defined as

$$\mathcal{Q}(a^n \bar{a}^m) = \hat{a}^m \hat{a}^n. \quad (2.59)$$

The linearity of \mathcal{Q} then implies that each analytic function f on \mathcal{P} is mapped to

$$\mathcal{Q}(f) = \int \frac{i d\bar{a} \wedge da}{2\pi\hbar} \int \frac{i d\bar{\lambda} \wedge d\lambda}{2\pi\hbar} \exp\left(\frac{\lambda}{\hbar}(\hat{a} - \bar{a})\right) \exp\left(-\frac{\bar{\lambda}}{\hbar}(\hat{a} - a)\right) f(a, \bar{a}). \quad (2.60)$$

Direct computation shows that

$$\mathcal{Q}(f) = \int \frac{i d\bar{a} \wedge da}{2\pi\hbar} \hat{\Delta}(a, \bar{a}) f(a, \bar{a}), \quad (2.61)$$

where

$$\hat{\Delta}(a, \bar{a}) = \int \frac{i d\bar{\lambda} \wedge d\lambda}{2\pi\hbar} |\lambda\rangle \exp\left(\frac{\bar{a}a - \bar{\lambda}a - \bar{a}\lambda}{\hbar}\right) \langle \bar{\lambda}|. \quad (2.62)$$

The kernel in Eq. (2.62) is attributed to Glauber and Sudarshan [60, 61]. It satisfies several axioms encoding Hermiticity and normalization:

$$\hat{\Delta}^\dagger(a, \bar{a}) = \hat{\Delta}(a, \bar{a}), \quad \text{tr}(\hat{\Delta}(a, \bar{a})) = 1, \quad \int \frac{i d\bar{a} \wedge da}{2\pi\hbar} \hat{\Delta}(a, \bar{a}) = \hat{1}. \quad (2.63)$$

Fourth, by using the properties of coherent states in Eq. (2.58), the inverse of the quantization map in Eq. (2.61) is found as

$$\mathcal{Q}^{-1}(\hat{f})(a, \bar{a}) = e^{-\bar{a}a/\hbar} \langle \bar{a} | \hat{f} | a \rangle. \quad (2.64)$$

This designates a unique phase space function $f \in C^\infty(\mathcal{P})$ to each operator $\hat{f} \in \text{Ops}(\mathcal{H})$. The phase space formulation of quantum mechanics is facilitated by this map \mathcal{Q}^{-1} .

The star product is defined by Eq. (2.23). By using Eqs. (2.61) and (2.64), it follows that $(f \star g)(a, \bar{a})$ is given by the integral

$$\int \frac{i d\bar{a}_1 \wedge da_1}{2\pi\hbar} \frac{i d\bar{a}_2 \wedge da_2}{2\pi\hbar} e^{-\bar{a}a/\hbar} \langle \bar{a} | \hat{\Delta}(a_1, \bar{a}_1) \hat{\Delta}(a_2, \bar{a}_2) | a \rangle f(a_1, \bar{a}_1) g(a_2, \bar{a}_2). \quad (2.65)$$

By explicit evaluation of this integral, it follows that

$$f \star g = f \exp\left(\hbar \frac{\overleftarrow{\partial}}{\partial a} \frac{\overrightarrow{\partial}}{\partial \bar{a}}\right) g. \quad (2.66)$$

This star product would be referred to as the star product of the Wick kind.

The exponential in Eq. (2.66) exactly implements the operator product between normal-ordered operators via Wick's theorem. To see this, observe the correspondences

$$\begin{aligned} \hat{a}\hat{a} &= : \hat{a}\hat{a} : \quad \leftrightarrow \quad \bar{a} \star a = \bar{a}a, \\ \hat{a}\hat{a} &= : \hat{a}\hat{a} : + \hbar \hat{1} \quad \leftrightarrow \quad a \star \bar{a} = a\bar{a} + \hbar. \end{aligned} \quad (2.67)$$

Here, $\bar{a}a = a\bar{a}$ describes the commutative product for $C^\infty(\mathcal{P})$. Another helpful exercise is

$$\begin{aligned} : \hat{a}\hat{a}^2 : : \hat{a}^3\hat{a} : &= : \hat{a}^4\hat{a}^3 : + 6\hbar : \hat{a}^3\hat{a}^2 : + 6\hbar^2 : \hat{a}^2\hat{a} : , \\ \Leftrightarrow (\bar{a}a^2) \star (\bar{a}^3a) &= \bar{a}^4a^3 + 6\hbar\bar{a}^3a^2 + 6\hbar^2\bar{a}^2a , \end{aligned} \quad (2.68)$$

where the power of \hbar equals the number of Wick contractions. It should be clear that

$$\mathcal{Q}^{-1}(\hat{f}) = f \iff \hat{f} = \mathcal{Q}(f) = : f(\hat{a}, \hat{a}) : . \quad (2.69)$$

The deformed Poisson bracket is defined by Eq. (2.26). The Wick star product in Eq. (2.66) gives

$$\{f, g\}^* = \frac{1}{i} \sum_{\ell=0}^{\infty} \frac{\hbar^\ell}{(\ell+1)!} f \left[\left(\frac{\overleftarrow{\partial}}{\partial a} \frac{\overrightarrow{\partial}}{\partial \bar{a}} \right)^{\ell+1} - \left(\frac{\overleftarrow{\partial}}{\partial \bar{a}} \frac{\overrightarrow{\partial}}{\partial a} \right)^{\ell+1} \right] g , \quad (2.70)$$

where the integer ℓ can be interpreted as loop order in a diagrammatic computation: see App. A.2. Also, compare Eq. (2.70) with the deformed Poisson bracket due to the Moyal star product in Eq. (2.25),

$$\{f, g\}^* = \sum_{k=0}^{\infty} \frac{(i\hbar/2)^{2k}}{(2k+1)!} f \left[\left(\frac{\overleftarrow{\partial}}{\partial x} \frac{\overrightarrow{\partial}}{\partial p} - \frac{\overleftarrow{\partial}}{\partial p} \frac{\overrightarrow{\partial}}{\partial x} \right)^{2k+1} \right] g . \quad (2.71)$$

In Eq. (2.71), only the even powers of \hbar occurs due to symmetry properties. Again, $2k$ in Eq. (2.71) describes the loop order in the diagrammatic derivation of star product [62].

Finally, a density matrix $\hat{\rho}$ is mapped to the phase-space function

$$\rho(a, \bar{a}) = e^{-\bar{a}a/\hbar} \langle \bar{a} | \hat{\rho} | a \rangle , \quad (2.72)$$

which is known as Husimi Q representation [63]. This is still a quasiprobability distribution, since some of the Kolmogorov probability axioms have to be relaxed (due to the overcompleteness of coherent states, for instance). Yet, it holds that Eq. (2.72) is non-negative and bounded [64]. Physically, it is literally the probability for obtaining a coherent state in a measurement due to the Born rule. For a pure state $\hat{\rho} = |\psi\rangle\langle\psi|$, for instance, one finds $\rho(a, \bar{a}) = |e^{-\bar{a}a/2} \langle \bar{a} | \psi \rangle|^2$, where the normalization factor $e^{-\bar{a}a/2}$ is due to our convention.

The rest of the phase space formulation unfolds in the exact same fashion as before.

3 Scattering Theory

In Sec. 2, we have established the geometrical interpretations of classical and quantum time evolutions as symplectomorphisms and fuzzy diffeomorphisms, by means of the phase space formulations of classical and quantum mechanics. In this section, we apply such ideas to scattering theory.

Secs. 3.1 and 3.2 review the definition and computation of S-symplectomorphism by following Ref. [21]. Secs. 3.3 and 3.4 construct quantum scattering theory in the phase space formulation of quantum mechanics as the major achievement of this paper.

3.1 Classical Interaction Picture

To begin with, suppose a classical system defined on a generic symplectic manifold (\mathcal{P}, Ω) as the phase space. Suppose the Hamiltonian is given in the form

$$H(t) = H^\circ(t) + V(t). \quad (3.1)$$

The split in Eq. (3.1) defines time-dependent perturbation theory in the phase space formulation of classical mechanics. $H^\circ(t) \in C^\infty(\mathcal{P})$ is the free Hamiltonian, while $V(t) \in C^\infty(\mathcal{P})$ is the interaction Hamiltonian. The latter is treated perturbatively.

Let $U^\circ(t_1, t_2)$ and $U(t_1, t_2)$ be the time-evolution symplectomorphisms from time t_2 to time t_1 due to the Hamiltonians $H^\circ(t)$ and $H(t)$, respectively. They satisfy the usual axioms: $U(t_1, t_1) = \text{id}$, $U(t_1, t_2) = U(t_2, t_1)^{-1}$, $U(t_1, t_2) \circ U(t_2, t_3) = U(t_1, t_3)$.

For any time-dependent function $f(t) \in C^\infty(\mathcal{P})$ on the phase space, its *classical interaction picture* image is defined as the pullback [21, 65]

$$U^\circ(t_0, t)^*[f(t)] = f(t) \circ U^\circ(t, t_0), \quad (3.2)$$

where t_0 is a fixed time of one's choice, often set to zero.

The first expression in Eq. (3.2) shows that the classical interaction picture implements the pullback due to the time-evolution symplectomorphism from t to t_0 . At the same time, the second expression in Eq. (3.2) shows that the classical interaction picture means to simply insert the free-theory trajectory in the arguments of the function $f(t)$, evolved from t_0 to t . The reversal in time direction here is nothing more than the usual wisdom that shifting the argument of the function transforms the function in the reverse way.

3.2 S-symplectomorphism

Given the above definition of classical interaction picture, the idea of S-symplectomorphism arises. The S-symplectomorphism $S \in \text{Diff}(\mathcal{P}, \Omega)$ is a geometrical object defined strictly within classical physics [10–13, 15, 16, 21]. In short, it is the time-evolution symplectomorphism in the classical interaction picture.

Firstly, the point of departure is the classical time-dependent perturbation theory set up in Sec. 3.1. Let $\rho(t)$ be the probability distribution governed by the Liouville equation in Eq. (2.5). Let $\tilde{\rho}(t)$ be its classical interaction picture image. Consider time evolution between times t_\pm , so $\rho(t_+) = \rho(t_-) \circ U(t_-, t_+)$. It follows that

$$\begin{aligned} \tilde{\rho}(t_+) &= \tilde{\rho}(t_-) \circ U^\circ(t_0, t_-) \circ U(t_-, t_+) \circ U^\circ(t_+, t_0), \\ &= \tilde{\rho}(t_-) \circ \left(U^\circ(t_0, t_+) \circ U(t_+, t_-) \circ U^\circ(t_-, t_0) \right)^{-1}. \end{aligned} \quad (3.3)$$

Provided a well-defined limit

$$S = \lim_{t_\pm \rightarrow \pm\infty} U^\circ(t_0, t_+) \circ U(t_+, t_-) \circ U^\circ(t_-, t_0), \quad (3.4)$$

Eq. (3.3) implies

$$\tilde{\rho}(+\infty) = S^*[\tilde{\rho}(-\infty)], \quad (3.5)$$

meaning that the pullback S^* transforms the classical state at far past to the classical state at far future in the interaction picture.

Since $U^\circ(t_1, t_2)$ and $U(t_1, t_2)$ are symplectomorphisms for any t_1, t_2 , Eq. (3.4) defines a symplectomorphism as well, dubbed **S-symplectomorphism** [21]:

$$S \in \text{Diff}(\mathcal{P}, \Omega). \quad (3.6)$$

Secondly, we desire to evaluate the S-symplectomorphism explicitly as a differential operator. Let $\tilde{H}(t)$ and $\tilde{V}(t)$ be the classical interaction picture images of $H(t)$ and $V(t)$, respectively. By using Eq. (2.13c), it follows that

$$\begin{aligned} \text{Eq. (2.5)} \iff & U^\circ(t_0, t)^*[\dot{\rho}(t)] = \{U^\circ(t_0, t)^*[H(t)], U^\circ(t_0, t)^*[\rho(t)]\}, \\ \iff & \tilde{\dot{\rho}}(t) = \{\tilde{H}(t), \tilde{\rho}(t)\}, \\ \iff & \dot{\tilde{\rho}}(t) = \{\tilde{V}(t), \tilde{\rho}(t)\}, \end{aligned} \quad (3.7)$$

where $\tilde{\dot{\rho}}(t) = U^\circ(t_0, t)^*[\dot{\rho}(t)]$. The last line in Eq. (3.7) uses

$$\dot{\tilde{\rho}}(t) = \tilde{\dot{\rho}}(t) + \{\tilde{\rho}(t), \tilde{H}^\circ(t)\}, \quad (3.8)$$

which is not difficult to deduce from $\tilde{\rho}(t) = \rho(t) \circ U^\circ(t, t_0)$.

Eq. (3.7) derives the partial differential equation satisfied by $\tilde{\rho}(t)$, whose solution must reproduce the S-symplectomorphism in Eq. (3.5) as

$$\dot{\tilde{\rho}}(t) = X_{\tilde{V}(t)}[\tilde{\rho}(t)] \implies \tilde{\rho}(+\infty) = S^*[\tilde{\rho}(-\infty)]. \quad (3.9)$$

This derives explicit formulae for S^* , via the Dyson [42] and Magnus [40] series:

$$S^* = \text{Texp}\left(\int dt X_{\tilde{V}(t)}\right) = \exp(X_\chi). \quad (3.10)$$

The function χ in Eq. (3.10) is given by

$$\begin{aligned} \chi = & \int dt_1 \tilde{V}(t_1) + \frac{1}{2} \int_{t_1 > t_2} d^2t \{\tilde{V}(t_1), \tilde{V}(t_2)\} \\ & + \frac{1}{6} \int_{t_1 > t_2 > t_3} d^3t \left(\{\tilde{V}(t_1), \{\tilde{V}(t_2), \tilde{V}(t_3)\}\} + \{\tilde{V}(t_3), \{\tilde{V}(t_2), \tilde{V}(t_1)\}\} \right) + \dots \end{aligned} \quad (3.11)$$

The default integral domains are $(-\infty, +\infty)$.

In sum, we have defined the S-symplectomorphism $S \in \text{Diff}(\mathcal{P}, \Omega)$ in the phase space formulation of classical mechanics and derived explicit formulae for its computation as a differential operator via solving the Liouville equation in the classical interaction picture.

In a well-defined scattering problem, the limit in Eq. (3.4) constructively exists by finiteness of the integral in Eq. (3.11). This stipulates that the interaction Hamiltonian in the interaction picture, $\tilde{V}(t)$, should decay to zero in the limits $t \rightarrow \pm\infty$, in particular.

The function χ in Eq. (3.11) is an effective Hamiltonian that reproduces the entire time evolution from far past to far future within a unit dimensionless time. It will be referred to as the **classical eikonal**.

The formula $S^* = \exp(X_\chi)$ manifests the symplecticity of classical scattering. Probability is conserved by classical scattering.

3.3 Quantum Interaction Picture

Next, we construct quantum scattering theory in the phase space formulation.

To begin with, suppose the quantization of the classical system in Secs. 3.1 and 3.2 in terms of a well-behaved quantization map $\mathcal{Q} : C^\infty(\mathcal{P}) \rightarrow \text{Ops}(\mathcal{H})$. Let (\mathcal{P}, \star) be the resulting fuzzy phase space. The same split in Eq. (3.1) defines time-dependent perturbation theory in the phase space formulation of quantum mechanics, in which case the free and interaction Hamiltonians are quantized with respect to the ordering prescription stipulated by \mathcal{Q} : $\hat{H}^\circ(t) = \mathcal{Q}(H^\circ(t))$, $\hat{V}(t) = \mathcal{Q}(V(t))$

Let $U^{\star\circ}(t_1, t_2)$ and $U^\star(t_1, t_2)$ be the fuzzy time-evolution diffeomorphisms from time t_2 to time t_1 due to the Hamiltonians $H^\circ(t)$ and $H(t)$, respectively. They satisfy the usual axioms: $U^\star(t_1, t_1) = \text{id}$, $U^\star(t_1, t_2) = U^\star(t_2, t_1)^{-1}$, $U^\star(t_1, t_2) \circ U^\star(t_2, t_3) = U^\star(t_1, t_3)$. Here, we remind ourselves that a fuzzy diffeomorphism is a \star -preserving differential operator.

For any time-dependent function $f(t) \in C^\infty(\mathcal{P})$ on the fuzzy phase space, its *quantum interaction picture* image is defined as

$$U^{\star\circ}(t_0, t)[f(t)], \quad (3.12)$$

where t_0 is the fixed chosen time.

This is a natural generalization of Eq. (3.2) in the phase space formulation of quantum mechanics. Geometrically, Eq. (3.12) brings the phase-space function $f(t)$ to the time t_0 through the fuzzy diffeomorphism for free evolution. It is not difficult to see that Eq. (3.12) is equivalent to the standard definition of the quantum-mechanical interaction picture familiar from textbooks: use the intertwining identity in Eqs. (2.44) and (2.45).

3.4 Fuzzy S-diffeomorphism

Given the above definition of quantum interaction picture, the phase space formulation of quantum scattering theory unfolds in the following way.

Firstly, the point of departure is the time-dependent perturbation theory in the phase space formulation of quantum mechanics, set up in Sec. 3.3. Let $\rho(t)$ be a quasiprobability distribution governed by the quantum Liouville equation in Eq. (2.30). Let $\tilde{\rho}(t)$ be its quantum interaction picture image. Consider time evolution between times t_\pm , so $\rho(t_+) = U^\star(t_+, t_-)[\rho(t_-)]$. It follows that

$$\tilde{\rho}(t_+) = U^{\star\circ}(t_0, t_+)[U^\star(t_+, t_-)[U^{\star\circ}(t_-, t_0)[\tilde{\rho}(t_-)]]]. \quad (3.13)$$

Provided a well-defined limit

$$S^\star = \lim_{t_\pm \rightarrow \pm\infty} U^{\star\circ}(t_0, t_+) \circ U^\star(t_+, t_-) \circ U^{\star\circ}(t_-, t_0), \quad (3.14)$$

Eq. (3.13) implies

$$\tilde{\rho}(+\infty) = S^\star[\tilde{\rho}(-\infty)], \quad (3.15)$$

meaning that S^* transforms the quantum state at far past to the quantum state at far future in the interaction picture.

Since $U^{*\circ}(t_1, t_2)$ and $U^*(t_1, t_2)$ are fuzzy diffeomorphisms for any t_1, t_2 , Eq. (3.14) defines a fuzzy diffeomorphism as well:

$$S^* \in \text{Diff}(\mathcal{P}, \star). \quad (3.16)$$

We will refer to S^* in Eq. (3.16) as the *fuzzy S-diffeomorphism*.

Secondly, we desire to evaluate the fuzzy S-diffeomorphism explicitly as a differential operator. To this end, let us take $\tilde{H}(t)$ and $\tilde{V}(t)$ as the quantum interaction picture images of $H(t)$ and $V(t)$, respectively. By using Eq. (2.37b), it follows that

$$\begin{aligned} \text{Eq. (2.30)} \iff & U^{*\circ}(t_0, t)[\dot{\rho}(t)] = \{U^{*\circ}(t_0, t)[H(t)], U^{*\circ}(t_0, t)[\rho(t)]\}^*, \\ \iff & \tilde{\dot{\rho}}(t) = \{\tilde{H}(t), \tilde{\rho}(t)\}^*, \\ \iff & \dot{\tilde{\rho}}(t) = \{\tilde{V}(t), \tilde{\rho}(t)\}^*, \end{aligned} \quad (3.17)$$

where the last line uses a deformed version of Eq. (3.8) due to quantum interaction picture:

$$\dot{\tilde{\rho}}(t) = \tilde{\dot{\rho}}(t) + \{\tilde{\rho}(t), \tilde{H}^\circ(t)\}^*. \quad (3.18)$$

Eq. (3.17) derives the partial differential equation satisfied by $\tilde{\rho}(t)$, whose solution must reproduce the fuzzy S-diffeomorphism in Eq. (3.15) as

$$\dot{\tilde{\rho}}(t) = X_{\tilde{V}(t)}^*[\tilde{\rho}(t)] \implies \tilde{\rho}(+\infty) = S^*[\tilde{\rho}(-\infty)]. \quad (3.19)$$

This derives explicit formulae for S^* , via the Dyson [42] and Magnus [40] series:

$$S^* = \text{Texp}\left(\int dt X_{\tilde{V}(t)}^*\right) = \exp\left(X_{\chi^*}^*\right). \quad (3.20)$$

The function χ^* in Eq. (3.20) is given by

$$\begin{aligned} \chi^* = & \int dt_1 \tilde{V}(t_1) + \frac{1}{2} \int_{t_1 > t_2} d^2t \{\tilde{V}(t_1), \tilde{V}(t_2)\}^* \\ & + \frac{1}{6} \int_{t_1 > t_2 > t_3} d^3t \left(\{\tilde{V}(t_1), \{\tilde{V}(t_2), \tilde{V}(t_3)\}^*\}^* + \{\tilde{V}(t_3), \{\tilde{V}(t_2), \tilde{V}(t_1)\}^*\}^* \right) + \dots \end{aligned} \quad (3.21)$$

In sum, we have defined the fuzzy S-diffeomorphism $S^* \in \text{Diff}(\mathcal{P}, \star)$ in the phase space formulation of quantum mechanics and derived explicit formulae for its computation as a differential operator via solving the quantum Liouville equation in the quantum interaction picture.

Again, well-defined scattering problems stipulate an appropriate decaying behavior of $\tilde{V}(t)$ in the limits $t \rightarrow \pm\infty$, on account of the existence of the limit in Eq. (3.14) and the integral expression in Eq. (3.21).

The function χ^* in Eq. (3.21) is an effective Hamiltonian that reproduces the entire quantum-mechanical time evolution from far past to far future within a unit dimensionless time. It will be referred to as the *quantum eikonal*.

The formula $S^* = \exp(X_{\chi^*})$ manifests the fact that S^* is a \star -preserving map. This implies the conservation of probability by quantum scattering, based on identities such as the one explicated in Eq. (2.39). Therefore, the formula $S^* = \exp(X_{\chi^*})$ manifests unitarity of quantum scattering. Probability is conserved by quantum scattering.

It is not difficult to show that the quantum interaction picture smoothly reduces to the classical interaction picture:¹

$$\lim_{\hbar \rightarrow 0} U^{\star\circ}(t_1, t_2) = U^\circ(t_1, t_2)^* . \quad (3.22)$$

Therefore, it follows that

$$\lim_{\hbar \rightarrow 0} \text{Eq. (3.15)} = \text{Eq. (3.5)} , \quad (3.23)$$

$$\lim_{\hbar \rightarrow 0} \text{Eq. (3.19)} = \text{Eq. (3.9)} , \quad (3.24)$$

$$\lim_{\hbar \rightarrow 0} \text{Eq. (3.20)} = \text{Eq. (3.10)} , \quad (3.25)$$

$$\lim_{\hbar \rightarrow 0} \text{Eq. (3.21)} = \text{Eq. (3.11)} . \quad (3.26)$$

3.5 S-matrix

Lastly, for completeness, we might quickly record the standard, Hilbert-space-based construction of quantum scattering theory. Let $\hat{U}^\circ(t_1, t_2)$ and $\hat{U}(t_1, t_2)$ be the time-evolution unitary operators for the Hamiltonian operators $\hat{H}^\circ(t) = \mathcal{Q}(H^\circ(t))$ and $\hat{H}(t) = \mathcal{Q}(H(t))$. The ***S-matrix*** is defined as the limit

$$\hat{S} = \lim_{t_\pm \rightarrow \pm\infty} \hat{U}^\circ(t_0, t_+) \circ \hat{U}(t_+, t_-) \circ \hat{U}^\circ(t_-, t_0) . \quad (3.27)$$

Explicitly, the Dyson [42] and Magnus [40] expansions are given by

$$\hat{S} = \text{Texp} \left(\frac{1}{i\hbar} \int dt \tilde{V}(t) \right) = \exp \left(\frac{1}{i\hbar} \hat{\chi} \right) , \quad (3.28)$$

where $\tilde{V}(t)$ is the interaction Hamiltonian operator in the quantum-mechanical interaction picture constructed in the standard way, whose image under \mathcal{Q}^{-1} is precisely $\tilde{V}(t)$ in Sec. 3.4. In Eq. (3.28), the ***eikonal matrix*** $\hat{\chi}$ is

$$\begin{aligned} \hat{\chi} = & \int dt_1 \tilde{V}(t_1) + \frac{1}{2(i\hbar)} \int_{t_1 > t_2} d^2t [\tilde{V}(t_1), \tilde{V}(t_2)] \\ & + \frac{1}{6(i\hbar)^2} \int_{t_1 > t_2 > t_3} d^3t \left([\tilde{V}(t_1), [\tilde{V}(t_2), \tilde{V}(t_3)]] + [\tilde{V}(t_3), [\tilde{V}(t_2), \tilde{V}(t_1)]] \right) + \dots \end{aligned} \quad (3.29)$$

Eq. (3.28) clearly shows that the eikonal matrix $\hat{\chi}$ is an effective Hamiltonian operator that generates the entire time evolution from past infinity to future infinity within “ $\Delta t = 1$.”²

¹See Eq. (A.3). A slight subtlety in the notation $\tilde{V}(t)$ in Eqs. (3.20) and (3.21) is clarified in App. A.1. This caveat is yet absent in physically relevant examples featuring quadratic free Hamiltonians.

²We have removed a minus sign common in the current literature on account of this view.

4 Classical Limits

Sec. 3 has defined various constructs in classical and quantum scattering theory. This section establishes exact relations between them, with a focus on the classical limit.

4.1 Eikonal Matrix $\hat{\chi}$ → Classical Eikonal χ

We begin with the relation between the eikonal matrix $\hat{\chi}$ in Eq. (3.29), the quantum eikonal χ^* in Eq. (3.21), and the classical eikonal χ in Eq. (3.11):

$$\hat{\chi} \xleftarrow{\text{equiv.}} \chi^* \xrightarrow{\hbar \rightarrow 0} \chi. \quad (4.1)$$

Firstly, the quantum eikonal χ^* is the equivalent counterpart of the eikonal matrix $\hat{\chi}$ in the phase space formulation. To show this, apply the inverse of a quantization map, $\mathcal{Q}^{-1} : \text{Ops}(\mathcal{H}) \rightarrow C^\infty(\mathcal{P})$, to the formula for $\hat{\chi}$ in Eq. (3.29). It follows that

$$\mathcal{Q}^{-1}(\hat{\chi}) = \chi^*. \quad (4.2)$$

Secondly, the classical eikonal χ is the classical limit of the quantum eikonal χ^* . The formula in Eq. (3.21) clearly establishes that

$$\lim_{\hbar \rightarrow 0} \chi^* = \chi, \quad (4.3)$$

as the deformed Poisson bracket smoothly reduce to the Poisson bracket in the $\hbar \rightarrow 0$ limit. Eqs. (4.2) and (4.3) together verifies the relation between $\hat{\chi}$, χ^* , and χ stated in Eq. (4.1).

4.2 Adjoint Action of S-matrix \hat{S} → S-symplectomorphism S^*

Next, we investigate the relationship between the S-matrix \hat{S} in Eq. (3.28), the fuzzy S-diffeomorphism S^* in Eq. (3.20), and the S-symplectomorphism S in Eq. (3.10):

$$\text{Ad}_{\hat{S}} \xleftarrow{\text{equiv.}} S^* \xrightarrow{\hbar \rightarrow 0} S^*. \quad (4.4)$$

Firstly, the relation established in Eq. (4.2) implies that the fuzzy S-diffeomorphism S^* is the equivalent counterpart of the adjoint action of the S-matrix. To show this, apply the intertwining identity in Eq. (2.45) to the formulae $\hat{S} = \exp(\hat{\chi}/i\hbar)$, $S^* = \exp(X_{\chi^*}^*)$ and $S^* = \exp(X_\chi)$ in Eqs. (3.28) and (3.10). Since Eq. (4.2) holds, it follows that

$$\text{Ad}_{\hat{S}} \circ \mathcal{Q} = \mathcal{Q} \circ S^*. \quad (4.5)$$

That is, the quantization map \mathcal{Q} intertwines between the adjoint action of the S-matrix and the fuzzy S-diffeomorphism.

Secondly, the pullback S^* of S-symplectomorphism is the classical limit of the fuzzy S-diffeomorphism S^* . Based on the formulae $S^* = \exp(X_{\chi^*}^*)$ and $S^* = \exp(X_\chi)$ in Eqs. (3.10) and (3.20), the limit established in Eq. (4.3) implies that

$$\lim_{\hbar \rightarrow 0} S^* = S^*. \quad (4.6)$$

In particular, the deformed Hamiltonian vector field $X_{\chi^*}^*$, as a differential operator, smoothly approaches to the Hamiltonian vector field X_χ . Eqs. (4.5) and (4.6) together verifies the relation between \hat{S} , S^* , and S stated in Eq. (4.4).

4.3 S-matrix → No Good Limit

Note the crucial role of the phase space formulation of quantum mechanics in establishing the relations in Eqs. (4.1) and (4.4). For instance, it does not make sense to equate a phase-space function χ with a limit of an operator $\hat{\chi}$. However, it does make sense to equate a phase-space function χ with a limit of a phase space function χ^* . In this manner, the classical limits are established as precise mathematical equalities, not as mere arguments appealing to the correspondence principle.

Note also the crucial role of the adjoint action in Eq. (4.4). In particular, suppose we investigate the classical limit of the S-matrix \hat{S} directly. Its image under \mathcal{Q}^{-1} is given by

$$\mathcal{Q}^{-1}(\hat{S}) = \exp^*\left(\frac{1}{i\hbar}\chi^*\right) = 1 + \sum_{n=1}^{\infty} \frac{1}{n!(i\hbar)^n} \underbrace{\chi^* \star \cdots \star \chi^*}_{n \text{ times}}, \quad (4.7)$$

whose $\hbar \rightarrow 0$ limit is ill-defined. We also clarify that the \star -exponential function \exp^* has appeared for the first time in Eq. (4.7); all exponentials so far have been the ordinary one. Namely, compare Eq. (4.7) with

$$\mathcal{Q}^{-1} \circ \text{Ad}_{\hat{S}} \circ \mathcal{Q} = \exp\left(X_{\chi^*}^*\right) = 1 + \sum_{n=1}^{\infty} \frac{1}{n!} (X_{\chi^*}^*)^n, \quad (4.8)$$

which describes the ordinary exponentiation of a differential operator $X_{\chi^*}^*$.

4.4 Impulse Formulae

We end with a remark on impulse formulae. The celebrated Kosower, Maybe, O'Connell formalism [22] provided a concrete framework for obtaining the impulse of classical observables from the S-matrix \hat{S} . The framework of S-symplectomorphism S , however, provides a purely classical implementation: the nested bracket formula due to Ref. [19], which also traces back to Refs. [23, 24]. Certainly, the analysis of this paper establishes how this classical framework is the faithful $\hbar \rightarrow 0$ limit of a quantum framework.

First of all, let us review Ref. [19]'s nested bracket formula:

$$\Delta[f] = \{f, \chi\} + \frac{1}{2!} \{\{f, \chi\}, \chi\} + \frac{1}{3!} \{\{\{f, \chi\}, \chi\}, \chi\} + \cdots. \quad (4.9)$$

This computes the impulse of a classical observable $f \in C^\infty(\mathcal{P})$ in classical scattering, in terms of the classical eikonal χ . Mathematically, Eq. (4.9) defines a differential operator $\Delta : C^\infty(\mathcal{P}) \rightarrow C^\infty(\mathcal{P})$ on phase-space functions which we may refer to as *classical impulse operator*. Geometrically, Eq. (4.9) can be rewritten as

$$\Delta[f] = (S^{-1})^*[f] - f = \sum_{n=1}^{\infty} \frac{1}{n!} (-X_\chi)^n[f], \quad (4.10)$$

where $(S^{-1})^*[f]$ in Eq. (4.10) computes the pullback of the function f by the map S^{-1} . Due to the very geometrical meaning of the S-symplectomorphism S , this is exactly the pullback of f from the *final* phase space to the *initial* phase space; hence $(S^{-1})^*[f] - f$ compute the impulse of f in classical scattering. Therefore, Eq. (4.10) provides a purely classical derivation of an impulse formula for classical observables on phase space.

Next, let us consider the impulse in quantum scattering. The Kosower, Maybe, O'Connell framework [22] identifies the impulse of an operator $\hat{f} \in \text{Ops}(\mathcal{H})$ as the adjoint action $\hat{S}^{-1} \hat{f} \hat{S} = \text{Ad}_{\hat{S}^{-1}}[\hat{f}]$. In the density matrix formulation of quantum mechanics, this is derived as follows. First, the expectation value of \hat{f} is found by taking the trace with the density matrix. Second, the S-matrix acts on the density matrix as the adjoint action $\text{Ad}_{\hat{S}}$. Third, this is translated to $\text{Ad}_{\hat{S}^{-1}}$ on the operator \hat{f} via the cyclic property of trace.

To carry out this derivation in the phase space formulation of quantum mechanics, one uses the identity that the trace of an operator \hat{f} equals the integral of $\mathcal{Q}^{-1}(\hat{f})$ over the entire phase space with respect to the Liouville measure μ , as is explored previously in Eqs. (2.27) and (2.39). Consequently, the phase space formulation computes the expectation value of a quantum observable $f \in C^\infty(\mathcal{P})$ by integrating its star product with the quasiprobability distribution over \mathcal{P} . In the scattering setup, the expectation value at far future is

$$\int \mu \tilde{\rho}(+\infty) \star f = \int \mu (S^*[\tilde{\rho}(-\infty)]) \star f = \int \mu \tilde{\rho}(-\infty) \star (S^{*-1}[f]), \quad (4.11)$$

where we have used Eqs. (3.15), (4.5), and the cyclic property of trace (recall Eq. (2.39)):

$$\int \mu \mathcal{Q}^{-1}(\hat{S}) \star \tilde{\rho}(-\infty) \star \mathcal{Q}^{-1}(\hat{S}^{-1}) \star f = \int \mu \tilde{\rho}(-\infty) \star \mathcal{Q}^{-1}(\hat{S}^{-1}) \star f \star \mathcal{Q}^{-1}(\hat{S}). \quad (4.12)$$

Therefore, the expectation value of f at far future equals the expectation value of $S^{*-1}[f]$ evaluated at far past, for any ensemble state $\tilde{\rho}(t)$ in the quantum interaction picture.

As a result, the impulse of a quantum observable $f \in C^\infty(\mathcal{P})$ can be defined independently of the smearing ensemble states as

$$\Delta^*[f] = S^{*-1}[f] - f = \sum_{n=1}^{\infty} \frac{1}{n!} (-X_{\chi^*}^*)^n[f], \quad (4.13)$$

which defines the *quantum impulse operator* $\Delta^* : C^\infty(\mathcal{P}) \rightarrow C^\infty(\mathcal{P})$. Note that $\tilde{\rho}(t)$ in Eqs. (4.11) and (4.12) is merely employed as a dummy object in this derivation. In terms of the quantum eikonal χ^* , it is convenient to utilize right actions to write Eq. (4.13) as

$$\Delta^*[f] = \{f, \chi^*\}^* + \frac{1}{2!} \{\{f, \chi^*\}^*, \chi^*\}^* + \frac{1}{3!} \{\{\{f, \chi^*\}^*, \chi^*\}^*, \chi^*\}^* + \dots \quad (4.14)$$

Certainly, Eq. (4.14) smoothly approaches to Eq. (4.9) in the $\hbar \rightarrow 0$ limit. In conclusion, we have shown that Ref. [19]'s classical impulse formula arises as the faithful $\hbar \rightarrow 0$ limit of the quantum impulse formula in the phase space formulation. In precise terms, we have established a yet another set of exact equalities about classical limit:

$$\text{Ad}_{\hat{S}^{-1}} - \text{id} \quad \xleftarrow{\text{equiv.}} \quad \Delta^* \quad \xrightarrow{\hbar \rightarrow 0} \quad \Delta. \quad (4.15)$$

The first arrow in Eq. (4.15) represents

$$(\text{Ad}_{\hat{S}^{-1}} - \text{id}) \circ \mathcal{Q} = \mathcal{Q} \circ \Delta^*, \quad (4.16)$$

which is implied by Eq. (4.5). The second arrow in Eq. (4.15) represents

$$\lim_{\hbar \rightarrow 0} \Delta^* = \lim_{\hbar \rightarrow 0} (S^{*-1} - \text{id}) = (S^{-1})^* - \text{id} = \Delta, \quad (4.17)$$

which is implied by Eq. (4.6).

Note that both Δ and Δ^* are differential operators acting on phase-space functions. Unlike Δ , however, Δ^* generates \hbar -dependencies in general even when acted on functions with no \hbar dependencies. Note also that nothing prevents one from implementing the Kosower, Maybe, O'Connell formalism [22] in the phase space formulation:

$$\hat{S} = \hat{1} - \frac{1}{i\hbar} \hat{T} \implies \Delta^*[f] = \{\mathcal{Q}^{-1}(\hat{T}), f\}^* + \frac{1}{i\hbar} \mathcal{Q}^{-1}(\hat{T}^\dagger) \star \{\mathcal{Q}^{-1}(\hat{T}), f\}^*. \quad (4.18)$$

The smoothness of classical limit, however, is not manifest in this approach. The so-called superclassical terms arise from each of $\{\mathcal{Q}^{-1}(\hat{T}), f\}^*$ and $\mathcal{Q}^{-1}(\hat{T}^\dagger) \star \{\mathcal{Q}^{-1}(\hat{T}), f\}^*/i\hbar$ while $\mathcal{Q}^{-1}(\hat{T}) = -\chi^* - \chi^* \star \chi^*/2i\hbar - \dots$ does not admit a nice classical limit as explored earlier in Sec. 4.3. In contrast, the adjoint actions in Eq. (4.14) describe a definite classical limit.

5 Quantum Eikonal from Magnus Expansion

The phase space formulation of classical and quantum scattering theory now stands well-established, by virtue of the analyses provided by Secs. 2, 3, and 4.

The eikonals χ and χ^* deserve a spotlight. They efficiently encapsulate the complete information about classical and quantum scattering as scalar functions on phase space, while also manifesting the conservation of probability via $S^* = \exp(X_\chi)$ and $S^* = \exp(X_{\chi^*}^*)$. Their explicit formulae are given by the Magnus expansions in Eqs. (3.11) and (3.21).

In this last section, we urge for a concrete understanding on the quantum eikonal χ^* in terms of its explicit evaluation. The key observation of this paper is that the formula in Eq. (3.21) simply \hbar -deforms each Poisson bracket in Eq. (3.11). This facilitates a principled approach for computing the quantum eikonal in a diagrammatic language.

In this paper, we limit our scope up to the third order in the Magnus expansion. Nevertheless, the loop order can be raised indefinitely thanks to the systematic formulation in terms of deformed Poisson brackets. Also, our approach straightforwardly applies to quantum field theory by taking an infinite-dimensional phase space, as shown in App. A.4.

For the reader's sake, the Magnus expansions in Eqs. (3.11) and (3.21) are reproduced below. The classical eikonal χ is given at each order as

$$\chi_{(1)} = \int dt_1 \tilde{V}(t_1), \quad (5.1a)$$

$$\chi_{(2)} = \frac{1}{2} \int_{t_1 > t_2} d^2t \{\tilde{V}(t_1), \tilde{V}(t_2)\}, \quad (5.1b)$$

$$\chi_{(3)} = \frac{1}{6} \int_{t_1 > t_2 > t_3} d^3t \left(\{\tilde{V}(t_1), \{\tilde{V}(t_2), \tilde{V}(t_3)\}\} + \{\tilde{V}(t_3), \{\tilde{V}(t_2), \tilde{V}(t_1)\}\} \right), \quad (5.1c)$$

while the quantum eikonal χ^* is given at each order as

$$\chi_{(1)}^* = \int dt_1 \tilde{V}(t_1), \quad (5.2a)$$

$$\chi_{(2)}^* = \frac{1}{2} \int_{t_1 > t_2} d^2t \{\tilde{V}(t_1), \tilde{V}(t_2)\}^*, \quad (5.2b)$$

$$\chi_{(3)}^* = \frac{1}{6} \int_{t_1 > t_2 > t_3} d^3t \left(\{\tilde{V}(t_1), \{\tilde{V}(t_2), \tilde{V}(t_3)\}^*\}^* + \{\tilde{V}(t_3), \{\tilde{V}(t_2), \tilde{V}(t_1)\}^*\}^* \right). \quad (5.2c)$$

5.1 Classical Eikonal

We begin by clarifying the foundations of our diagrammatic framework for Magnus expansion in phase space. Readers familiar with the work [20] can directly jump to Sec. 5.2.

Here, the geometrical premise is a Poisson manifold (\mathcal{P}, Π) equipped with coordinates ϕ^I . The coordinate derivative $\partial_I = \partial/\partial\phi^I$ is a differential operator that acts on functions $f \in C^\infty(\mathcal{P})$ as $\partial_I[f]$. The Poisson bracket is given by

$$\{f, g\} = \Pi^{IJ} \partial_I[f] \partial_J[g], \quad (5.3)$$

where $\Pi^{IJ} = -\Pi^{JI}$ are the components of the **Poisson tensor** Π . In symplectic manifolds, $\Pi^{IJ} = (\omega^{-1})^{IJ}$. For simplicity, we assume that Π^{IJ} are constants.

5.1.1 Tensor Graphs

A graphical representation of Eq. (5.3) is facilitated by utilizing the following two methods of visualization.

The first is the *differentiation balloon notation* of Penrose [66, 67], incorporated as a part in his renowned graphical notation [3, 4, 66, 67] for tensors. The coordinate derivative ∂_I is represented as a balloon whose tail describes the index I :

$$\partial_I [\quad] \quad \rightsquigarrow \quad \text{Diagram: a circle with a tail labeled } I \quad . \quad (5.4)$$

The Leibniz rule, $\partial_I[f g] = (\partial_I[f])g + f(\partial_I[g])$, is graphically represented as

$$\text{Diagram 1} = \text{Diagram 2} + \text{Diagram 3}, \quad (5.5)$$

where the triangle and diamond represent the scalar fields f and g , respectively. In Eq. (5.5), the explicit index I is omitted since it essentially serves as a dummy. The reader is encouraged to adopt—or invent—their preferred intuition for comprehending the visual rule in Eq. (5.5). For instance, one might imagine the balloon “digesting” each component, much like an enzyme acting on a molecular complex. In Ref. [20], the process is instead envisioned as “popping” the balloon like a bubble, thereby reducing it to smaller pieces.

The second is an *arrow representation for Poisson tensor*, which is an instance of bird-tracks [68] notation:

$$\Pi^{IJ} = -\Pi^{JI} \quad \rightsquigarrow \quad I \xleftarrow{} J = -I \xrightarrow{} J. \quad (5.6)$$

Here, the arrowhead is the symbol for Π , on which the two lines representing indices I, J are attached. Flipping the arrow simply changes the sign, encoding antisymmetry. In fact, Eq. (5.6) yields a simplification of the Kontsevich [37] graph notation for constant Π^{IJ} .

By incorporating the differentiation balloon in the birdtracks grammar, the Poisson bracket in Eq. (5.3) is graphically represented as

$$\{ , \} \rightsquigarrow \text{Diagram} , \quad (5.7)$$

where the arguments f and g will be inserted in the first and second slots/balloons. Index contraction means to glue the ends of two lines in the graphical notation [3, 4, 66–68].

Next, a graphical representation of the Magnus expansion in Eq. (5.1) is facilitated by introducing the following two rules. First, $\tilde{V}(t)$ is represented as a round blob with label t :

$$\tilde{V}(t) \rightsquigarrow \text{Diagram} . \quad (5.8)$$

Second, the phase-space derivatives of $\tilde{V}(t)$ are simply denoted as

$$\partial_I[\tilde{V}(t)] \rightsquigarrow \text{Diagram} = \text{Diagram} , \quad (5.9a)$$

$$\partial_J[\partial_I[\tilde{V}(t)]] \rightsquigarrow \text{Diagram} = \text{Diagram} , \quad (5.9b)$$

and so on. This essentially declares each n^{th} derivative of $\tilde{V}(t)$ as a new tensor in the graphical notation.

As a result, Eq. (5.1) is graphically represented as

$$\chi_{(1)} \rightsquigarrow \int dt_1 \left[\text{Diagram} \right] , \quad (5.10a)$$

$$\chi_{(2)} \rightsquigarrow \frac{1}{2} \int_{t_1 > t_2} dt^2 \left[\text{Diagram} \right] , \quad (5.10b)$$

$$\chi_{(3)} \rightsquigarrow \frac{1}{6} \int_{t_1 > t_2 > t_3} dt^3 \left[\text{Diagram} + \text{Diagram} \right] , \quad (5.10c)$$

where the nested Poisson brackets have turned into nested balloons.

5.1.2 Intermediate Form via Bubble Popping

Regarding explicit evaluation of Eq. (5.10), the nested brackets are fully expanded out in the purely diagrammatic language via the Leibniz rule in Eq. (5.5). This procedure might be dubbed *bubble popping*, following Ref. [20].

Take the first term in the integrand of Eq. (5.10c), for instance. The diagrammatic Leibniz rule in Eq. (5.5) is applied as

$$\text{Diagram} = \text{Diagram} + \text{Diagram} , \quad (5.11a)$$

which then boils down to

$$\text{Diagram with a circle around } t_2 \text{ and } t_3 = \text{Diagram with } t_1, t_2, t_3 \text{ in a row} + \text{Diagram with a loop from } t_1 \text{ to } t_3 \quad (5.11b)$$

by adopting the simplified notation proposed in Eq.(5.9). By adding the image under $t_1 \leftrightarrow t_3$ exchange, it is easy to see that $\chi_{(3)}$ in Eq.(5.1c) is brought to

$$\frac{1}{6} \int_{t_1 > t_2 > t_3} d^3t \left[\text{Diagram with two horizontal lines and a loop} + \text{Diagram with a vertex } t_1 \text{ branching to } t_2 \text{ and } t_3 + \text{Diagram with a triangle } t_1, t_2, t_3 \right], \quad (5.12)$$

which we name the *intermediate form* of $\chi_{(3)}$. Obtaining the intermediate form of $\chi_{(n)}$ means to expand out $n - 2$ nontrivially nested Poisson brackets by using the Leibniz rule in Eq.(5.5): “pop all balloons.” Via the abbreviation rule in Eq.(5.9), the outcome is represented as an integral whose integrand is a weighted sum of time-labeled graphs.

Generally speaking, this process may involve flipping some arrows via Eq.(5.6). Also, it should be clarified that the value of a diagram is left unchanged by planar isotopy:

$$\text{Diagram with a loop from } t_1 \text{ to } t_3 = \text{Diagram with a vertex } t_1 \text{ branching to } t_3 = \text{Diagram with a vertex } t_2 \text{ branching to } t_3 = \text{Diagram with a vertex } t_1 \text{ branching to } t_3 \quad . \quad (5.13)$$

5.1.3 Feynman Graphs

The graphical notation introduced above is a way of rewriting tensors. However, we eventually transition to the *Feynman graph notation* [69] where each edge is not merely a tensor (as numerator) but a propagator (as numerator with denominator).

The Heaviside step function is defined such that

$$\Theta(t_1, t_2) = \begin{cases} 1 & \text{if } t_1 > t_2, \\ 0 & \text{if } t_1 < t_2. \end{cases} \quad (5.14)$$

As explicated at length in App. A.4 for both particles and fields, the *retarded propagator* of the free theory arises by combining the Poisson tensor $\Pi^{I_1 I_2}$ (as Pauli-Jordan function) with the step function $\Theta(t_1, t_2)$. Based on this fact, an integral of a tensor graph is converted to a Feynman graph as

$$\int_{t_1 > t_2} d^2t \left[\text{Diagram with two horizontal lines} \right] = \int d^2t \left[\text{Diagram with two horizontal lines} \Theta(t_1, t_2) \right] = \text{Feynman graph} . \quad (5.15)$$

In a Feynman graph such as the last diagram in Eq.(5.15), the vertices are unlabeled since the times associated to them are dummy integration variables. Also, the edges are marked with a different kind of arrowhead to represent the retarded propagator.

5.1.4 Final Form via Freeing

By Eq. (5.15), the second-order eikonal $\chi_{(2)}$ in Eq. (5.10b) is brought to the *final form* as

$$\chi_{(2)} \quad \rightsquigarrow \quad \frac{1}{2} \bullet \text{---} \bullet \quad . \quad (5.16)$$

Obtaining the final form of the n^{th} -order eikonal $\chi_{(n)}$ means to represent it as a weighted sum of Feynman graphs where each edge describes the retarded propagator.

To obtain the final form of the third-order eikonal $\chi_{(3)}$, we recall its intermediate form obtained in Eq. (5.12). The first term in Eq. (5.12) is straightforwardly boiled down to a Feynman graph as

$$\int_{t_1 > t_2 > t_3} d^3 t \left[\begin{array}{c} \bullet \leftarrow \bullet \leftarrow \bullet \\ t_1 \quad t_2 \quad t_3 \end{array} \right] = \bullet \leftarrow \bullet \leftarrow \bullet \leftarrow \bullet \quad , \quad (5.17)$$

which repeats the exercise in Eq. (5.15).

However, a nontrivial gymnastics is required for the second term in Eq. (5.12). The Poisson tensors connect between times (t_1, t_2) and (t_1, t_3) , which do not align with the time ordering $t_1 > t_2 > t_3$ prescribed by the integration domain. Notably, this mismatch can be handled by symmetrizing over $t_2 \leftrightarrow t_3$ exchange via change of integration variables:³

$$\begin{aligned} & \int_{t_1 > t_2 > t_3} d^3 t \left[\begin{array}{c} \bullet \leftarrow \bullet \\ t_1 \quad t_2 \\ \quad \quad t_3 \end{array} \right] \\ &= \frac{1}{2} \int_{t_1 > t_2 > t_3} d^3 t \left[\begin{array}{c} \bullet \leftarrow \bullet \\ t_1 \quad t_2 \\ \quad \quad t_3 \end{array} \right] + \frac{1}{2} \int_{t_1 > t_3 > t_2} d^3 t \left[\begin{array}{c} \bullet \leftarrow \bullet \\ t_1 \quad t_3 \\ \quad \quad t_2 \end{array} \right], \quad (5.18) \\ &= \frac{1}{2} \int_{t_1 > t_2, t_1 > t_3} d^3 t \left[\begin{array}{c} \bullet \leftarrow \bullet \\ t_1 \quad t_2 \\ \quad \quad t_3 \end{array} \right] = \frac{1}{2} \bullet \leftarrow \bullet \leftarrow \bullet \quad . \end{aligned}$$

In the second equality, we have used a planar isotopy à la Eq. (5.13).

The gymnastics demonstrated in Eq. (5.18) will be referred to as the *freeing* operation, which induces a factor $1/2$ of a combinatorial origin. The inverse of this factor, 2 , will be referred to as the *freeing factor*.

As is explained in Ref. [20], the freeing factor is well-formulated in precise mathematical terms. The V-shaped graph in the first line of Eq. (5.18) defines a partial ordering between its time labels: $\{t_1 > t_2, t_1 > t_3\}$. This is relevant to its promotion to a Feynman graph: each retarded propagator encodes a step function, stipulating $t_1 > t_2$ and $t_1 > t_3$. On the other hand, the integral domain is given as a total ordering between t_1, t_2, t_3 . Crucially, there are two *linear extensions* of the partial ordering $\{t_1 > t_2, t_1 > t_3\}$ to a total ordering: $t_1 > t_2 > t_3$ and $t_1 > t_3 > t_2$. The freeing factor 2 is the number of such linear extensions.

³This gymnastics amounts to the identity $\Theta(t_1, t_2) \Theta(t_2, t_3) = \Theta(t_1, t_2) \Theta(t_2, t_3) + \Theta(t_1, t_2) \Theta(t_3, t_2)$.

5.1.5 Magnus Coefficient

Eventually, $\chi_{(1)}, \chi_{(2)}, \chi_{(3)}$ are found in the final form as

$$\chi_{(1)} \rightsquigarrow \bullet , \quad (5.19a)$$

$$\chi_{(2)} \rightsquigarrow \frac{1}{2} \bullet \bullet , \quad (5.19b)$$

$$\chi_{(3)} \rightsquigarrow \frac{1}{3} \bullet \bullet \bullet + \frac{1}{12} \bullet \bullet \bullet + \frac{1}{12} \bullet \bullet \bullet . \quad (5.19c)$$

In general, let us define that a *classical Magnus graph* is a connected directed acyclic graph with n vertices and zero loops. The final form of the n^{th} -order classical eikonal $\chi_{(n)}$ describes a weighted sum of such graphs:

$$\chi_{(n)} \rightsquigarrow \sum_{\mathcal{G} \in \text{Mag}(n,0)} \mu(\mathcal{G}) \mathcal{G} . \quad (5.20)$$

Here, $\text{Mag}(n,0)$ is the set of classical Magnus graphs with n vertices. In this way, each classical Magnus graph \mathcal{G} is assigned with a unique coefficient $\mu(\mathcal{G})$, which may be referred to as the *Magnus coefficient*. It holds generically true that $\mu(\mathcal{G}) = \mu(\mathcal{G}^\top)$, if \mathcal{G}^\top denotes the transpose of \mathcal{G} : the graph obtained from \mathcal{G} by reversing its orientation structure. This property is inherited from a \mathbb{Z}_2 symmetry in the Magnus expansion (see Eq. (3.11)).

With hindsight, it is helpful to multiply $\mu(\mathcal{G})$ by the symmetry factor $\sigma(\mathcal{G})$ of \mathcal{G} :

$$\omega(\mathcal{G}) = \mu(\mathcal{G}) \sigma(\mathcal{G}) , \quad (5.21)$$

which could be called *reduced Magnus coefficient*. For instance, Eq. (5.19) describes that

$$\begin{aligned} \omega(\bullet) &= 1, & \omega(\bullet \bullet \bullet) &= \frac{1}{3}, \\ \omega(\bullet \bullet) &= \frac{1}{2}, & \omega(\bullet \bullet \bullet) &= \omega(\bullet \bullet \bullet) = \frac{1}{6}. \end{aligned} \quad (5.22)$$

Note that some graphs do not contribute to the classical eikonal by having zero coefficient, as is substantiated at order $n = 4$:

$$\begin{aligned} \omega(\bullet \bullet \bullet \bullet) &= \frac{1}{4}, & \omega(\bullet \bullet \bullet \bullet) &= 0, \\ \omega(\bullet \bullet \bullet \bullet) &= \omega(\bullet \bullet \bullet \bullet) = \frac{1}{12}, & \omega(\bullet \bullet \bullet \bullet) &= \frac{1}{6}. \end{aligned} \quad (5.23)$$

Also, some graphs start to exhibit negative coefficients from order $n = 5$.

The coefficients of classical Magnus graphs have been well-studied. Ref. [20] shows that the reduced Magnus coefficient $\omega(\mathcal{G})$ generalizes a graph function previously defined by Murua [70] for rooted tree graphs (up to conventional sign factor $(-1)^{|\mathcal{G}|-1}$). In the Hopf-algebraic framework [71], $\omega(\mathcal{G})$ serves as an inverse to the graph function $e(\mathcal{G})$ in the antipode sense, where $e(\mathcal{G})$ is the freeing factor for \mathcal{G} divided by $|\mathcal{G}|!$.

5.2 Quantum Eikonal (Symmetric Ordering)

Provided the preliminary discussion in Sec. 5.1, this subsection computes the quantum eikonal for systems quantized with the Moyal star product.

Here, the geometrical premise is a linear Poisson manifold (\mathcal{P}, Π) . In terms of linear coordinates ϕ^I , the Moyal star product is defined as

$$f \star g = f \exp \left(\overleftarrow{\partial}_I \beta \Pi^{IJ} \overrightarrow{\partial}_J \right) g. \quad (5.24)$$

Then (\mathcal{P}, \star) is the quantization of the classical system (\mathcal{P}, Π) in a symmetric ordering prescription: Eq. (5.24) treats all coordinates ϕ^I on the same footing (is ignorant of polarization data). For brevity, we have desired to take the deformation parameter as

$$\beta = i\hbar/2. \quad (5.25)$$

Eq. (5.24) reproduces Eq. (2.25) for $\mathcal{P} = \mathbb{R}^2$ with $\Pi = \partial_x \wedge \partial_p$.

5.2.1 Graphical Notation

The deformed Poisson bracket due to the Moyal star product in Eq. (5.24) is

$$\sum_{k=0}^{\infty} \frac{\beta^{2k}}{(2k+1)!} \left(\partial_{I_1} [\dots \partial_{I_{2k+1}} [f]] \right) \Pi^{I_1 J_1} \dots \Pi^{I_{2k+1} J_{2k+1}} \left(\partial_{J_1} [\dots \partial_{J_{2k+1}} [g]] \right), \quad (5.26)$$

which reduces to Eq. (2.71) for $\mathcal{P} = \mathbb{R}^2$. For an intuitive diagrammatic representation, we introduce a fuzzy line as a new graphic element:

$$\{ , \}^* \rightsquigarrow \text{fuzzy line} \quad . \quad (5.27)$$

That is, the deformed Poisson bracket in Eq. (5.27) is literally the Poisson bracket in Eq. (5.7) *made fuzzy*. With this notation, Eq. (5.26) translates to

$$\begin{aligned} & \text{fuzzy line} \\ &= \text{fuzzy line} + \frac{\beta^2}{3!} \text{fuzzy line} + \frac{\beta^4}{5!} \text{fuzzy line} + \dots, \end{aligned} \quad (5.28)$$

whose right-hand side is a direct application of the graphical notation set up in Sec. 5.1.1.

For simplicity of our notation, we also regard that

$$\text{fuzzy line} \quad \text{means} \quad \text{fuzzy line}, \quad (5.29)$$

meaning that the balloon enclosing $\tilde{V}(t)$ can be omitted for fuzzy lines as well (cf. Eq. (5.9)).

With this understanding, Eq. (5.2) is graphically represented as

$$\chi_{(1)}^* \rightsquigarrow \int dt_1 \left[\begin{array}{c} \bullet \\ t_1 \end{array} \right], \quad (5.30a)$$

$$\chi_{(2)}^* \rightsquigarrow \frac{1}{2} \int_{t_1 > t_2} dt^2 t \left[\begin{array}{cc} \bullet & \bullet \\ t_1 & t_2 \end{array} \right], \quad (5.30b)$$

$$\chi_{(3)}^* \rightsquigarrow \frac{1}{6} \int_{t_1 > t_2 > t_3} dt^3 t \left[\begin{array}{ccc} \bullet & \bullet & \bullet \\ t_1 & t_2 & t_3 \end{array} \right] + \left[\begin{array}{ccc} \bullet & \bullet & \bullet \\ t_3 & t_2 & t_1 \end{array} \right]. \quad (5.30c)$$

Compare this with Eq. (5.10).

5.2.2 Evaluation

We now perform the diagrammatic evaluation of the quantum eikonal in Eq. (5.30). Once all fuzzy lines are unpacked into ordinary lines, the procedure takes two steps as before: bubble popping (Leibniz rule) and freeing (counting linear extensions).

The evaluation of Eqs. (5.30a) and (5.30b) is straightforward; hence we consider the third-order quantum eikonal in Eq. (5.30c).

To begin with, all the fuzzy lines must be unpacked via Eq. (5.28). The first term in the integrand of Eq. (5.30c), for instance, is unpacked as

$$\bullet \leftarrow \left(\begin{array}{c} \bullet \\ t_2 \\ t_3 \end{array} \right) + \frac{\beta^2}{3!} \left[\bullet \leftarrow \left(\begin{array}{c} \bullet \\ t_2 \\ t_3 \end{array} \right) + \bullet \leftarrow \left(\begin{array}{ccc} \bullet & \bullet \\ t_1 & t_2 & t_3 \end{array} \right) \right] + \mathcal{O}(\beta^4). \quad (5.31)$$

The $\mathcal{O}(\beta^0)$ part is of course the classical term evaluated in Eq. (5.11a). The $\mathcal{O}(\beta^2)$ part, on the other hand, describes the leading quantum contribution.

Next, we implement the bubble popping. For example, take the $\mathcal{O}(\beta^2)$ part of Eq. (5.31). There are two diagrams. By applying the Leibniz rule in Eq. (5.5), the first diagram is evaluated as

$$\bullet \leftarrow \left(\begin{array}{ccc} \bullet & \bullet & \bullet \\ t_1 & t_2 & t_3 \end{array} \right) + \left(\begin{array}{ccc} \bullet & \bullet & \bullet \\ t_1 & t_2 & t_3 \end{array} \right), \quad (5.32a)$$

whereas the second diagram is evaluated as

$$\left(\begin{array}{ccc} \bullet & \bullet & \bullet \\ t_1 & t_2 & t_3 \end{array} \right) + 3 \left(\begin{array}{ccc} \bullet & \bullet & \bullet \\ t_1 & t_2 & t_3 \end{array} \right) + 3 \left(\begin{array}{ccc} \bullet & \bullet & \bullet \\ t_1 & t_2 & t_3 \end{array} \right) + \left(\begin{array}{ccc} \bullet & \bullet & \bullet \\ t_1 & t_2 & t_3 \end{array} \right). \quad (5.32b)$$

Then the intermediate form of the third-order quantum eikonal at two loops is found via the sum of Eqs. (5.32a) and (5.32b) plus its image under $t_1 \leftrightarrow t_3$ exchange.

Finally, we implement the freeing. Take the sum of the last diagrams in Eqs. (5.32a) and (5.32b), for instance. Upon integration over the domain $t_1 > t_2 > t_3$, it is

$$\int_{t_1 > t_2 > t_3} d^3 t \left[\begin{array}{c} \text{Diagram with } t_1 \text{ at bottom, } t_2 \text{ in middle, } t_3 \text{ at top, with a loop from } t_1 \text{ to } t_3 \text{ and a loop from } t_2 \text{ to } t_3 \end{array} \right] + \int_{t_2 > t_1 > t_3} d^3 t \left[\begin{array}{c} \text{Diagram with } t_2 \text{ at top, } t_1 \text{ in middle, } t_3 \text{ at bottom, with a loop from } t_2 \text{ to } t_3 \text{ and a loop from } t_1 \text{ to } t_3 \end{array} \right], \quad (5.33)$$

where a change of integration variables is used. By using planar isotopy, Eq. (5.33) becomes

$$\int_{t_1 > t_3, t_2 > t_3} d^3 t \left[\begin{array}{c} \text{Diagram with } t_1 \text{ at top, } t_3 \text{ at bottom, and } t_2 \text{ in middle, with a loop from } t_1 \text{ to } t_3 \text{ and a loop from } t_2 \text{ to } t_3 \end{array} \right] = \text{Diagram with } t_1 \text{ at top, } t_3 \text{ at bottom, and } t_2 \text{ in middle, with a loop from } t_1 \text{ to } t_3 \text{ and a loop from } t_2 \text{ to } t_3. \quad (5.34)$$

From the calculations detailed above, it is not difficult to see that the final form of the third-order quantum eikonal $\chi_{(3)}^*$ at two loops describes the sum

$$\begin{aligned} \frac{\beta^2}{6} \text{Diagram with } t_1 \text{ at top, } t_3 \text{ at bottom, and } t_2 \text{ in middle, with a loop from } t_1 \text{ to } t_3 \text{ and a loop from } t_2 \text{ to } t_3} &+ \frac{\beta^2}{12} \text{Diagram with } t_1 \text{ at top, } t_3 \text{ at bottom, and } t_2 \text{ in middle, with a loop from } t_1 \text{ to } t_3 \text{ and a loop from } t_2 \text{ to } t_3} \\ &+ \frac{\beta^2}{18} \text{Diagram with } t_1 \text{ at top, } t_3 \text{ at bottom, and } t_2 \text{ in middle, with a loop from } t_1 \text{ to } t_3 \text{ and a loop from } t_2 \text{ to } t_3} + \frac{\beta^2}{36} \text{Diagram with } t_1 \text{ at top, } t_3 \text{ at bottom, and } t_2 \text{ in middle, with a loop from } t_1 \text{ to } t_3 \text{ and a loop from } t_2 \text{ to } t_3} \\ &+ \frac{\beta^2}{12} \text{Diagram with } t_1 \text{ at top, } t_3 \text{ at bottom, and } t_2 \text{ in middle, with a loop from } t_1 \text{ to } t_3 \text{ and a loop from } t_2 \text{ to } t_3} + \frac{\beta^2}{18} \text{Diagram with } t_1 \text{ at top, } t_3 \text{ at bottom, and } t_2 \text{ in middle, with a loop from } t_1 \text{ to } t_3 \text{ and a loop from } t_2 \text{ to } t_3} + \frac{\beta^2}{36} \text{Diagram with } t_1 \text{ at top, } t_3 \text{ at bottom, and } t_2 \text{ in middle, with a loop from } t_1 \text{ to } t_3 \text{ and a loop from } t_2 \text{ to } t_3. \end{aligned} \quad (5.35)$$

This concludes a demonstration for the diagrammatic evaluation of the quantum eikonal in Moyal quantization (symmetric ordering).

Crucially, Eq. (5.35) describes a collection of directed *acyclic* graphs. Cyclic graphs are forbidden since any chain of retarded propagators (step functions) evaluates to zero: they are incompatible with time ordering.

By working in the same fashion, it can be found that the third-order quantum eikonal $\chi_{(3)}^*$ describes the sum of the following two groups of terms:

$$\left(\begin{aligned} \frac{1}{3} \sum_{2|a, 2|b} \frac{\beta^{a+b-2}}{a!b!} \text{Diagram with } t_1 \text{ at top, } t_3 \text{ at bottom, and } t_2 \text{ in middle, with a loop from } t_1 \text{ to } t_3 \text{ and a loop from } t_2 \text{ to } t_3} &+ \frac{1}{12} \sum_{2|a} \frac{\beta^{2a-2}}{a!^2} \text{Diagram with } t_1 \text{ at top, } t_3 \text{ at bottom, and } t_2 \text{ in middle, with a loop from } t_1 \text{ to } t_3 \text{ and a loop from } t_2 \text{ to } t_3} \\ &+ \frac{1}{12} \sum_{2|a, 2|b, a \neq b} \frac{2\beta^{a+b-2}}{a!b!} \text{Diagram with } t_1 \text{ at top, } t_3 \text{ at bottom, and } t_2 \text{ in middle, with a loop from } t_1 \text{ to } t_3 \text{ and a loop from } t_2 \text{ to } t_3} \\ &+ \frac{1}{12} \sum_{2|a} \frac{\beta^{2a-2}}{a!^2} \text{Diagram with } t_1 \text{ at top, } t_3 \text{ at bottom, and } t_2 \text{ in middle, with a loop from } t_1 \text{ to } t_3 \text{ and a loop from } t_2 \text{ to } t_3} + \frac{1}{12} \sum_{2|a, 2|b, a \neq b} \frac{2\beta^{a+b-2}}{a!b!} \text{Diagram with } t_1 \text{ at top, } t_3 \text{ at bottom, and } t_2 \text{ in middle, with a loop from } t_1 \text{ to } t_3 \text{ and a loop from } t_2 \text{ to } t_3 \end{aligned} \right), \quad (5.36a)$$

$$\left(\frac{\beta^{a+b+c-2}}{6} \sum_{2|(a+b), 2|c} \frac{1}{a!b!c!} \text{Diagram with } t_1 \text{ at top, } t_3 \text{ at bottom, and } t_2 \text{ in middle, with a loop from } t_1 \text{ to } t_3 \text{ and a loop from } t_2 \text{ to } t_3 \right. \\ \left. + \frac{\beta^{a+b+c-2}}{3} \sum_{2|a, 2|b, 2|c} \frac{1}{a!b!c!} \text{Diagram with } t_1 \text{ at top, } t_3 \text{ at bottom, and } t_2 \text{ in middle, with a loop from } t_1 \text{ to } t_3 \text{ and a loop from } t_2 \text{ to } t_3 \right). \quad (5.36b)$$

Here, $a, b, c \geq 1$ are positive integers indicating the multiplicity of each edge. We have explicitly verified Eq. (5.36) up to $\ell = 101$ loops by numerical means.

The astute reader will point out that the first group of terms, Eq. (5.36a), simply equals the third-order classical eikonal $\chi_{(3)}$ in Eq. (5.19c) if all lines are promoted to fuzzy lines:

$$\text{Fuz}(\chi_{(3)}) \rightsquigarrow \frac{1}{3} \text{ (fuzzy line)} + \frac{1}{12} \text{ (fuzzy line)} + \frac{1}{12} \text{ (fuzzy line)} . \quad (5.37)$$

Let us recall to Eq. (5.37) as the *fuzzification* of $\chi_{(3)}$. In contrast, the second group of terms, Eq. (5.36b), does not arise in this way. Hence a qualitative difference is implied between Eqs. (5.36a) and (5.36b). At $\mathcal{O}(\beta^2)$, Eq. (5.37) reproduces the third and fourth columns in Eq. (5.35) but not the first and second columns.

In fact, we can consider the following noncommutative diagram.

$$\begin{array}{ccc} \text{Eq. (5.30)} & \xrightarrow{\text{unpack then pop bubbles}} & \chi_{(n)}^* \\ \uparrow \text{fuzzify} & & \uparrow \text{fuzzify} \\ \text{Eq. (5.10)} & \xrightarrow{\text{pop bubbles}} & \chi_{(n)} \end{array} \quad (5.38)$$

While $\chi_{(n)}^*$ is the desired answer for the quantum eikonal, $\text{Fuz}(\chi_{(n)})$ is what one obtains by replacing every edge in the final form of the classical eikonal $\chi_{(n)}$ with the fuzzy line. Crucially, we find $\chi_{(n)}^* \neq \text{Fuz}(\chi_{(n)})$ from $n = 3$.

The mismatch $\chi_{(n)}^* - \text{Fuz}(\chi_{(n)})$ precisely originates from the fact that the Leibniz rule in Eq. (5.5) does not apply for balloons attached with fuzzy lines, since Eq. (5.28) describe a collection of higher-derivative operators. Thus one must unpack all fuzzy lines to ordinary lines via Eq. (5.28) before initiating the bubble popping process, as is clarified at the beginning of Sec. 5.2.2. In other words, $\text{Fuz}(\chi_{(n)})$ is what one would get if the Leibniz rule is mistakenly applied for balloons attached with fuzzy lines.

5.2.3 Magnus-Moyal Coefficient

Let us define that a *Magnus graph of the first kind* is a connected directed acyclic graph. The final form of the n^{th} -order quantum eikonal $\chi_{(n)}^*$ in Moyal quantization is represented as a weighted sum of such graphs:

$$\chi_{(n)}^* \rightsquigarrow \sum_{\ell=0}^{\infty} \sum_{\mathcal{G} \in \text{Mag}(n, \ell)} \beta^\ell \mu_1(\mathcal{G}) \mathcal{G} , \quad (5.39)$$

where $\text{Mag}(n, \ell)$ is the set of Magnus graphs of the first kind with n vertices and ℓ loops. In this way, each $\mathcal{G} \in \text{Mag}(n, \ell)$ is assigned with a unique coefficient $\mu_1(\mathcal{G})$. This defines the *Magnus-Moyal coefficient* of \mathcal{G} .

From the property of the deformed Poisson bracket, it is immediate that this Magnus-Moyal coefficient coincides with the Magnus coefficient defined in Sec. 5.1.5 at zero loops: $\mu_1(\mathcal{G}) = \mu(\mathcal{G})$ if $\mathcal{G} \in \text{Mag}(n, 0)$. Another immediate fact is that $\mu_1(\mathcal{G}) = 0$ at odd loop orders: $2 \nmid \ell$. The \mathbb{Z}_2 symmetry $\mu(\mathcal{G}^\top) = \mu(\mathcal{G})$ continues to hold.

Again, it is desirable to work with *reduced Magnus-Moyal coefficient*:

$$\omega_1(\mathcal{G}) = \mu_1(\mathcal{G}) \sigma(\mathcal{G}). \quad (5.40)$$

For example, Eq. (5.36) describes that

$$\omega_1 \left(\begin{array}{c} a \quad b \\ \bullet - \bullet - \bullet \end{array} \right) = \omega \left(\begin{array}{c} \bullet - \bullet - \bullet \end{array} \right) \cdot \begin{cases} 1 & \text{if } a, b \text{ are both odd} \\ 0 & \text{otherwise} \end{cases}, \quad (5.41a)$$

$$\omega_1 \left(\begin{array}{c} a \\ \bullet \leftarrow \bullet \\ b \end{array} \right) = \omega \left(\begin{array}{c} \bullet \leftarrow \bullet \end{array} \right) \cdot \begin{cases} 1 & \text{if } a, b \text{ are both odd} \\ 0 & \text{otherwise} \end{cases}, \quad (5.41b)$$

$$\omega_1 \left(\begin{array}{c} a \quad b \\ \bullet \leftarrow \bullet \leftarrow \bullet \\ c \end{array} \right) = \begin{cases} 1/6 & \text{if } (a, b, c) \text{ is (odd,even,odd) or (even,odd,odd)} \\ 1/3 & \text{if } (a, b, c) \text{ is (odd,odd,even)} \\ 0 & \text{otherwise} \end{cases}, \quad (5.41c)$$

compactly summarizing all Magnus-Moyal coefficients at three vertices and all loops.

The equalities in Eqs. (5.41a) and (5.41b) encode our earlier observation that a part of $\chi_{(3)}^*$ simply recycles the classical eikonal $\chi_{(3)}$ via fuzzification. Hence Eq. (5.41c) describes the “genuinely quantum” part of $\chi_{(3)}^*$ that cannot be straightforwardly derived from $\chi_{(3)}$.

For a precise mathematical formulation, let $\text{Prim}(n, \ell)$ be the subset of $\text{Mag}(n, \ell)$ whose elements are simple. A graph is simple if it has at most one edge between any two vertices. Elements of $\text{Prim}(n, \ell)$ are called **primaries of the first kind**. Accordingly, $\mathcal{G} \in \text{Mag}(n, \ell)$ is a **descendant** of $\mathcal{G}_0 \in \text{Prim}(n, \ell_0)$ if \mathcal{G} arises by giving an edge multiplicity to \mathcal{G}_0 . The set of descendants of $\mathcal{G}_0 \in \text{Mag}(n, \ell_0)$ is denoted as $\text{Desc}(\mathcal{G}_0)$. For example,

$$\begin{array}{c} \text{Diagram of a complex graph with multiple edges between vertices} \end{array} \in \text{Desc} \left(\begin{array}{c} \bullet - \bullet - \bullet \\ \bullet \leftarrow \bullet \leftarrow \bullet \\ \bullet \end{array} \right). \quad (5.42)$$

Meanwhile, $\mathcal{G} \in \text{Mag}(n, \ell)$ is a **Moyal-descendant** of $\mathcal{G}_0 \in \text{Mag}(n, 0)$ if every edge multiplicity given to \mathcal{G}_0 for obtaining \mathcal{G} is odd. For example, Eq. (5.42) does not describe a Moyal descendant. Finally, $\mathcal{G} \in \text{Mag}(n, \ell)$ is **trivial** if it is a descendant of a classical Magnus graph: $\mathcal{G} \in \text{Desc}(\mathcal{G}_0)$ for $\mathcal{G}_0 \in \text{Mag}(n, 0)$. $\mathcal{G} \in \text{Mag}(n, \ell)$ is **nontrivial** if it is not trivial. Fuzzification Fuz is a linear map that outputs a weighted sum of trivial Moyal-descendants.

With these definitions, it can be shown for any n that

$$\chi_{(n)}^* - \text{Fuz}(\chi_{(n)}) \rightsquigarrow \sum_{k=1}^{\infty} \sum_{\substack{\mathcal{G} \in \text{Mag}(n, 2k) \\ \text{nontrivial}}} \beta^{2k} \cdot \frac{\omega_1(\mathcal{G})}{\sigma(\mathcal{G})} \mathcal{G}, \quad (5.43)$$

from which Eqs. (5.41a) and (5.41b) follow as

$$\mathcal{G} \text{ trivial Moyal-descendant of } \mathcal{G}_0 \implies \omega_1(\mathcal{G}) = \omega(\mathcal{G}_0), \quad (5.44a)$$

$$\mathcal{G} \text{ trivial but not Moyal-descendant} \implies \omega_1(\mathcal{G}) = 0. \quad (5.44b)$$

Thus, it suffices to determine the coefficients of nontrivial graphs. At $n = 3$, the triangle in Eq. (5.41c) is the only topology of a nontrivial primary. At $n = 4$, there are four topologies with one (\diamond , \blacktriangleleft), two (\blacktriangleright), and three (\blacklozenge) loops when orientation is ignored. At $n = 5$, there are 18 such topologies.

5.3 Quantum Eikonal (Normal Ordering)

Finally, this subsection computes the quantum eikonal for systems quantized with the Wick star product, such as quantum field theories.

Here, the geometrical premise is a Kähler vector space or a suitable generalization. This is a linear Poisson manifold (\mathcal{P}, Π) endowed with a rank-two tensor $W = W^{IJ} \partial_I \otimes \partial_J$, which we call the *Wightman tensor*. Importantly, it is related to the Poisson tensor as

$$\frac{1}{i} (W^{IJ} - W^{JI}) = \Pi^{IJ}. \quad (5.45)$$

We suppose linear coordinates ϕ^I such that the components W^{IJ} are constants. The Wick star product is defined as

$$f \star g = f \exp \left(\overleftarrow{\partial}_I \hbar W^{IJ} \overrightarrow{\partial}_J \right) g. \quad (5.46)$$

Eq. (5.46) reproduces Eq. (2.66) for $\mathcal{P} \cong \mathbb{C}^1$ by taking $W = \partial_a \otimes \partial_{\bar{a}}$, which shows that the physical content of the Wightman tensor is the very Wick contraction between a and \bar{a} . See App. A.3 for more details on the mathematical setup of this subsection.

5.3.1 Graphical Notation

We shall begin by constructing the graphical notation for Wick star product. As in Sec. 5.1, we start with tensor graphs and then transition to Feynman graphs.

The Wightman tensor will be represented as a red line:

$$W^{IJ} \quad \rightsquigarrow \quad I \xrightarrow{\text{red}} J. \quad (5.47)$$

The Wightman tensor does not exhibit any index symmetry. Eq. (5.45) translates to

$$\frac{1}{i} (\xleftarrow{\text{red}} - \xrightarrow{\text{red}}) = \xleftarrow{\text{black}}. \quad (5.48)$$

The Wick star product in Eq. (5.46) then describes

$$f \star g \quad \rightsquigarrow \quad \blacktriangle \blacklozenge + \frac{\hbar^1}{1!} \blacktriangle \xleftarrow{\text{red}} \blacklozenge + \frac{\hbar^2}{2!} \blacktriangle \circlearrowleft \blacklozenge + \frac{\hbar^3}{3!} \blacktriangle \circlearrowright \blacklozenge + \mathcal{O}(\hbar^4). \quad (5.49)$$

Here, the weights $1/1!, 1/2!, 1/3!, \dots$ serve as symmetry factors for edge multiplicity.

The deformed Poisson bracket $\{f, g\}^*$ due to the Wick star product in Eq. (5.46) is

$$\frac{1}{i} \sum_{\ell=0}^{\infty} \frac{\hbar^\ell}{(\ell+1)!} \left(\partial_{I_1} [\dots \partial_{I_{\ell+1}} [f]] \right) \left(\begin{matrix} W^{I_1 J_1} \dots W^{I_{\ell+1} J_{\ell+1}} \\ -W^{J_1 I_1} \dots W^{J_{\ell+1} I_{\ell+1}} \end{matrix} \right) \left(\partial_{J_1} [\dots \partial_{J_{\ell+1}} [g]] \right), \quad (5.50)$$

which reduces to Eq. (2.70) for $\mathcal{P} = \mathbb{C}^1$. In the graphical notation, Eq. (5.50) translates to

$$\frac{1}{i} (\blacktriangle \xleftarrow{\text{red}} \blacklozenge - \blacktriangle \xrightarrow{\text{red}} \blacklozenge) + \frac{\hbar}{2!i} (\blacktriangle \circlearrowleft \blacklozenge - \blacktriangle \circlearrowright \blacklozenge) + \frac{\hbar^2}{3!i} (\blacktriangle \circlearrowright \blacklozenge - \blacktriangle \circlearrowleft \blacklozenge) + \mathcal{O}(\hbar^4). \quad (5.51)$$

Physically, Eq. (5.51) visualizes the pings and pongs of quantum excitations exchanged between f and g .

As a bi-differential operator, the deformed Poisson bracket $\{ \cdot, \cdot \}^*$ is represented as

$$\begin{aligned}
 \text{Diagram: Two circles connected by a wavy line} &= \frac{1}{i} \left[\text{Diagram: Two circles connected by a red double line} - \text{Diagram: Two circles connected by a blue double line} \right] \\
 &+ \frac{\hbar}{2!i} \left[\text{Diagram: Two circles connected by a red triple line} - \text{Diagram: Two circles connected by a blue triple line} \right] \\
 &+ \frac{\hbar^2}{3!i} \left[\text{Diagram: Two circles connected by a red quadruple line} - \text{Diagram: Two circles connected by a blue quadruple line} \right] \\
 &+ \mathcal{O}(\hbar^3),
 \end{aligned} \tag{5.52}$$

where we have employed the notation in Eq. (5.27) again.

Surely, the diagrammatic Leibniz rule in Eq. (5.5) applies to balloons attached to red lines. The Magnus expansion for the quantum eikonal is again given by Eq. (5.30), yet with the definition in Eq. (5.52).

Lastly, we describe the transition to Feynman graphs. As is explicated at length for both particles and fields in App. A.4, the **positive-frequency retarded propagator** arises by combining the Wightman tensor $W^{I_1 I_2}$ (as Wightman function) with the step function $\Theta(t_1, t_2)$. The positive-frequency retarded propagator is represented as a red arrow:

$$\text{Diagram: Two circles connected by a red arrow} = \int d^2t \partial_{I_1}[\tilde{V}(t_1)] \left(W^{I_1 I_2} \Theta(t_1, t_2) \right) \partial_{I_2}[\tilde{V}(t_2)]. \tag{5.53a}$$

Similarly, the **negative-frequency retarded propagator** arises by combining the transposed Wightman tensor $W^{I_2 I_1}$ with the step function $\Theta(t_1, t_2)$. The negative-frequency retarded propagator is represented as a blue arrow:

$$\text{Diagram: Two circles connected by a blue arrow} = \int d^2t \partial_{I_1}[\tilde{V}(t_1)] \left(W^{I_2 I_1} \Theta(t_1, t_2) \right) \partial_{I_2}[\tilde{V}(t_2)]. \tag{5.53b}$$

To clarify, these are exactly the positive- and negative-frequency parts of the retarded propagator defined in Sec. 5.1.3, up to customary $\pm i$ factors:

$$\text{Diagram: Two circles connected by a black arrow} = -i \text{ (Diagram: Two circles connected by a red arrow)} + i \text{ (Diagram: Two circles connected by a blue arrow)}. \tag{5.54}$$

To be explicit, the retarded propagator is

$$\text{Diagram: Two circles connected by a black arrow} = \int d^2t \partial_{I_1}[\tilde{V}(t_1)] \left(\Pi^{I_1 I_2} \Theta(t_1, t_2) \right) \partial_{I_2}[\tilde{V}(t_2)]. \tag{5.55}$$

A crucial feature of the quantum eikonal is that it cannot be represented solely in terms of the retarded propagator in Eq. (5.55), unlike as in the classical case. Namely, the retarded propagator must resolve into more fundamental building blocks, Eqs. (5.53a) and (5.53b).

Note that the colors red and blue indicate whether the index flow in the Wightman tensor aligns with the time flow in the step function. In Eq. (5.53a), they are aligned as $I_1 \leftarrow I_2$ and $t_1 \leftarrow t_2$. In Eq. (5.53b), they are anti-aligned as $I_1 \rightarrow I_2$ and $t_1 \leftarrow t_2$. In fact, this analysis reveals that there lie two independent notions of ordering in our graphical notation: *operator ordering* and *time ordering*. This point will be revisited several times.

Finally, the counterpart of Eq. (5.15) is

$$\int_{t_1 > t_2} d^2t \left[\begin{array}{cc} \bullet & \bullet \\ t_1 & t_2 \end{array} \right] = \int d^2t \left[\begin{array}{cc} \bullet & \bullet \\ t_1 & t_2 \end{array} \right] \Theta(t_1, t_2) = \bullet \xrightarrow{\text{red}} \bullet, \quad (5.56a)$$

$$\int_{t_1 > t_2} d^2t \left[\begin{array}{cc} \bullet & \bullet \\ t_1 & t_2 \end{array} \right] = \int d^2t \left[\begin{array}{cc} \bullet & \bullet \\ t_1 & t_2 \end{array} \right] \Theta(t_1, t_2) = \bullet \xleftarrow{\text{blue}} \bullet. \quad (5.56b)$$

Here, the arrows put on the tensor graphs represent the propagating direction of quantum excitations: the index flow of Wightman tensors. On the other hand, the arrows put on the Feynman graphs represent the time direction: the time flow stipulated by step functions.

5.3.2 Evaluation

We now perform the diagrammatic evaluation of the quantum eikonal in Eq. (5.30) by using the deformed Poisson bracket in Eq. (5.52).

The computation is trivial at orders $n = 1$ and $n = 2$. In particular, $\chi_{(2)}^*$ is found as

$$\frac{1}{2i} \left(\bullet \xrightarrow{\text{red}} \bullet - \bullet \xleftarrow{\text{blue}} \bullet \right) + \frac{\hbar}{4i} \left(\bullet \circlearrowleft \bullet - \bullet \circlearrowright \bullet \right) + \mathcal{O}(\hbar^3) = \frac{1}{2} \bullet \text{---} \bullet. \quad (5.57)$$

Again, fuzzification reproduces the entire answer at this order: $\chi_{(2)}^* = \text{Fuz}(\chi_{(2)})$. Hence it suffices to focus on the third-order quantum eikonal, $\chi_{(3)}^*$. The procedure is very much the same as in Sec. 5.2.2: unpacking, bubble popping, and freeing. Yet, the process can be streamlined a bit more by recalling the lessons learned in Secs. 5.2.2 and 5.2.3.

We begin with unpacking. The counterpart of Eq. (5.31) is given by

$$\begin{aligned} \bullet \text{---} \bullet &= \bullet \xleftarrow{\text{---}} \bullet \\ &+ \frac{\hbar}{2i^2} \left[\begin{array}{c} \bullet \xleftarrow{\text{---}} \bullet + \bullet \xrightarrow{\text{---}} \bullet \\ - \bullet \xleftarrow{\text{---}} \bullet - \bullet \xrightarrow{\text{---}} \bullet \\ + \dots \end{array} \right] \\ &+ \mathcal{O}(\hbar^2), \end{aligned} \quad (5.58)$$

where the one-loop part describes a sum of eight terms.

Next, we demonstrate the bubble popping at one loop. Due to the lessons in Secs. 5.2.2 and 5.2.3, we expect that the result will be classified into three categories: linear (L), V-shaped (V), and triangle (T). Regarding this point, the first and second columns in the

bracketed group of terms in Eq. (5.58) play different roles:

$$\begin{array}{c} \text{Diagram 1: } t_1 \xrightarrow{\text{red}} \text{circle } t_2 \xrightarrow{\text{red}} t_3 \\ \text{Diagram 2: } t_1 \xrightarrow{\text{red}} t_2 \xrightarrow{\text{red}} t_3 \end{array} - \dots \rightarrow \text{L, V categories ,} \quad (5.59\text{a})$$

$$\begin{array}{c} \text{Diagram 1: } t_1 \xrightarrow{\text{red}} \text{circle } t_2 \xrightarrow{\text{red}} t_3 \\ \text{Diagram 2: } t_1 \xleftarrow{\text{red}} t_2 \xrightarrow{\text{red}} t_3 \end{array} - \dots \rightarrow \text{L, T categories .} \quad (5.59\text{b})$$

With the expectation that the T category of diagrams will be only of a genuine interest, we extract the triangle diagrams from Eq. (5.59b). The result is the sum

$$+ \begin{array}{c} \text{Diagram 1: } t_1 \xrightarrow{\text{red}} t_2 \xrightarrow{\text{red}} t_3 \\ \text{Diagram 2: } t_1 \xrightarrow{\text{red}} t_2 \xrightarrow{\text{red}} t_3 \\ \text{Diagram 3: } t_1 \xrightarrow{\text{red}} t_2 \xrightarrow{\text{red}} t_3 \\ \text{Diagram 4: } t_1 \xrightarrow{\text{red}} t_2 \xrightarrow{\text{red}} t_3 \end{array} - \dots + \dots , \quad (5.60)$$

multiplied by an overall coefficient 2.

Crucially, the graphs in Eq. (5.60) are all *acyclic*, even though a loop is formed. This is because the very structure of the Wick star product (normal ordering) strictly forbids exchanging quantum excitations in a cycle. We shall remind ourselves that our graphical calculus have been computing operator products in essence, which describe one-dimensional arrays (strings) of objects. For instance, the third triangle diagram in Eq. (5.60) arises as

$$\langle 0 | \hat{V}(t_2) \hat{V}(t_3) \hat{V}(t_1) | 0 \rangle \sim \langle 0 | \begin{array}{c} \text{Diagram 3: } t_1 \xrightarrow{\text{red}} t_2 \xrightarrow{\text{red}} t_3 \\ \text{Diagram 4: } t_1 \xrightarrow{\text{red}} t_2 \xrightarrow{\text{red}} t_3 \\ \text{Diagram 5: } t_1 \xrightarrow{\text{red}} t_2 \xrightarrow{\text{red}} t_3 \end{array} | 0 \rangle , \quad (5.61)$$

which clearly shows that a cycle cannot occur. The red lines are the Wick contractions; the directions of arrows are pulled back from the ordering for a linear array of operators.

With this remark made, we find the image of Eq. (5.60) under $t_1 \leftrightarrow t_3$ exchange. Using planar isotopy, it boils down to

$$+ \begin{array}{c} \text{Diagram 1: } t_1 \xrightarrow{\text{red}} t_2 \xrightarrow{\text{red}} t_3 \\ \text{Diagram 2: } t_1 \xrightarrow{\text{red}} t_2 \xrightarrow{\text{red}} t_3 \\ \text{Diagram 3: } t_1 \xrightarrow{\text{red}} t_2 \xrightarrow{\text{red}} t_3 \\ \text{Diagram 4: } t_1 \xrightarrow{\text{red}} t_2 \xrightarrow{\text{red}} t_3 \end{array} - \dots - \dots + \dots . \quad (5.62)$$

Eventually, the sum of Eqs. (5.60) and (5.62) derives that the triangle contribution to the intermediate form of $\chi_{(3)}^*$ at one loop is given by the integration of the following over the domain $t_1 > t_2 > t_3$. Incorporating the overall coefficient 1/6 in Eq. (5.30c), we find

$$\frac{\hbar}{6i^2} \left(\begin{array}{c} \text{Diagram 1: } t_1 \xrightarrow{\text{red}} t_2 \xrightarrow{\text{red}} t_3 \\ \text{Diagram 2: } t_1 \xrightarrow{\text{red}} t_2 \xrightarrow{\text{red}} t_3 \\ \text{Diagram 3: } t_1 \xrightarrow{\text{red}} t_2 \xrightarrow{\text{red}} t_3 \\ \text{Diagram 4: } t_1 \xrightarrow{\text{red}} t_2 \xrightarrow{\text{red}} t_3 \end{array} + 2 \begin{array}{c} \text{Diagram 1: } t_1 \xrightarrow{\text{red}} t_2 \xrightarrow{\text{red}} t_3 \\ \text{Diagram 2: } t_1 \xrightarrow{\text{red}} t_2 \xrightarrow{\text{red}} t_3 \\ \text{Diagram 3: } t_1 \xrightarrow{\text{red}} t_2 \xrightarrow{\text{red}} t_3 \\ \text{Diagram 4: } t_1 \xrightarrow{\text{red}} t_2 \xrightarrow{\text{red}} t_3 \end{array} - \dots - \dots - \dots - \dots \right) . \quad (5.63)$$

Finally, we transition to Feynman graphs. For triangles, there is no room for freeing since the retarded propagators will completely resolve the ordering between vertices. Hence the triangle contribution to the final form of $\chi_{(3)}^*$ is found as

$$\begin{aligned} & \frac{\hbar}{3i^2} \left(\begin{array}{c} \text{Diagram 1: } \text{triangle with red edges} \\ \text{Diagram 2: } \text{triangle with blue edges} \end{array} \right) \\ & - \frac{\hbar}{6i^2} \left(\begin{array}{c} \text{Diagram 3: } \text{triangle with red edges} \\ \text{Diagram 4: } \text{triangle with blue edges} \\ \text{Diagram 5: } \text{triangle with red edges} \\ \text{Diagram 6: } \text{triangle with blue edges} \end{array} \right), \end{aligned} \quad (5.64)$$

while computation shows that every L or V term arises from the fuzzification $\text{Fuz}(\chi_{(3)})$.

This concludes a demonstration for the diagrammatic evaluation of the quantum eikonal in Wick quantization (normal ordering). By working in the same fashion, it can be found that the final form of $\chi_{(3)}^*$ is given by

$$\begin{aligned} & \left(\frac{1}{3} \text{Diagram 7: } \text{horizontal wavy line} + \frac{1}{12} \text{Diagram 8: } \text{wavy line with two vertices} + \frac{1}{12} \text{Diagram 9: } \text{wavy line with two vertices} \right) \\ & + \sum_{a,b,c} \frac{\hbar^{a+b+c-2}}{3i^2 a! b! c!} \left(\begin{array}{c} \text{Diagram 10: } \text{triangle with red edges} \\ \text{Diagram 11: } \text{triangle with blue edges} \end{array} \right) \\ & - \sum_{a,b,c} \frac{\hbar^{a+b+c-2}}{6i^2 a! b! c!} \left(\begin{array}{c} \text{Diagram 12: } \text{triangle with red edges} \\ \text{Diagram 13: } \text{triangle with blue edges} \\ \text{Diagram 14: } \text{triangle with red edges} \\ \text{Diagram 15: } \text{triangle with blue edges} \end{array} \right), \end{aligned} \quad (5.65)$$

where $a, b, c \geq 1$ are positive integers indicating the multiplicity of each edge. Note that the trivial and nontrivial parts due to fuzzification are cleanly split. We have explicitly verified Eq. (5.65) up to $\ell = 22$ loops by numerical means.

5.3.3 Magnus-Wick Coefficient

In Sec. 5.1.5, we defined classical Magnus graphs as connected directed acyclic graphs with zero loops. In fact, a classical Magnus graph $\mathcal{G} \in \text{Mag}(n, 0)$ can be regarded as a pair $\mathcal{G} = (\mathcal{X}, \rightarrow_T)$. \mathcal{X} is a connected unoriented graph with no loops, while \rightarrow_T is an acyclic orientation structure on \mathcal{X} . The orientation structure \rightarrow_T defines a partial ordering between the vertices of \mathcal{G} , which encodes time ordering.

In Sec. 5.2.3, we defined Magnus graphs of the first kind as connected directed acyclic graphs. In fact, a Magnus graph of the first kind $\mathcal{G} \in \text{Mag}(n, \ell)$ can be regarded as a pair $\mathcal{G} = (\mathcal{X}, \rightarrow_T)$. \mathcal{X} is a connected unoriented graph, while \rightarrow_T is an acyclic orientation structure on \mathcal{X} . The orientation structure \rightarrow_T defines a partial ordering between the vertices of \mathcal{G} , which encodes time ordering.

Here, let us define that a **Magnus graph of the second kind** is a pair $\mathcal{G} = (\mathcal{X}, \rightarrow_T, \rightarrow_O)$. \mathcal{X} is a connected unoriented graph, while \rightarrow_T and \rightarrow_O are two independent acyclic orientation structures on \mathcal{X} . Physically, \rightarrow_T encodes the **time ordering** whereas \rightarrow_O encodes

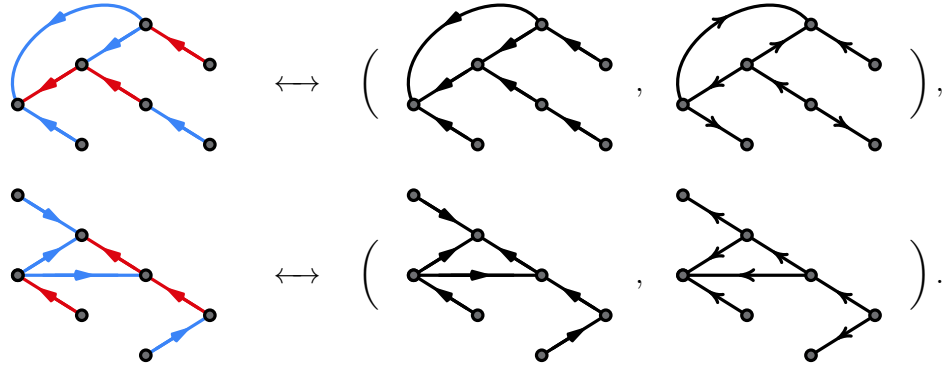


Figure 3. The bichrome notation for doubly directed graphs stands as a technique of visualization that aims to efficiently display two orientation structures within a single diagram. In this figure, the same $\mathcal{G} \in \text{Mag}^2(7, 1)$ is drawn, while emphasizing the time ordering \rightarrow_T (first row) or the operator ordering \rightarrow_O (second row).

$$\begin{aligned}
 G_{\text{retarded}}^+ &= \int d^2t \partial_{I_1}[\tilde{V}(t_1)] \left(\begin{array}{c} W \\ I_1 \quad I_2 \end{array} \times \begin{array}{c} \Theta \\ t_1 \quad t_2 \end{array} \right) \partial_{I_2}[\tilde{V}(t_2)] = \text{“ } \bullet \leftarrow \bullet \text{”} \\
 G_{\text{retarded}}^- &= \int d^2t \partial_{I_1}[\tilde{V}(t_1)] \left(\begin{array}{c} W \\ I_1 \quad I_2 \end{array} \times \begin{array}{c} \Theta \\ t_1 \quad t_2 \end{array} \right) \partial_{I_2}[\tilde{V}(t_2)] = \text{“ } \bullet \rightarrow \bullet \text{”}
 \end{aligned}$$

Figure 4. A graphical representation of Eqs. (5.53a) and (5.53b). Ideally, we would have drawn two arrows per each edge to visualize a doubly directed graph.

the *operator ordering*. The set of Magnus graphs of the second kind with n vertices and ℓ loops will be denoted as $\text{Mag}^2(n, \ell)$.

The presence of an additional orientation structure \rightarrow_O in Magnus graphs of the second kind traces back to the fact that Wick quantization (normal ordering) has demanded polarization as an additional geometric structure on the phase space. Moyal quantization (symmetric ordering), in contrast, stipulates no such structure. Physically, Moyal quantization employs a symmetric propagator between quantum fluctuations, sensitive only to time ordering. For Wick quantization, however, one additionally needs to specify which end is a (annihilation) and which end is \bar{a} (creation) when contracting quantum fluctuations.

To understand why and how our notation for Feynman graphs in Secs. 5.3.1 and 5.3.2 has described Magnus graphs of the second kind, recall the remark in Sec. 5.3.1 that the index flow due to the Wightman tensor W^{IJ} and the time ordering due to the step functions in the retarded propagators define separate acyclic orientations. Recall also Eq. (5.61) to understand how the index flow of the Wightman tensor describes the propagating direction of quantum fluctuations.

To be explicit about these points, we have provided an example of the breakdown

$\mathcal{G} = (\mathcal{X}, \rightarrow_T, \rightarrow_O)$ in Fig. 3. Also, in Fig. 4, we have shown the explicit equivalence between the bichrome notation we have been employing and the implementation of Magnus graphs of the second kind as doubly directed acyclic graphs.

The final form of the n^{th} -order quantum eikonal $\chi_{(n)}^*$ in Wick quantization describes a weighted sum of Magnus graphs of the second kind:

$$\chi_{(n)}^* \rightsquigarrow \sum_{\ell=0}^{\infty} \sum_{\mathcal{G} \in \text{Mag}^2(n, \ell)} \frac{\hbar^\ell}{i^{n-1}} \mu_2(\mathcal{G}) \mathcal{G}. \quad (5.66)$$

In this way, each $\mathcal{G} \in \text{Mag}^2(n, \ell)$ is assigned with a unique coefficient $\mu_2(\mathcal{G})$, which defines the **Magnus-Wick coefficient** of \mathcal{G} .

Again, it is desirable to define **reduced Magnus-Wick coefficient**:

$$\omega_2(\mathcal{G}) = \mu_2(\mathcal{G}) \sigma(\mathcal{G}). \quad (5.67)$$

Of course, the symmetry factor $\sigma(\mathcal{G})$ concerns both \rightarrow_T and \rightarrow_O . Eq. (5.65) boils down to

$$\omega_2 \left(\begin{array}{c} a \\ \bullet \cdots \bullet \\ b \end{array} \right) = \omega \left(\begin{array}{c} \bullet \cdots \bullet \\ \bullet \end{array} \right) \cdot \begin{cases} +1 & \text{if monochrome} \\ -1 & \text{otherwise} \end{cases}, \quad (5.68a)$$

$$\omega_2 \left(\begin{array}{c} a \\ \bullet \\ b \end{array} \right) = \omega_2 \left(\begin{array}{c} a \\ \bullet \\ b \end{array} \right) = \omega \left(\begin{array}{c} \bullet \\ \bullet \\ \bullet \end{array} \right) \cdot \begin{cases} +1 & \text{if monochrome} \\ -1 & \text{otherwise} \end{cases}, \quad (5.68b)$$

$$\omega_2 \left(\begin{array}{c} a \\ \bullet \\ b \\ c \end{array} \right) = \begin{cases} 1/3 & \text{if monochrome} \\ -1/6 & \text{otherwise} \end{cases}, \quad (5.68c)$$

where a, b, c are edge multiplicities. To clarify, the arguments of ω_2 in Eq. (5.68) are meant to be colored with red and blue. That is, we have stipulated only the time ordering \rightarrow_T on the left-hand side.

It should be clear that $\mathcal{G} = (\mathcal{X}, \rightarrow_T, \rightarrow_O) \in \text{Mag}^2(n, \ell)$ is **monochrome** iff $\rightarrow_T = \pm \rightarrow_O$. Specifically, \mathcal{G} is **monochrome red** iff $\rightarrow_T = + \rightarrow_O$ and **monochrome blue** iff $\rightarrow_T = - \rightarrow_O$.

It should be also clear that a multiplied edge in any Magnus graph must have the same orientation structure due to the acyclicity condition. In particular, the same color must be shared to qualify as a Magnus graph of the second kind:

$$\begin{array}{c} \bullet \\ \bullet \\ \bullet \end{array} \notin \text{Mag}^2(3, 1), \quad \begin{array}{c} \bullet \\ \bullet \\ \bullet \end{array} \notin \text{Mag}^2(3, 3), \quad \dots. \quad (5.69)$$

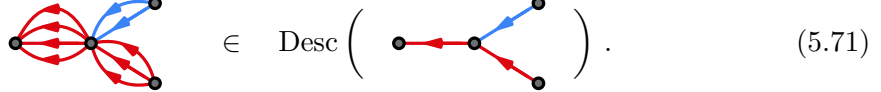
On a related note, only six coloring schemes exist for the triangle diagrams in Eq. (5.68c). The forbidden cases are

$$\begin{array}{c} a \\ \bullet \\ b \\ c \end{array}, \quad \begin{array}{c} a \\ \bullet \\ b \\ c \end{array}. \quad (5.70)$$

The allowed cases are shown in Eq. (5.65).

Eq. (5.68) provides a compact summary of the Magnus-Wick coefficients at three vertices and all loops. Again, the equalities in Eqs. (5.68a) and (5.68b) reflect the fact that a part of $\chi_{(3)}^*$ simply recycles the classical eikonal $\chi_{(3)}$ via fuzzification as stated in Eq. (5.65).

For a precise mathematical formulation of this observation, let $\text{Prim}^2(n, \ell)$ be the subset of $\text{Mag}^2(n, \ell)$ whose elements are simple. Elements of $\text{Prim}^2(n, \ell)$ are called *primaries of the second kind*. Accordingly, $\mathcal{G} \in \text{Mag}^2(n, \ell)$ is a *descendant* of $\tilde{\mathcal{G}}_0 \in \text{Prim}^2(n, \ell_0)$ if \mathcal{G} arises by giving an edge multiplicity to $\tilde{\mathcal{G}}_0$. The set of descendants of $\tilde{\mathcal{G}}_0 \in \text{Mag}^2(n, \ell_0)$ is denoted as $\text{Desc}(\tilde{\mathcal{G}}_0)$. For example,



$$\text{in } \text{Desc} \left(\text{primary graph} \right).$$
(5.71)

An element of $\text{Mag}(n, \ell)$ is either a descendant or a primary.

Let $\mathcal{G}_0 = (\mathcal{X}, \rightarrow_T) \in \text{Mag}(n, 0)$ be a classical Magnus graph. Then $\tilde{\mathcal{G}}_0 = (\mathcal{X}, \rightarrow_T, \rightarrow_O) \in \text{Mag}^2(n, 0)$ is said to be a *bicoloring* of \mathcal{G}_0 for an acyclic orientation structure \rightarrow_O on \mathcal{X} . Specifically, let $\gamma : \text{Mag}(n, 0) \rightarrow \text{Mag}^2(n, 0)$ be the bicoloring map such that $\tilde{\mathcal{G}}_0 = \gamma(\mathcal{G}_0)$. The *red number* of γ is the number of edges on which $\rightarrow_T = + \rightarrow_O$ is denoted as $n_+(\gamma)$. The *blue number* of γ is the number of edges on which $\rightarrow_T = - \rightarrow_O$ is denoted as $n_-(\gamma)$. These are the number of reds and blues which the bicoloring γ chooses.

Any primary of the second kind $\tilde{\mathcal{G}}_0 \in \text{Prim}^2(n, \ell)$ is a bicoloring of a primary of the first kind $\mathcal{G}_0 \in \text{Prim}(n, \ell)$. A unique bicoloring map γ exists such that $\tilde{\mathcal{G}}_0 = \gamma(\mathcal{G}_0)$.

Finally, $\mathcal{G} \in \text{Mag}^2(n, \ell)$ is *trivial* if it is a descendant of a bicoloring of a classical Magnus graph: $\mathcal{G} \in \text{Desc}(\gamma(\mathcal{G}_0))$ for $\mathcal{G}_0 \in \text{Mag}(n, 0)$. $\mathcal{G} \in \text{Mag}^2(n, \ell)$ is *nontrivial* if it is not trivial.

In the context of Wick quantization, fuzzification Fuz is a linear map that outputs a weighted sum of trivial Magnus graphs of the second kind. That is, a classical Magnus graph $\mathcal{G}_0 \in \text{Mag}(n, 0)$ is mapped to a weighted sum of elements from $\text{Desc}(\gamma(\mathcal{G}_0))$.

With these definitions, it holds at any n that

$$\chi_{(n)}^* - \text{Fuz}(\chi_{(n)}) \rightsquigarrow \sum_{\ell=1}^{\infty} \sum_{\substack{\mathcal{G} \in \text{Mag}(n, \ell) \\ \text{nontrivial}}} \frac{\hbar^\ell}{i^{n-1}} \cdot \frac{\omega_2(\mathcal{G})}{\sigma(\mathcal{G})} \mathcal{G},$$
(5.72)

which implies

$$\tilde{\mathcal{G}}_0 = \gamma(\mathcal{G}_0) \text{ for } \mathcal{G}_0 \in \text{Mag}(n, 0) \implies \omega_2(\tilde{\mathcal{G}}_0) = (-1)^{n_-(\gamma)} \omega(\mathcal{G}_0). \quad (5.73)$$

Furthermore, our explorations up to the order $n = 3$ has confirmed that

$$\mathcal{G} \in \text{Desc}(\tilde{\mathcal{G}}_0) \implies \omega_2(\mathcal{G}) = \omega_2(\tilde{\mathcal{G}}_0),$$
(5.74)

where $\mathcal{G} \in \text{Mag}^2(n, \ell)$ and $\tilde{\mathcal{G}}_0 \in \text{Prim}^2(n, \ell_0)$.

It might suffice to determine the coefficients of nontrivial primaries, the insight of which may provide some guidance when exploring higher orders.

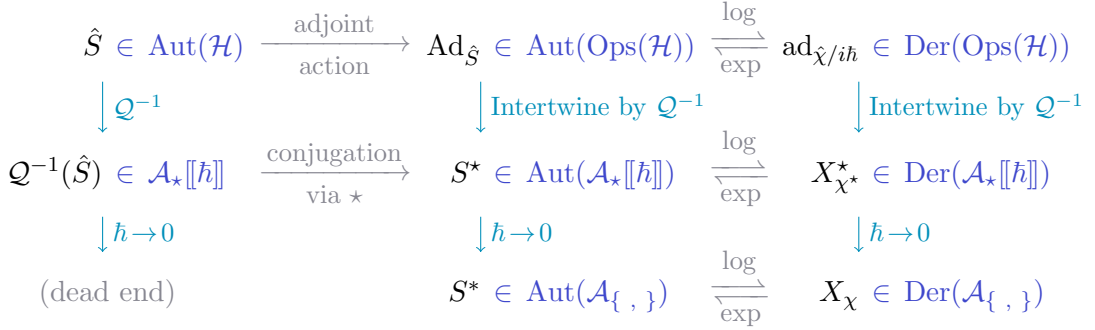


Figure 5. Summary of exact relations in classical and quantum scattering theory. Here, we pursue mathematical precision. Classical observables in the phase space formulation are identified as elements of the Poisson algebra $\mathcal{A}_{\{, \}}$. Quantum observables in the phase space formulation are identified as formal power series in \hbar whose coefficients are elements of the noncommutative ring \mathcal{A}_* . Also, Aut and Der are notations for the sets of automorphisms and derivations, respectively.

6 Summary and Outlook

In this paper, we established classical and quantum scattering theory in the phase space formulation. The classical and quantum scattering processes are geometrically interpreted as symplectomorphisms and fuzzy diffeomorphisms mapping the initial phase space to the final phase space. The logarithm of these maps via Magnus expansion defines the classical and quantum eikons as phase-space functions, serving as generators of scattering. Consequently, exact relations are established between

$$\begin{array}{ll}
\hat{S} & \text{S-matrix ,} \\
S^* & \text{Fuzzy S-diffeomorphism ,} \\
S & \text{S-symplectomorphism ,}
\end{array}
\quad
\begin{array}{ll}
\hat{\chi} & \text{Eikonal Matrix ,} \\
\chi^* & \text{Quantum Eikonal ,} \\
\chi & \text{Classical Eikonal .}
\end{array}
\quad (6.1)$$

The first row yields the second row through adjoint actions while using quantization map as an intertwiner. The second row yields the third row through the literal $\hbar \rightarrow 0$ limit. The first and second columns are in exponential/log relationships up to necessary refinements. The details are reviewed in Fig. 5.

The power of the phase space formulation shines at both conceptual and practical realms. Conceptually, the phase space formulation facilitates the very rigorous comparison between classical and quantum scattering theories by formulating quantum-mechanical operators in the same “data type” as classical observables: phase-space functions. Moreover, the phase space formulation also manifests the well-definedness of the classical limit in terms of deformed Poisson bracket and Hamiltonian vector fields.

Practically, the phase space formulation straightforwardly establishes the fact that the quantum eikonal arises by simply deforming each Poisson bracket in the Magnus formula for the classical eikonal. This leads to a systematic and principled approach to computing the quantum eikonal to arbitrary number of loops at any order, as is concretely demonstrated in detail in Sec. 5. The generality of this formalism ensures that both symmetric and normal orderings are handled within the same framework, providing a complete operational definition of Magnus coefficients for both Moyal and Wick quantizations.

Specifically, it is shown that the Magnus expansion in deformation quantization defines two new graph functions $\omega_1(\mathcal{G})$ and $\omega_2(\mathcal{G})$ on singly and doubly directed acyclic graphs. For concreteness, a detailed analysis is given for graphs with three vertices. The relevant graphs split into linear, V-shaped, and triangle categories based on the idea of descendants and primaries, the last of which being only nontrivial. The triangle category describes numbers $1/3$ or $\pm 1/6$, depending on the parity of edge multiplicities (for Moyal quantization) or the sign flip associated with the transposed Wightman tensor (for Wick quantization).

In a mathematician's perspective, this work connects between various branches of mathematics from symplectic geometry and noncommutative algebra to combinatorics and graph theory. In a physicist's perspective, this work promotes and formulates intuitive analogies into precise equalities, clarifies good and bad pathways for the classical limit, and derives explicit results about the systematic evaluation of the quantum eikonal.

We end with a few remarks on generalizations and future directions.

First of all, it should be clear that the results of this paper applies to a general class of systems. In the main parts of this paper, we have presumed the following conditions for the sake of concreteness in our exposition:

- (a) The classical phase space is a symplectic manifold.
- (b) The quantum system is realized concretely on a Hilbert space so that the phase space formulation arises by a well-behaved quantization map.
- (c) The phase space is a real plane or a complex plane.
- (d) The star product is associative.

However, these premises can all be relaxed except (d). The minimal requirement is a fuzzy phase space with an associative star product whose classical limit yields any Poisson manifold. The definitions of S, S^*, χ, χ^* all survive, as well as the Dyson/Magnus formulae.

- (a) In Poisson manifolds, $S \in \text{Diff}(\mathcal{P}, \{ \ , \ \})$ is the Poisson diffeomorphism from the initial phase space to the final phase space. The classical eikonal $\chi \in \mathcal{A}_{\{ \ , \ \}}$ is defined by $S^* = \exp(X_\chi)$. The Liouville measure is lost, but the Hamiltonian equations of motion or the Liouville equation can still be posited and studied. Physically speaking, one can define and compute S, S^*, χ, χ^* without requiring an action principle [21].
- (b) In formal (not necessarily strict) deformation quantization, $S^* \in \text{Aut}(\mathcal{A}_\star[[\hbar]])$ is the formal fuzzy diffeomorphism from the initial fuzzy phase space to the final fuzzy phase space. The quantum eikonal $\chi^* \in \mathcal{A}_\star[[\hbar]]$ is a formal power series in \hbar , defined by $S^* = \exp(X_{\chi^*}^*)$. Here, one loses the convergence of power series in \hbar or the Hilbert space \mathcal{H} . Physically speaking, one can define and compute S, S^*, χ, χ^* for systems whose perturbation theory yields only asymptotic series in the loop expansion.
- (c) The phase can be nonlinear, compact, or curved. In particular, it is well-established that the phase space formulation for spin takes the two-sphere $\mathcal{P} = S^2$ as the phase space via an explicit, well-behaved quantizer \mathcal{Q} [72]. The compactness of the phase space corresponds to the finite dimension $2j + 1$ of the spin- $2j$ Hilbert space.

Regarding (d), our framework has stipulated Jacobi identity and the associativity of star product as crucial axioms. Relaxing them will lead to rather radical generalizations but still could be of a physical interest, regarding magnetic monopoles [73, 74].

Eventually, the above generalizations at the geometry level will boil down to generalizations at the combinatorics and graph theory level. For example, suppose one quantizes a generic Poisson manifold \mathcal{P} by the Kontsevich quantization formula [37]: non-constant Π^{IJ} . Then the Magnus expansions describe weighted sum of Kontsevich graphs multiplied by factors of step functions, which will define *Magnus-Kontsevich* coefficients. What are the Magnus-Kontsevich coefficients at, say, three vertices and one loop? What is the all-orders formula? Do the ideas about descendants and primaries generalize? The linear Poisson manifold $\mathcal{P} = T^*\mathfrak{g}$ for a Lie algebra \mathfrak{g} would provide a nice cubic specialization. Physically, these explorations might connect with the perturbation theory of open strings [75].

The recursion relations and Hopf-algebraic formulations for the quantum eikonal remain to be an open problem, although those are the natural future avenues as per Ref. [20].

Another open avenue is Magnus coefficients for symplectic perturbations [76, 77], relevant to magnetic couplings. This means to implement interactions by modifying the symplectic structure instead of the Hamiltonian [78, 79], which induces several subtleties. The believed formula for the classical eikonal may need to be proven, while partial progress has been made by Ref. [77].

It may be interesting to investigate global properties of S-symplectomorphisms. Strictly speaking, our formulae for the eikonals have worked within local patches.

The treatment of field-theoretical S-matrices in this paper is based on second quantization, as is elaborated in App. A.4. It will be interesting to investigate if a first-quantized framework is viable, in which case the map S in general may describe a morphism in the symplectic category: “S-morphism.”

Acknowledgements.—The author is grateful to Li Guo, Jung-Wook Kim, Sungsoo Kim, Jianrong Li, and Toby Saunders-A’Court for discussions, from which he learned many insights about Magnus expansion. J.-H.K. is supported by the Department of Energy (Grant No. DE-SC0011632) and by the Walter Burke Institute for Theoretical Physics.

A Appendices

A.1 More on Interaction Pictures

In Secs. 3.1 and 3.3, we defined the classical and quantum interaction picture images as

$$\tilde{f}(t) = U^\circ(t_0, t)^*[f(t)], \quad \tilde{f}^*(t) = U^{*\circ}(t_0, t)[f(t)]. \quad (\text{A.1})$$

A subtle point worth clarifying is that they differ in general, as explicit examples show:

$$U^{*\circ}(t_0, t) \neq U^\circ(t_0, t)^* \implies \exists f(t) \text{ s.t. } \tilde{f}^*(t) \neq \tilde{f}(t). \quad (\text{A.2})$$

However, it still holds that the latter retrieves the former in the classical limit:

$$\lim_{\hbar \rightarrow 0} U^{*\circ}(t_1, t_2) = U^\circ(t_1, t_2)^* \implies \lim_{\hbar \rightarrow 0} \tilde{f}^*(t) = \tilde{f}(t) \quad \forall f(t). \quad (\text{A.3})$$

This can be shown by using the Magnus [40] series for $U^{*\circ}(t_1, t_2)$ and $U^\circ(t_1, t_2)^*$. Note that Eq. (A.3) is a concretely formulated equation about differential operators.

A summary can be given in terms of the following (non)commutative diagram.

$$\begin{array}{ccccc} & & \tilde{f}(t) & & \\ & \xleftarrow{\mathcal{Q}} & & \xrightarrow{\mathcal{Q}} & f(t) \\ \text{Ad}_{\hat{U}^\circ(t_0, t)} \downarrow & & U^{*\circ}(t_0, t) \nearrow & & \downarrow U^\circ(t_0, t)^* \\ \tilde{f}(t) & \xleftarrow{\mathcal{Q}} & \tilde{f}^*(t) & \xrightarrow{\hbar \rightarrow 0} & \tilde{f}(t) \end{array} \quad (\text{A.4})$$

Namely, quantization does not commute with interaction picture, although classical limit closes the square:

$$\mathcal{Q} \circ \left(\text{Quantum Interaction Picture} \right) \neq \left(\text{Classical Interaction Picture} \right) \circ \mathcal{Q}. \quad (\text{A.5})$$

Crucially, however, physically relevant examples tend to achieve the equality $\tilde{f}^*(t) = \tilde{f}(t)$ by prescribing a simple free Hamiltonian. First, suppose quantization in symmetric ordering: Sec. 2.2.1. A quadratic free Hamiltonian, such as $p^2/2m$, keeps the free evolution linear as $x \mapsto x+pt/m$, $p \mapsto p$, in which case the interaction picture preserves the symmetric ordering. Second, suppose quantization in normal ordering: Sec. 2.2.5. The harmonic free Hamiltonian in Eq. (2.54) keeps the free evolution holomorphic in the sense that no mixing between a and \bar{a} develops: $a \mapsto a e^{-i\omega t}$, $\bar{a} \mapsto \bar{a} e^{+i\omega t}$ (that is, no Bogoliubov β coefficient). As a result, the interaction picture preserves the normal ordering. More explicitly, one can verify $U^{*\circ}(t_0, t) = U^\circ(t_0, t)^*$ directly by showing that $X_{\bar{a}a}^* = X_{\bar{a}a}$.

The precise criterion for the equality $\tilde{f}^*(t) = \tilde{f}(t)$ is the preservation of operator ordering by free time evolution. We may impose that *the free theory respects the quantization* in this precise sense, as an optional consistency condition in the quantum theory of scattering with a nicely behaving classical limit.

Despite this caveat, the formulae in Eqs. (3.20) and (3.21) is exact since $\tilde{V}(t)$ in Sec. 3.4 denotes $U^{*\circ}(t_0, t)[V(t)]$: the symbol of $\tilde{V}(t)$ ($\neq \hat{V}(t)$). Generally speaking, this develops \hbar corrections from $\tilde{V}(t)$ in Sec. 3.2, which denotes $U^\circ(t_0, t)^*[V(t)]$. However, one should feel free to regard that we have presumed the consistency between free theory and quantization.

A.2 In Background Perturbation Theory

This appendix provides an optional analysis on background field theory computations. This is in consideration of the exploration given in Ref. [80], where the vacuum expectation value of the eikonal matrix $\hat{\chi}$ is compared with the classical eikonal. In our framework, such vacuum expectation values essentially compute the symbol of operators via \mathcal{Q}^{-1} . Thus, provided a correct interpretation of notations, our conclusions will be

$$\chi^* = \langle \hat{\chi} \rangle_{\text{bkgd}} \implies \chi = \lim_{\hbar \rightarrow 0} \langle \hat{\chi} \rangle_{\text{bkgd}}, \quad (\text{A.6})$$

as well as

$$\exp^* \left(\frac{1}{i\hbar} \chi^* \right) = \langle \hat{S} \rangle_{\text{bkgd}}. \quad (\text{A.7})$$

First of all, we review the fact that star products admit path integral derivations: recall the brief comments given around Eqs. (2.70) and (2.71). For the Moyal star product, a worldline path integral derivation is nicely detailed in Ref. [62] (see also Ref. [75]).

For the Wick star product, we may take the formula in Eq. (2.64) as the starting point. Its right-hand side can be reinterpreted as a path integral

$$\int_a^{\bar{a}} \mathcal{D}\lambda \mathcal{D}\bar{\lambda} \exp \left(\frac{1}{\hbar} \left(\bar{a}(\lambda(t_+) - a) - \int_{t_-}^{t_+} dt \bar{\lambda}(t) \dot{\lambda}(t) \right) \right) f(\lambda(t_0), \bar{\lambda}(t_0)), \quad (\text{A.8})$$

the boundary conditions for which are $\lambda(t_-) = a$ and $\bar{\lambda}(t_+) = \bar{a}$. Here, t_+ , t_- , and t_0 fixed arbitrary times such that $t_+ > t_0 > t_-$. This freedom is due to the fact that the action in Eq. (A.8) defines a topological (reparametrization-invariant) theory [62]: phase space action with zero Hamiltonian.

By expanding around a static background as $\lambda(t) = a + \delta a(t)$ and $\bar{\lambda}(t) = \bar{a} + \delta \bar{a}(t)$, one then finds that Eq. (2.64) can be recast to

$$\mathcal{Q}^{-1}(\hat{f})(a, \bar{a}) = \langle f(a + \delta a(t_0), \bar{a} + \delta \bar{a}(t_0)) \rangle, \quad (\text{A.9})$$

which employs the path integration

$$\langle \dots \rangle = \int \mathcal{D}\delta a \mathcal{D}\delta \bar{a} \exp \left(-\frac{1}{\hbar} \int_{t_-}^{t_+} dt \delta \bar{a}(t) \delta \dot{a}(t) \right) \langle \dots \rangle \quad (\text{A.10})$$

with boundary conditions $\delta a(t_-) = 0$, $\delta \bar{a}(t_+) = 0$. As a result, the propagator is given by

$$\langle \delta a(t_1) \delta a(t_2) \rangle = 0, \quad \langle \delta a(t_1) \delta \bar{a}(t_2) \rangle = \hbar \Theta(t_1, t_2), \quad \langle \delta \bar{a}(t_1) \delta \bar{a}(t_2) \rangle = 0, \quad (\text{A.11})$$

where $\Theta(t_1, t_2)$ equals 1 if $t_1 > t_2$ and 0 if $t_1 < t_2$. Finally, the operator ordering is implemented as the time ordering in the path integral as

$$\mathcal{Q}^{-1}(\hat{f}\hat{g})(a, \bar{a}) = \langle f(a + \delta a(t_1), \bar{a} + \delta \bar{a}(t_1)) g(a + \delta a(t_2), \bar{a} + \delta \bar{a}(t_2)) \rangle, \quad (\text{A.12})$$

where t_1 and t_2 are arbitrary times such that $t_+ > t_1 > t_2 > t_-$. Again, such a freedom arises because the path integral is sensitive to only the ordering between t_1 and t_2 as the topological information [62]. Evaluating Eq. (A.12) with the propagator in Eq. (A.11) readily reproduces the Wick star product in Eq. (2.66), which sums over vacuum bubble diagrams arising from joining f and g as two vertices.

In the operator language, Eq. (A.9) could be described as

$$\mathcal{Q}^{-1}(\hat{f})(a, \bar{a}) = \langle 0 | : f(a + \widehat{\delta a}, \bar{a} + \widehat{\delta \bar{a}}) : | 0 \rangle, \quad (\text{A.13})$$

where a, \bar{a} are merely c-number variables; it is the fluctuation fields that are quantized. The vacuum ket (bra) in Eq. (A.13) is annihilated by $\widehat{\delta a}$ ($\widehat{\delta \bar{a}}$).

With this understanding, consider abbreviating Eqs. (A.9) or (A.13) to

$$\mathcal{Q}^{-1}(\hat{f}) = \langle \hat{f} \rangle_{\text{bkgd}}. \quad (\text{A.14})$$

In the path integral perspective, the definition of the right-hand side in Eq. (A.14) is to sum over vacuum bubble diagrams in a *background field theory* computation, which is indeed what Ref. [80] performs. We clarify that this path integral is with respect to the topological (zero-Hamiltonian) action. In the operator perspective, the definition of the right-hand side in Eq. (A.14) is to compute the vacuum expectation value with the crucial stipulation that both the quantization and vacuum are implemented with respect to the *fluctuation* fields.

With this clarification, we find Eq. (A.6) from $\chi^* = \mathcal{Q}^{-1}(\hat{\chi})$ in Eq. (4.2). For Eq. (A.7), consider the relation derived in Eq. (4.7).

A remark regarding Eq. (A.7) is that its path integral representation can take either of the following as the phase space action:

$$I_{\text{eff}}[x, p] = \int_0^1 dt \left(\frac{1}{2} \left(p(t) \dot{x}(t) - \dot{p}(t) x(t) \right) - \chi^*(x(t), p(t), t) \right), \quad (\text{A.15})$$

$$I[x, p] = \int_{-\infty}^{+\infty} dt \left(\frac{1}{2} \left(p(t) \dot{x}(t) - \dot{p}(t) x(t) \right) - \tilde{V}^*(x(t), p(t), t) \right). \quad (\text{A.16})$$

This is indeed consistent with the fact that χ^* is the effective Hamiltonian reproducing the time evolution within unit time. Specifically, it can be seen that

$$\int \mathcal{D}x \mathcal{D}p e^{-I_{\text{eff}}[x, p]/i\hbar} = \langle \exp(\hat{\chi}/i\hbar) \rangle_{\text{bkgd}} = \langle \hat{S} \rangle_{\text{bkgd}} = \int \mathcal{D}x \mathcal{D}p e^{-I[x, p]/i\hbar}, \quad (\text{A.17})$$

as the exponential $\exp(\hat{\chi}/i\hbar)$ merges with the exponentiated topological part of the action in the path integral. For the free theory $H^\circ = p^2/2m$, for instance, Eq. (A.16) will precisely describe the perturbation theory of Ref. [80] that expands around a straight-line trajectory, provided a proper treatment of the interaction picture [20].

Finally, note the subtle difference between

$$i\hbar \langle \log \hat{S} \rangle_{\text{bkgd}} = i\hbar \log^* \mathcal{Q}^{-1}(\hat{S}) = \chi^*, \quad (\text{A.18a})$$

$$i\hbar \log \langle \hat{S} \rangle_{\text{bkgd}} = i\hbar \log \mathcal{Q}^{-1}(\hat{S}), \quad (\text{A.18b})$$

where \log^* is an inverse of \exp^* via $\log^* \circ \mathcal{Q}^{-1} = \mathcal{Q}^{-1} \circ \log$. As is shown in Eq. (A.18a), \hbar -deformed functions such as \log^* or \exp^* translate to ordinary functions acting inside the vacuum expectation value. As is shown in Eq. (A.18b), however, ordinary functions such as \log or \exp simply act outside the expectation value. As should be clear from Eq. (A.14), $\langle \rangle_{\text{bkgd}}$ is essentially synonymous to \mathcal{Q}^{-1} : extracting the symbol.

A.3 More on Wightman Tensor

In Sec. 5.3, an oscillator is viewed as a Hamiltonian system that takes a Kähler vector space as the phase space, on which the Wightman tensor is defined to yield the Wick star product. This appendix elaborates on the details of this construction.

Concretely, suppose N -dimensional harmonic oscillator. The phase space is the Kähler vector space $\mathcal{P} = \mathbb{C}^N$ with complex coordinates a_α . The **Kähler triple** is formed by metric A , symplectic form Ω , and complex structure J such that $A(X, Y) = \Omega(J(X), Y)$:

$$A = \delta^{\bar{\beta}\alpha} \left(d\bar{a}_\beta \otimes da_\alpha + da_\alpha \otimes d\bar{a}_\beta \right), \quad (\text{A.19})$$

$$\Omega = i \left(d\bar{a}^\alpha \otimes da_\alpha - da_\alpha \otimes d\bar{a}^\alpha \right), \quad (\text{A.20})$$

where $\bar{a}_\beta = [a_\beta]^*$. Note that one takes $\bar{a}^\alpha = \bar{a}_\beta \delta^{\bar{\beta}\alpha}$ via the metric.

The inverse metric A^{-1} is the pointwise inverse of A :

$$A^{-1} = \frac{\partial}{\partial a_\alpha} \otimes \frac{\partial}{\partial \bar{a}^\alpha} + \frac{\partial}{\partial \bar{a}^\alpha} \otimes \frac{\partial}{\partial a_\alpha}. \quad (\text{A.21})$$

The Poisson tensor Π is the pointwise inverse of ω :

$$\Pi = -i \frac{\partial}{\partial a_\alpha} \otimes \frac{\partial}{\partial \bar{a}^\alpha} + i \frac{\partial}{\partial \bar{a}^\alpha} \otimes \frac{\partial}{\partial a_\alpha}. \quad (\text{A.22a})$$

Crucially, the **Wightman tensor** W is defined as

$$W = \frac{1}{2} \left(A^{-1} + i\Pi \right) = \frac{\partial}{\partial a_\alpha} \otimes \frac{\partial}{\partial \bar{a}^\alpha}. \quad (\text{A.22b})$$

This is the pointwise inverse of the hermitian form $\langle \cdot, \cdot \rangle$ on \mathbb{C}^N , in fact. Its transpose is

$$W^\top = \frac{1}{2} \left(A^{-1} - i\Pi \right) = \frac{\partial}{\partial \bar{a}^\alpha} \otimes \frac{\partial}{\partial a_\alpha}. \quad (\text{A.22c})$$

Note the relation

$$\Pi = \frac{1}{i} \left(W - W^\top \right). \quad (\text{A.22d})$$

The Poisson bracket is defined as (regard I_1, I_2 as abstract indices)

$$\{f, g\} = f \left(\overleftarrow{\partial}_{I_1} \Pi^{I_1 I_2} \overrightarrow{\partial}_{I_2} \right) g = -i \frac{\partial f}{\partial a_\alpha} \frac{\partial g}{\partial \bar{a}^\alpha} + i \frac{\partial f}{\partial \bar{a}^\alpha} \frac{\partial g}{\partial a_\alpha}, \quad (\text{A.23a})$$

which arises from the Poisson tensor. The **Wightman bracket** is defined as

$$\{f, g\}^+ = f \left(\overleftarrow{\partial}_{I_1} W^{I_1 I_2} \overrightarrow{\partial}_{I_2} \right) g = \frac{\partial f}{\partial a_\alpha} \frac{\partial g}{\partial \bar{a}^\alpha}, \quad (\text{A.23b})$$

which arises from the Wightman tensor. The **transposed Wightman bracket** is defined as

$$\{f, g\}^- = f \left(\overleftarrow{\partial}_{I_1} W^{I_2 I_1} \overrightarrow{\partial}_{I_2} \right) g = \frac{\partial f}{\partial \bar{a}^\alpha} \frac{\partial g}{\partial a_\alpha} = \{g, f\}^+, \quad (\text{A.23c})$$

which arises from the transpose $(W^\top)^{I_1 I_2} = W^{I_2 I_1}$ of the Wightman tensor. Then we have

$$\{f, g\} = \frac{1}{i} \left(\{f, g\}^+ - \{f, g\}^- \right). \quad (\text{A.23d})$$

The Wick star product in Eq. (5.46) is an exponentiation of the Wightman bracket in Eq. (A.23b). That said, the Wightman bracket $\{f, g\}^+$ is the $\mathcal{O}(\hbar^1)$ part of $f \star g$.

A.4 Field Theory

This appendix shows that the results in Sections 2, 3, 4, and 5 universally apply to both particles and fields. Especially, we show that the final form of eikonal in Sec. 5 has precisely described Feynman diagrams in the retarded causality prescription, in both quantum mechanics and quantum field theory.

To recapitulate, the definitions of the retarded propagator and its positive- and negative-frequency parts were proposed in Eqs. (5.15), (5.53), and (5.55), with their relation stated in Eq. (5.54). For the reader's sake, we reproduce them below:

$$\text{---} \bullet \text{---} = \int d^2t \tilde{V}(t_1) \left(\overleftarrow{\partial}_{I_1} \Pi^{I_1 I_2} \Theta(t_1, t_2) \overrightarrow{\partial}_{I_2} \right) \tilde{V}(t_2), \quad (\text{A.24a})$$

$$\bullet \text{---} \bullet = \int d^2t \tilde{V}(t_1) \left(\overleftarrow{\partial}_{I_1} W^{I_1 I_2} \Theta(t_1, t_2) \overrightarrow{\partial}_{I_2} \right) \tilde{V}(t_2), \quad (\text{A.24b})$$

$$\bullet \text{---} \bullet = \int d^2t \tilde{V}(t_1) \left(\overleftarrow{\partial}_{I_1} W^{I_2 I_1} \Theta(t_1, t_2) \overrightarrow{\partial}_{I_2} \right) \tilde{V}(t_2), \quad (\text{A.24c})$$

where

$$\text{---} \bullet \text{---} = \frac{1}{i} \left(\bullet \text{---} \bullet - \bullet \text{---} \bullet \right). \quad (\text{A.24d})$$

Since we treat interactions perturbatively, it suffices to examine free theories. We also use the notations $d\xi = d\xi/2\pi$, $\delta(\xi) = 2\pi\delta(\xi)$.

Recalling a famous quote by Sidney Coleman, we first revisit the one-dimensional harmonic oscillator defined by Eqs. (2.52), (2.54), and (2.66). The phase space is $\mathcal{P} = \mathbb{R}^2 \cong \mathbb{C}^1$. The classical and quantum interaction pictures coincide as shown in App. A.1. The free time evolution $U^\circ(t, 0)$ acts on the phase space simply as a phase rotation, $a \mapsto a e^{-i\omega t}$, $\bar{a} \mapsto \bar{a} e^{i\omega t}$, where we take the fixed time slice as $t_0 = 0$ for simplicity. We then take the position variable x in Eq. (2.53) as a function on the phase space. Its interaction picture image $\tilde{x}(t)$ splits into the *positive- and negative- frequency parts* as

$$\tilde{x}(t) = \frac{1}{\sqrt{2m\omega}} a e^{-i\omega t} + \frac{1}{\sqrt{2m\omega}} \bar{a} e^{+i\omega t}. \quad (\text{A.25})$$

The Wick star product in Eq. (2.66) implies

$$\tilde{x}(t_1) \star \tilde{x}(t_2) = \tilde{x}(t_1) \tilde{x}(t_2) + \hbar W(t_1, t_2), \quad (\text{A.26})$$

which derives the *Wightman function* $W(t_1, t_2)$. The Poisson bracket in Eq. (2.52) implies

$$\{\tilde{x}(t_1), \tilde{x}(t_2)\} = \frac{1}{i} \left(W(t_1, t_2) - W(t_2, t_1) \right) = \Delta(t_1, t_2), \quad (\text{A.27})$$

which derives the *Pauli-Jordan function* $\Delta(t_1, t_2) = -\Delta(t_2, t_1)$. Explicitly,

$$W(t_1, t_2) = \frac{1}{2m\omega} e^{-i\omega(t_1-t_2)}, \quad \Delta(t_1, t_2) = -\frac{\sin(\omega(t_1-t_2))}{m\omega}. \quad (\text{A.28})$$

From the clarifications made in App. A.3, it should be clear that Eqs. (A.26) and (A.27) have computed the Wightman and Poisson brackets,

$$\begin{aligned}\tilde{x}(t_1) \left(\overleftarrow{\partial}_{I_1} W^{I_1 I_2} \overrightarrow{\partial}_{I_2} \right) \tilde{x}(t_2) &= W(t_1, t_2), \\ \tilde{x}(t_1) \left(\overleftarrow{\partial}_{I_1} \Pi^{I_1 I_2} \overrightarrow{\partial}_{I_2} \right) \tilde{x}(t_2) &= \Delta(t_1, t_2).\end{aligned}\quad (\text{A.29})$$

Here, I_1, I_2 are indices taking values in $\{1, 2\}$, which understands the phase space concretely as a real manifold \mathbb{R}^2 .

With this understanding, we consider the case in which the interaction Hamiltonian arises from a potential $v(x)$ in position space, so $\tilde{V}(x, p; t) = v(\tilde{x}(x, p; t))$. By using chain rule, Eq. (A.24) then boils down to

$$\bullet \text{---} \bullet = \int d^2t \ v'(\tilde{x}(t_1)) \left(\Delta(t_1, t_2) \Theta(t_1, t_2) \right) v'(\tilde{x}(t_2)), \quad (\text{A.30a})$$

$$\bullet \text{---} \bullet = \int d^2t \ v'(\tilde{x}(t_1)) \left(W(t_1, t_2) \Theta(t_1, t_2) \right) v'(\tilde{x}(t_2)), \quad (\text{A.30b})$$

$$\bullet \text{---} \bullet = \int d^2t \ v'(\tilde{x}(t_1)) \left(W(t_2, t_1) \Theta(t_1, t_2) \right) v'(\tilde{x}(t_2)), \quad (\text{A.30c})$$

which should be clear from Eq. (A.29).

Crucially, the bracketed terms in Eqs. (A.30a), (A.30b), and (A.30c) are respectively the *retarded propagator*, the *positive-frequency retarded propagator*, and the *negative-frequency retarded propagator*:

$$G_{\text{ret}}(t_1, t_2) = \Delta(t_1, t_2) \Theta(t_1, t_2), \quad (\text{A.31a})$$

$$G_{\text{ret}}^+(t_1, t_2) = W(t_1, t_2) \Theta(t_1, t_2), \quad (\text{A.31b})$$

$$G_{\text{ret}}^-(t_1, t_2) = W(t_2, t_1) \Theta(t_1, t_2). \quad (\text{A.31c})$$

To clarify, $G_{\text{ret}}^\pm(t_1, t_2)$ are the positive- and negative-frequency parts of $G_{\text{ret}}(t_1, t_2)$ up to the customary $\pm i$ factors:

$$G_{\text{ret}}(t_1, t_2) = \frac{1}{i} \left(G_{\text{ret}}^+(t_1, t_2) - G_{\text{ret}}^-(t_1, t_2) \right). \quad (\text{A.31d})$$

To see this, note first that the Wightman and Pauli-Jordan functions are *homogeneous* solutions to the harmonic oscillator equations of motion, which one can directly verify from their explicit form given in Eq. (A.28):

$$m \left(-\frac{\partial^2}{\partial t_1^2} - \omega^2 \right) W(t_1, t_2) = 0, \quad m \left(-\frac{\partial^2}{\partial t_1^2} - \omega^2 \right) \Delta(t_1, t_2) = 0. \quad (\text{A.32})$$

Similarly, it follows that $G_{\text{ret}}(t_1, t_2)$ in Eq. (A.47a) is the retarded Green's function solving the *inhomogeneous* equation

$$m \left(-\frac{\partial^2}{\partial t_1^2} - \omega^2 \right) G_{\text{ret}}(t_1, t_2) = \delta(t_1 - t_2). \quad (\text{A.33})$$

Consequently, Eq. (A.30) precisely describes the integrals that one obtains in a covariant perturbation theory in the retarded causality prescription. This establishes that the left-hand sides in Eq. (A.30) are Feynman diagrams in the precise sense, constructed with retarded propagators.

It is easy to generalize the above result to the case of an N -dimensional oscillator, in which case the indices I_1, I_2 are valued in a set of $2N$ integers. By promoting them to continuous labels, one obtains field theories without much difficulty.

Concretely, suppose the Klein-Gordon field in d spacetime dimensions. As a Hamiltonian system, it describes the infinite-dimensional phase space $\mathcal{P} = T^*(C^\infty(\mathbb{R}^{d-1}))$ whose coordinates are $\phi : \vec{x} \mapsto \phi^{\vec{x}}$ and $\pi : \vec{x} \mapsto \pi^{\vec{x}}$, where $\vec{x} \in \mathbb{R}^{d-1}$. In particular, the derivation of the Poisson bracket and Hamiltonian from the relativistic Lagrangian is a textbook matter. To establish the interpretation as an oscillator system, one considers the following change of coordinates as a generalization of Eq. (2.53):

$$\begin{aligned}\phi^{\vec{x}} &= \int \frac{d^{d-1}k}{2\omega(\vec{k})} \left(a_{\vec{k}} e^{i\vec{k}\cdot\vec{x}} + \bar{a}_{\vec{k}} e^{-i\vec{k}\cdot\vec{x}} \right), \\ \pi^{\vec{x}} &= \int d^{d-1}k \frac{1}{2i} \left(a_{\vec{k}} e^{i\vec{k}\cdot\vec{x}} - \bar{a}_{\vec{k}} e^{-i\vec{k}\cdot\vec{x}} \right).\end{aligned}\quad (\text{A.34})$$

Here, a dispersion relation $\omega(\vec{k}) = (\vec{k}^2 + \mu^2)^{1/2}$ is assumed for a rest-mass parameter μ . As is well-known, the Poisson bracket is then given by

$$\left(\overleftarrow{\partial}_{I_1} \Pi^{I_1 I_2} \overrightarrow{\partial}_{I_2} \right) = -i \int d^{d-1}k 2\omega(\vec{k}) \left(\overleftarrow{\frac{\delta}{\delta a_{\vec{k}}}} \overrightarrow{\frac{\delta}{\delta \bar{a}_{\vec{k}}}} - \overleftarrow{\frac{\delta}{\delta \bar{a}_{\vec{k}}}} \overrightarrow{\frac{\delta}{\delta a_{\vec{k}}}} \right). \quad (\text{A.35})$$

Here, I_1, I_2 may be identified with the continuous indices \vec{x}_1, \vec{x}_2 taking values in \mathbb{R}^{d-1} . Yet more elegantly, one can regard them as abstract indices given for the infinite-dimensional manifold \mathcal{P} .

Next, one quantizes the system in the normal ordering prescription, in which case the Wick contraction rule is

$$a_{\vec{k}_1} \star \bar{a}_{\vec{k}_2} = a_{\vec{k}_1} \bar{a}_{\vec{k}_2} + 2\hbar\omega(\vec{k}_1) \delta^{(d-1)}(\vec{k}_1 - \vec{k}_2). \quad (\text{A.36})$$

From the discussion around Eq. (2.67), it should be clear that Eq. (A.38) is a mere rewriting of the textbook equation,

$$\hat{a}_{\vec{k}_1} \hat{a}_{\vec{k}_2} = : \hat{a}_{\vec{k}_1} \hat{a}_{\vec{k}_2} : + 2\hbar\omega(\vec{k}_1) \delta^{(d-1)}(\vec{k}_1 - \vec{k}_2). \quad (\text{A.37})$$

Generalizing Eq. (2.66), the Wick star product is given by

$$\star = \exp \left(\overleftarrow{\partial}_{I_1} \hbar W^{I_1 I_2} \overrightarrow{\partial}_{I_2} \right) = \exp \left[\hbar \int d^{d-1}k 2\omega(\vec{k}) \left(\overleftarrow{\frac{\delta}{\delta a_{\vec{k}}}} \overrightarrow{\frac{\delta}{\delta \bar{a}_{\vec{k}}}} \right) \right]. \quad (\text{A.38})$$

The free Hamiltonian is

$$H^\circ = \int \frac{d^{d-1}k}{2\omega(\vec{k})} \left(\omega(\vec{k}) \bar{a}_{\vec{k}} a_{\vec{k}} \right). \quad (\text{A.39})$$

In turn, the interaction picture image of the “position variable” ϕ in Eq. (A.34) is

$$\tilde{\phi}^{\vec{x}}(t) = \int \frac{d^{d-1}k}{2\omega(\vec{k})} \left(a_{\vec{k}} e^{-i\omega(\vec{k})t+i\vec{k}\cdot\vec{x}} + \bar{a}_{\vec{k}} e^{i\omega(\vec{k})t-i\vec{k}\cdot\vec{x}} \right), \quad (\text{A.40})$$

yielding the split of the time-evolved free field into *positive- and negative-frequency parts*.

The Wick star product in Eq. (A.38) implies

$$\tilde{\phi}^{\vec{x}_1}(t_1) \star \tilde{\phi}^{\vec{x}_2}(t_2) = \tilde{\phi}^{\vec{x}_1}(t_1) \tilde{\phi}^{\vec{x}_2}(t_2) + \hbar W((t_1, \vec{x}_1), (t_2, \vec{x}_2)), \quad (\text{A.41})$$

where the **Wightman function** is defined as a function $W(x_1, x_2)$ of two spacetime points. The Poisson bracket in Eq. (A.35) then implies

$$\begin{aligned} \{\tilde{\phi}^{\vec{x}_1}(t_1), \tilde{\phi}^{\vec{x}_2}(t_2)\} &= \frac{1}{i} \left(W((t_1, \vec{x}_1), (t_2, \vec{x}_2)) - W((t_2, \vec{x}_2), (t_1, \vec{x}_1)) \right), \\ &= \Delta((t_1, \vec{x}_1), (t_2, \vec{x}_2)), \end{aligned} \quad (\text{A.42})$$

where the **Pauli-Jordan function** is defined as a function $\Delta(x_1, x_2) = -\Delta(x_2, x_1)$ of two spacetime points. Explicitly,

$$\begin{aligned} W(x_1, x_2) &= \int d^d k \delta(k^2 + \mu^2) \Theta(k^0) e^{ik(x_1 - x_2)}, \\ \Delta(x_1, x_2) &= \frac{1}{i} \int d^d k \delta(k^2 + \mu^2) \operatorname{sgn}(k^0) e^{ik(x_1 - x_2)}. \end{aligned} \quad (\text{A.43})$$

Again, Eqs. (A.41) and (A.42) have computed the Wightman and Poisson brackets,

$$\begin{aligned} \tilde{\phi}^{\vec{x}_1}(t_1) \left(\overleftarrow{\partial}_{I_1} W^{I_1 I_2} \overrightarrow{\partial}_{I_2} \right) \tilde{\phi}^{\vec{x}_2}(t_2) &= W((t_1, \vec{x}_1), (t_2, \vec{x}_2)), \\ \tilde{\phi}^{\vec{x}_1}(t_1) \left(\overleftarrow{\partial}_{I_1} \Pi^{I_1 I_2} \overrightarrow{\partial}_{I_2} \right) \tilde{\phi}^{\vec{x}_2}(t_2) &= \Delta((t_1, \vec{x}_1), (t_2, \vec{x}_2)). \end{aligned} \quad (\text{A.44})$$

It should be clear that Eq. (A.44) has merely rewritten the textbook equations about Wick contraction and commutator between fields at different points.

With this understanding, we consider the typical situation in which the interaction Hamiltonian arises from a potential $v : \mathbb{R} \rightarrow \mathbb{R}$:

$$V = \int d^{d-1}x v(\phi^{\vec{x}}) \implies \tilde{V}(t) = \int d^{d-1}x v(\tilde{\phi}^{\vec{x}}(t)). \quad (\text{A.45})$$

By using chain rule, Eq. (A.24) then boils down to

$$\bullet \text{---} \bullet = \int_{t_1, t_2, \vec{x}_1, \vec{x}_2} v'(\tilde{\phi}^{\vec{x}_1}(t_1)) \left(\Delta((t_1, \vec{x}_1), (t_2, \vec{x}_2)) \Theta(t_1, t_2) \right) v'(\tilde{\phi}^{\vec{x}_2}(t_2)), \quad (\text{A.46a})$$

$$\bullet \text{---} \bullet = \int_{t_1, t_2, \vec{x}_1, \vec{x}_2} v'(\tilde{\phi}^{\vec{x}_1}(t_1)) \left(W((t_1, \vec{x}_1), (t_2, \vec{x}_2)) \Theta(t_1, t_2) \right) v'(\tilde{\phi}^{\vec{x}_2}(t_2)), \quad (\text{A.46b})$$

$$\bullet \text{---} \bullet = \int_{t_1, t_2, \vec{x}_1, \vec{x}_2} v'(\tilde{\phi}^{\vec{x}_1}(t_1)) \left(W((t_2, \vec{x}_2), (t_1, \vec{x}_1)) \Theta(t_1, t_2) \right) v'(\tilde{\phi}^{\vec{x}_2}(t_2)), \quad (\text{A.46c})$$

which follows from Eq. (A.44). Here, we have abbreviated $\int dt_1 dt_2 d^{d-1}x_1 d^{d-1}x_2$ as $\int_{t_1, t_2, \vec{x}_1, \vec{x}_2}$.

Crucially, the bracketed terms in Eqs. (A.46a), (A.46b), and (A.46c) describe respectively the **retarded propagator**, the **positive-frequency retarded propagator**, and the **negative-frequency retarded propagator**:

$$G_{\text{ret}}(x_1, x_2) = \Delta(x_1, x_2) \Theta(x_1^0, x_2^0), \quad (\text{A.47a})$$

$$G_{\text{ret}}^+(x_1, x_2) = W(x_1, x_2) \Theta(x_1^0, x_2^0), \quad (\text{A.47b})$$

$$G_{\text{ret}}^-(x_1, x_2) = W(x_2, x_1) \Theta(x_1^0, x_2^0). \quad (\text{A.47c})$$

To clarify, $G_{\text{ret}}^\pm(x_1, x_2)$ are the positive- and negative-frequency parts of $G_{\text{ret}}(x_1, x_2)$ up to the customary $\pm i$ factors:

$$G_{\text{ret}}(x_1, x_2) = \frac{1}{i} \left(G_{\text{ret}}^+(x_1, x_2) - G_{\text{ret}}^-(x_1, x_2) \right). \quad (\text{A.47d})$$

To see this, note first that the Wightman and Pauli-Jordan functions are *homogeneous* solutions to the Klein-Gordon equation, which one can directly verify from the on-shell support $\delta(k^2 + \mu^2)$ in Eq. (A.43):

$$\left(\partial_1^2 - \mu^2 \right) W(t_1, t_2) = 0, \quad \left(\partial_1^2 - \mu^2 \right) \Delta(t_1, t_2) = 0. \quad (\text{A.48})$$

Similarly, it follows that $G_{\text{ret}}(t_1, t_2)$ in Eq. (A.47a) is the retarded Green's function solving the following *inhomogeneous* Klein-Gordon equation, which is a well-known fact:

$$\left(\partial_1^2 - \mu^2 \right) G_{\text{ret}}(x_1, x_2) = \delta^{(d)}(x_1 - x_2). \quad (\text{A.49})$$

Eventually, we switch to the conventional notation in quantum field theory via

$$\tilde{\phi}^{\vec{x}}(t) = \phi_{\text{I}}(x) \quad \text{where} \quad x = (t, \vec{x}) \in \mathbb{R}^{1, d-1}, \quad (\text{A.50})$$

where the subscript I signifies “interaction picture.” Then Eq. (A.46) is brought to

$$\bullet \text{---} \bullet = \int d^d x_1 d^d x_2 v'(\phi_{\text{I}}(x_1)) G_{\text{ret}}(x_1, x_2) v'(\phi_{\text{I}}(x_2)), \quad (\text{A.51a})$$

$$\bullet \text{---} \bullet = \int d^d x_1 d^d x_2 v'(\phi_{\text{I}}(x_1)) G_{\text{ret}}^+(x_1, x_2) v'(\phi_{\text{I}}(x_2)), \quad (\text{A.51b})$$

$$\bullet \text{---} \bullet = \int d^d x_1 d^d x_2 v'(\phi_{\text{I}}(x_1)) G_{\text{ret}}^-(x_1, x_2) v'(\phi_{\text{I}}(x_2)), \quad (\text{A.51c})$$

Evidently, Eq. (A.51) describes nothing but Feynman diagrams in the retarded causality prescription. Specifically, these are precisely the integrals that one encounters when computing the S-matrix in the operator formalism via the interaction picture. This establishes that the left-hand sides in Eq. (A.30) have described Feynman diagrams in the precise sense, constructed with the quantum field theoretical retarded propagators.

In conclusion, we have established that the final forms of eikonals in Sec. 5 are Feynman diagrams in the retarded causality prescription, for both quantum mechanics and quantum field theory. We have simply examined single-multiplicity lines since it is easy to derive the same conclusion for multiplied lines as well.

To clarify, however, these diagrams compute operators. That is, the output is operator-valued. It is not a matrix element. For instance, take the cubic potential $v(\phi) = g\phi^3/3!$. Then the second-order classical eikonal, $\chi_{(2)}$, is found from Eq. (A.51a) as

$$\frac{1}{2} \bullet \text{---} \bullet = \frac{g^2}{8} \int d^d x_1 d^d x_2 (\phi_{\text{I}}(x_1))^2 G_{\text{ret}}(x_1, x_2) (\phi_{\text{I}}(x_2))^2. \quad (\text{A.52})$$

This is simply a normal-ordered operator described in the phase space formulation: Eq. (A.52) is equivalent to Eq. (4.11) of Ref. [39].

Finally, the demonstration of this appendix should also clarify that our results for the final form of eikonals were manifestly Lorentz covariant: just interpret the diagrams as in Eq. (A.51).

In fact, an elaborate framework known as Peierls bracket [81–83] or covariant phase space [84] can readily manifest covariance in all intermediate steps in our formalism: perturbative algebraic quantum field theory [85]. Namely, we take \mathcal{P} as the space of solutions to free field equations and work with its Poisson and Wightman structures which arise through the Pauli-Jordan and Wightman functions, which avoids the $1 + (d - 1)$ decomposition. There is not enough space to delve into this direction in this paper, but we hope to do so in a future work.

References

- [1] S. Eilenberg and S. MacLane, “General theory of natural equivalences,” *Transactions of the american mathematical society* **58** no. 2, (1945) 231–294.
- [2] S. Mac Lane, *Categories for the working mathematician*, vol. 5. Springer Science & Business Media, 1998.
- [3] R. Penrose, *Tensor methods in algebraic geometry*. PhD thesis, St John’s Coll., Cambridge, 1956.
- [4] R. Penrose, “Applications of negative dimensional tensors,” *Combinatorial mathematics and its applications* **1** (1971) 221–244.
- [5] A. Joyal and R. Street, “The geometry of tensor calculus, I,” *Advances in mathematics* **88** no. 1, (1991) 55–112.
- [6] P. J. Freyd and D. N. Yetter, “Braided compact closed categories with applications to low dimensional topology,” *Advances in mathematics* **77** no. 2, (1989) 156–182.
- [7] P. Selinger, “A survey of graphical languages for monoidal categories,” in *New structures for physics*, pp. 289–355. Springer, 2010.
- [8] B. Coecke, “Kindergarten quantum mechanics: Lecture notes,” in *AIP Conference Proceedings*, vol. 810, pp. 81–98, American Institute of Physics. 2006. [quant-ph/0510032](https://arxiv.org/abs/quant-ph/0510032).
- [9] B. Coecke and A. Kissinger, “Categorical quantum mechanics i: causal quantum processes,” *Categories for the Working Philosopher* (2015) 286–328.
- [10] W. Hunziker, “The S-matrix in classical mechanics,” *Communications in Mathematical Physics* **8** no. 4, (1968) 282–299.
- [11] B. Simon, “Wave operators for classical particle scattering,” *Communications in Mathematical Physics* **23** no. 1, (1971) 37–48.
- [12] I. W. Herbst, “Classical scattering with long range forces,” *Communications in Mathematical Physics* **35** no. 3, (1974) 193–214.
- [13] S. Sokolov, “Classical analogues of the moeller operators, of the pearson example and of the birmann-kato invariance principle,” *Il Nuovo Cimento A (1965-1970)* **52** no. 1, (1979) 1–22.
- [14] T. Osborn, R. Froese, and S. Howes, “Levinson’s theorems in classical scattering,” *Physical Review A* **22** no. 1, (1980) 101.
- [15] H. Narnhofer and W. Thirring, “Canonical scattering transformation in classical mechanics,” *Physical Review A* **23** no. 4, (1981) 1688.
- [16] W. Thirring, “Classical scattering theory,” in *New Developments in Mathematical Physics*, pp. 3–28. Springer, 1981.

- [17] N. Levinson, “On the uniqueness of the potential in a schrodinger equation for a given asymptotic phase,” *Kgl. Danske Videnskab Selskab. Mat. Fys. Medd.* **25** (1949) .
- [18] J.-H. Kim and S. Lee, “Symplectic perturbation theory in massive ambitwistor space: a zig-zag theory of massive spinning particles,” [arXiv:2301.06203 \[hep-th\]](https://arxiv.org/abs/2301.06203).
- [19] J.-H. Kim, J.-W. Kim, and S. Lee, “Massive twistor worldline in electromagnetic fields,” *JHEP* **08** (2024) 080, [arXiv:2405.17056 \[hep-th\]](https://arxiv.org/abs/2405.17056).
- [20] J.-H. Kim, J.-W. Kim, S. Kim, and S. Lee, “Classical eikonal from Magnus expansion,” *JHEP* **01** (2025) 111, [arXiv:2410.22988 \[hep-th\]](https://arxiv.org/abs/2410.22988).
- [21] J.-H. Kim, “Manifest symplecticity in classical scattering,” [arXiv:2511.07387 \[hep-th\]](https://arxiv.org/abs/2511.07387).
- [22] D. A. Kosower, B. Maybee, and D. O’Connell, “Amplitudes, Observables, and Classical Scattering,” *JHEP* **02** (2019) 137, [arXiv:1811.10950 \[hep-th\]](https://arxiv.org/abs/1811.10950).
- [23] R. Gonzo and C. Shi, “Scattering and Bound Observables for Spinning Particles in Kerr Spacetime with Generic Spin Orientations,” *Phys. Rev. Lett.* **133** no. 22, (2024) 221401, [arXiv:2405.09687 \[hep-th\]](https://arxiv.org/abs/2405.09687).
- [24] P. H. Damgaard, E. R. Hansen, L. Planté, and P. Vanhove, “Classical observables from the exponential representation of the gravitational S-matrix,” *JHEP* **09** (2023) 183, [arXiv:2307.04746 \[hep-th\]](https://arxiv.org/abs/2307.04746).
- [25] J. E. Moyal, “Quantum mechanics as a statistical theory,” *Proc. Cambridge Phil. Soc.* **45** (1949) 99–124.
- [26] H. J. Groenewold, “On the Principles of elementary quantum mechanics,” *Physica* **12** (1946) 405–460.
- [27] H. Weyl, “Quantenmechanik und gruppentheorie,” *Zeitschrift für Physik* **46** no. 1, (1927) 1–46.
- [28] E. P. Wigner, “On the quantum correction for thermodynamic equilibrium,” *Phys. Rev.* **40** (1932) 749–760.
- [29] T. L. Curtright and C. K. Zachos, “Quantum Mechanics in Phase Space,” *Asia Pac. Phys. Newslett.* **1** (2012) 37–46, [arXiv:1104.5269 \[physics.hist-ph\]](https://arxiv.org/abs/1104.5269).
- [30] C. Zachos, D. Fairlie, and T. Curtright, “Quantum mechanics in phase space: an overview with selected papers,”.
- [31] U. Leonhardt, *Measuring the quantum state of light*, vol. 22. Cambridge university press, 1997.
- [32] F. Bayen, M. Flato, C. Fronsdal, A. Lichnerowicz, and D. Sternheimer, “Quantum mechanics as a deformation of classical mechanics,” *Letters in Mathematical Physics* **1** no. 6, (1977) 521–530.
- [33] F. Bayen, M. Flato, C. Fronsdal, A. Lichnerowicz, and D. Sternheimer, “Deformation theory and quantization. i. deformations of symplectic structures,” *Annals of Physics* **111** no. 1, (1978) 61–110.
- [34] F. Bayen, M. Flato, C. Fronsdal, A. Lichnerowicz, and D. Sternheimer, “Deformation theory and quantization. ii. physical applications,” *Annals of Physics* **111** no. 1, (1978) 111–151.
- [35] F. A. Berezin, “General concept of quantization,” *Communications in Mathematical Physics* **40** no. 2, (1975) 153–174.

[36] B. V. Fedosov, “A simple geometrical construction of deformation quantization,” *Journal of differential geometry* **40** no. 2, (1994) 213–238.

[37] M. Kontsevich, “Deformation quantization of Poisson manifolds,” *Letters in Mathematical Physics* **66** (2003) 157–216.

[38] A. Weinstein, “Deformation quantization,” *Astérisque* **227** (1995) 389–409.

[39] A. Brandhuber, G. R. Brown, P. Pichini, G. Travaglini, and P. Vives Matasan, “The Magnus expansion in relativistic quantum field theory,” [arXiv:2512.05017 \[hep-th\]](https://arxiv.org/abs/2512.05017).

[40] W. Magnus, “On the exponential solution of differential equations for a linear operator,” *Communications on pure and applied mathematics* **7** no. 4, (1954) 649–673.

[41] A. M. Vershik, I. M. Gel’fand, and M. I. Graev, “Representations of the group of diffeomorphisms,” *Russian Mathematical Surveys* **30** no. 6, (1975) 1.

[42] F. J. Dyson, “The S matrix in quantum electrodynamics,” *Phys. Rev.* **75** (1949) 1736–1755.

[43] J. R. Shewell, “On the formation of quantum-mechanical operators,” *American Journal of Physics* **27** no. 1, (1959) 16–21.

[44] N. H. McCoy, “On the function in quantum mechanics which corresponds to a given function in classical mechanics,” *Proceedings of the National Academy of Sciences* **18** no. 11, (1932) 674–676.

[45] R. L. Stratonovich, “On distributions in representation space,” *SOVIET PHYSICS JETP-USSR* **4** no. 6, (1957) 891–898.

[46] J. C. Várilly and J. M. Gracia-Bondia, “The Moyal representation for spin,” *Annals Phys.* **190** (1989) 107–148.

[47] M. Raymer, “Measuring the quantum mechanical wave function,” *Contemporary Physics* **38** no. 5, (1997) 343–355.

[48] L. A. M. Souza, M. C. Nemes, M. F. Santos, and J. G. P. de Faria, “Quantifying the decay of quantum properties in single-mode states,” *Opt. Commun.* **281** (2008) 4696, [arXiv:0710.5930 \[quant-ph\]](https://arxiv.org/abs/0710.5930).

[49] N. Wheeler, “Phase space formulation of the quantum mechanical particle-in-a-box problem,” *Reed College Physics Department* (2000). <https://www.reed.edu/physics/faculty/wheeler/documents/Quantum%20Mechanics/Miscellaneous%20Essays/Phase%20Space%20in%20a%20Box.pdf>. Retrieved Dec 28, 2025.

[50] R. L. Hudson, “When is the wigner quasi-probability density non-negative?,” *Reports on Mathematical Physics* **6** no. 2, (1974) 249–252.

[51] I. Arnold, V. *Mathematical Methods of Classical Mechanics*, vol. 60 of *Graduate Texts in Mathematics*. Springer-Verlag, New York, 2nd ed., 1989.

[52] A. Connes, *Noncommutative geometry*. Academic Press, 1994.

[53] J. M. Gracia-Bondia, J. C. Várilly, and H. Figueroa, *Elements of noncommutative geometry*. Springer Science & Business Media, 2013.

[54] R. J. Szabo, “Quantum field theory on noncommutative spaces,” *Phys. Rept.* **378** (2003) 207–299, [arXiv:hep-th/0109162](https://arxiv.org/abs/hep-th/0109162).

[55] I. M. Gel’fand and M. A. Naimark, “On the imbedding of normed rings into the ring of operators in hilbert space,” *Matematicheskii Sbornik* **12** no. 2, (1943) 197–217.

[56] I. E. Segal, “Irreducible representations of operator algebras,” *Bulletin of the American Mathematical Society* **53** (1947) 73–88.

[57] R. Montgomery, “An algebraic perspective on manifolds, their tangent vectors, covectors, and diffeomorphisms.” Math 208 lecture notes, University of California Santa Cruz, 2016. <https://people.ucsc.edu/~rmont/classes/ManifoldsI/Lectures/RingStrucB.pdf>. Retrieved Dec 14, 2025.

[58] M. Oliva, D. Kakofengitis, and O. Steuernagel, “Anharmonic quantum mechanical systems do not feature phase space trajectories,” [arXiv:1611.03303 \[quant-ph\]](https://arxiv.org/abs/1611.03303).

[59] B. C. Hall, “Lie groups, lie algebras, and representations,” in *Quantum Theory for Mathematicians*, pp. 333–366. Springer, 2013.

[60] R. J. Glauber, “The quantum theory of optical coherence,” *Physical Review* **130** no. 6, (1963) 2529.

[61] E. Sudarshan, “Equivalence of semiclassical and quantum mechanical descriptions of statistical light beams,” *Physical Review Letters* **10** no. 7, (1963) 277.

[62] A. Cattaneo, B. Keller, C. Torossian, and A. Bruguieres, *Déformation, quantification, théorie de Lie*. Société mathématique de France, 2005. 11.3. The Moyal star product from path integrals.

[63] K. Husimi, “Some formal properties of the density matrix,” *Proceedings of the Physico-Mathematical Society of Japan. 3rd Series* **22** no. 4, (1940) 264–314.

[64] N. D. Cartwright, “A non-negative wigner-type distribution,” *Physica A: Statistical Mechanics and its Applications* **83** no. 1, (1976) 210–212.

[65] W. B. Campbell, P. Finkler, C. E. Jones, and M. N. Misheloff, “Path Integral Formulation of Scattering Theory,” *Phys. Rev. D* **12** (1975) 2363–2369.

[66] R. Penrose, *The road to reality: A complete guide to the laws of the universe*. Random house, 2005. Figures 14.6, 14.7, 14.17, 14.18, 14.21.

[67] R. Penrose and W. Rindler, *Spinors and space-time: Volume 1, Two-spinor calculus and relativistic fields*, vol. 1. Cambridge University Press, 1984. Appendix: Diagrammatic Notation.

[68] P. Cvitanovic, *Group theory: birdtracks, Lie's, and exceptional groups*. Princeton University Press, 2008.

[69] R. P. Feynman, “Space-time approach to nonrelativistic quantum mechanics,” *Rev. Mod. Phys.* **20** (1948) 367–387.

[70] A. Murua, “The Hopf Algebra of Rooted Trees, Free Lie Algebras, and Lie Series,” *Foundations of Computational Mathematics* **6** no. 4, (2006) 387–426. <https://doi.org/10.1007/s10208-003-0111-0>.

[71] D. Calaque, K. Ebrahimi-Fard, and D. Manchon, “Two interacting Hopf algebras of trees: A Hopf-algebraic approach to composition and substitution of B-series,” *Advances in Applied Mathematics* **47** no. 2, (2011) 282–308. <https://www.sciencedirect.com/science/article/pii/S0196885810000990>.

[72] J. C. Várilly and J. Gracia-Bondia, “The Moyal representation for spin,” *Annals of physics* **190** no. 1, (1989) 107–148.

[73] R. J. Szabo, “Magnetic monopoles and nonassociative deformations of quantum theory,” *J. Phys. Conf. Ser.* **965** no. 1, (2018) 012041, [arXiv:1709.10080 \[hep-th\]](https://arxiv.org/abs/1709.10080).

[74] I. Bakas and D. Lüst, “3-Cocycles, Non-Associative Star-Products and the Magnetic Paradigm of R-Flux String Vacua,” *JHEP* **01** (2014) 171, [arXiv:1309.3172 \[hep-th\]](https://arxiv.org/abs/1309.3172).

[75] A. S. Cattaneo and G. Felder, “A path integral approach to the kontsevich quantization formula,” *Communications in Mathematical Physics* **212** (2000) 591–611.

[76] J.-H. Kim, “Worldline formalism in phase space,” [arXiv:2509.06058 \[hep-th\]](https://arxiv.org/abs/2509.06058).

[77] S. Kim, H. Lee, and S. Lee, “Classical eikonal in relativistic scattering,” [arXiv:2509.01922 \[hep-th\]](https://arxiv.org/abs/2509.01922).

[78] J.-M. Souriau, “Structure des systemes dynamiques dunod,” *Paris, 1970. Department of Mathematics and Statistics, The University of Calgary, Calgary, Alberta, Canada, T2N 1N4* (1970) .

[79] F. J. Dyson, “Feynman’s proof of the Maxwell equations,” *American Journal of Physics* **58** no. 3, (1990) 209–211.

[80] K. Haddad, G. U. Jakobsen, G. Mogull, and J. Plefka, “Unitarity and the On-Shell Action of Worldline Quantum Field Theory,” [arXiv:2510.00988 \[hep-th\]](https://arxiv.org/abs/2510.00988).

[81] R. E. Peierls, “The Commutation laws of relativistic field theory,” *Proc. Roy. Soc. Lond. A* **214** (1952) 143–157.

[82] D. M. Marolf, “Poisson brackets on the space of histories,” *Annals Phys.* **236** (1994) 374–391, [arXiv:hep-th/9308141](https://arxiv.org/abs/hep-th/9308141).

[83] M. Duetsch and K. Fredenhagen, “The Master Ward Identity and generalized Schwinger-Dyson equation in classical field theory,” *Commun. Math. Phys.* **243** (2003) 275–314, [arXiv:hep-th/0211242](https://arxiv.org/abs/hep-th/0211242).

[84] E. Witten, “Interacting Field Theory of Open Superstrings,” *Nucl. Phys. B* **276** (1986) 291–324.

[85] K. Fredenhagen and K. Rejzner, “Perturbative algebraic quantum field theory,” in *Winter School in Mathematical Physics: Mathematical Aspects of Quantum Field Theory*, pp. 17–55. Springer, 8, 2012. [arXiv:1208.1428 \[math-ph\]](https://arxiv.org/abs/1208.1428).